Title
Proteins at the Saccharomyces cerevisiae Lipid Droplet

Author
Currie, Erin

Publication Date
2014

Peer reviewed|Thesis/dissertation

Proteins at the *Saccharomyces cerevisiae* Lipid Droplet

by

Erin Currie

DISSERTATION

Submitted in partial satisfaction of the requirements for the degree of

DOCTOR OF PHILOSOPHY

in

Cell Biology

in the

GRADUATE DIVISION

of the

UNIVERSITY OF CALIFORNIA, SAN FRANCISCO

Acknowledgements

Acknowledgements

Text and figures in Chapter 2 were submitted to the *Journal of Lipid Research* entitled "High Confidence Proteomic Analysis of Yeast Lipid Droplets Identifies Additional Droplet Proteins and Reveals Connections to Dolichol Synthesis and Sterol Acetylation" by Erin Currie, Xiuling Guo, Romain Christiano, Chandramohan Chitraju, Nora Kory , Kenneth Harrison, Joel Haas, Tobias C. Walther, and Robert V. Farese, Jr. The authors would like to thank Crystal Herron and John Carroll for editorial assistance, Beth Cimini, Ellen Edenberg, Manuele Piccolis, and Andrew Nguyen for technical assistance, and Natalie Krahmer, Charles Waechter, and Jeffrey Rush for advice. This work was supported by NIH grants RO1-GM09984 (to R.F.), GM097194 (T.C.W.), and The G. Harold and Leila Y. Mathers Charitable Foundation (to T.C.W). E.C was supported in part by a grant from NSF.

Text and figures in Chapter 4 were published as a Perspective in *Cell Metabolism* (Vol. 18, June 2013) entitled "Cellular Fatty Acid Metabolism and Cancer," by Erin Currie, Almut Schulze, Rudolf Zechner, Tobias C. Walther, and Robert V. Farese Jr. The authors would like to thank Gary Howard for editorial assistance.

Text and figures in Chapters 1 and 3 are unpublished.

Personal Acknowledgements

To my partner, Adam Weisbart, I give the utmost thanks for the love and support that has carried me through the final years of this madcap pursuit. You're crazy for staying by my crazy self through this whole crazy process and I don't know if I could have done it without you. Credenza.

To my "Girls," Dr. Beth Cimini, Dr. Ellen Edenberg, Dr. Heather Eshleman, Dr. Erica Moehle, and Dr. Argenta Price, I give the utmost thanks for the love and support. I don't know if I could have done this without your listening ears, helpful advice, and affirmations through so many "learning experiences."

To my parents, Bill Currie and Linda Bothwell and Lisa and Steve Bird, I give the utmost thanks for the love and support. They may not have understood much of what I had to say about graduate school, but they patiently listened to all of it.

The members of my thesis committee, Dr. Nevan Krogan, Dr. Peter Walter, and Dr. Keith Yamamoto, were sources of great wisdom. I appreciate their insightful comments in my committee meetings and their patient ears outside. And I always knew they enjoyed my thesis committee meetings, even if it was just for the baked goods.

The many labmates that I have had during my tenure in the Farese Lab have all contributed to my growth as a scientist. In particular, I would like to thank Dr. Lauren Herl Martens and Dr. Joel Haas for sharing the graduate student experience with me. Additionally, Dr. Carrie Grueter, Dr. Laura Mitic, and Dr. Caroline Mrejen were great role models as successful female scientists.

And, finally, I give thanks to my mentor and PI, Dr. Bob Farese Jr. He is full of enthusiasm and ideas that inspire his lab members. I appreciate his support through the ups and downs of graduate school and his support of and belief in me as a scientist. He has taught me much more than just how to be a scientist.

Abstract

Lipid droplets (LDs) are ubiquitous and dynamic organelles whose major functions are in lipid metabolism. They are unique among organelles because they have a phospholipid monolayer and neutral lipid core. This unique architecture puts unusual biological constraints upon many basic organelle process including biogenesis, protein targeting, and degradation. While they are the focus of much research on the biochemical, cell biological, and physiological levels, many basic questions about LD biology remain unanswered, such as Where and how are LDs formed? What proteins are at the LD and how do they target there? and How are LDs regulated and degraded? Overall, understanding the biology of LDs has broad implications for many human diseases including lipodystrophy, cachexia, metabolic syndrome, non-alcoholic fatty liver disease, atherosclerosis, neutral lipid storage disease, and cancer.

We used *Saccharomyces cerevisiae* as a model organism to make inroads into several of the unanswered questions. We used protein correlation profiling and quantitative proteomics to produce a high confidence list of proteins localized to the LD to begin to answer the question of what proteins are at the LD. We conducted a genome wide visual screen for genetic requirements of LD formation and protein targeting to the LD and explored the targeting of ergosterol synthetic enzymes to the LD on a cell biological level to begin to answer the questions of how LDs are formed and how do proteins target the LD?

Table of Contents

List of Tables

List of Figures

Chapter 1:
Introduction to Lipid Droplets

Introduction to Lipid Droplets

The lipid droplet (LD) is an ubiquitous organelle whose major functions include lipid storage and metabolism. Long thought to be mostly inert, the LD is now recognized as a *bona fide* organelle that has dynamic size, number, distribution, and protein composition (Farese and Walther, 2009). LD proteins include a family of structural proteins (Brasaemle, 2007), many enzymes involved in lipid metabolism, and an assortment of proteins with other functions. Protein localization to the LD can be regulated by many factors including development (e.g., histones (Cermelli et al., 2006)) or phospholipid content (e.g., CCT1 in flies (Krahmer et al., 2011)).

The LD has a unique architecture for an intracellular organelle with a phospholipid (PL) monolayer and neutral lipid core. The neutral lipid core is primarily composed of triaclyglycerols (TG) and sterol esters (SE) in which the ratio of TG to SE varies by cell type. Adipocyte LDs are primarily TG (Zweytick et al., 2000), yeast have ratios of roughly 1:1 TG:SE (Leber et al., 1994), while macrophage foam cells, involved in atherosclerotic plaques, contain mostly SE (McGookey and Anderson, 1983). Hepatocyte LDs can be primarily either, depending upon conditions: TG in classic diet-induced fatty liver (Sozio et al., 2010) or SE in mice lacking the oxysterol receptor LXRα (Peet et al., 1998).

Because of its unique architecture, biogenesis of the LD is governed by different principles than the biogenesis of other organelles. Formation and growth of the LD requires both PL and neutral lipid synthesis. Relatively little is known about how LDs are formed. It is commonly accepted that LDs arise from the endoplasmic reticulum (ER) because the TG synthetic enzymes (e.g. mammalian DGAT1 and DGAT2, yeast Dga1 and Lro1) are ER localized (reviewed in

Goodman, 2008 and Walther and Farese, 2012), although it is clear that proteins can target to the LD either at the moment of LD formation or later (e.g. Erg6 and Dga1, respectively, in yeast (Jacquier et al., 2011)). Many screens have been done in several model systems for changes to LD morphology, however none have identified protein machinery that is essential for LD formation (e.g. *Drosophila* S2 cells in Guo et al., 2008, *C. elegans* in Ashrafi et al., 2003, *S. cerevisiae* in Fei et al., 2008a and b). The LD research field has recently come to view the problem of LD formation in light of emulsion physics (Thiam et al., 2013) which is able to explain why the only protein requirements for LD formation discovered are neutral lipid synthetic enzymes (e.g. murine adipocytes in Harris et al., 2011, *S. cerevisiae* in Sandager et al, 2002)

The PL monolayer imposes unique structural requirements upon proteins that target to the LD, for example, prohibiting transmembrane proteins and favoring structures that can localize to the interface by dipping segments into the hydrophobic phase, such as proteins with hydrophobic sequences (Martin and Partin, 2006, Wilfling et al., 2013) or amphipathic helices (Brasaemle et al., 2007). How and why proteins target to the LD is a major question that remains unanswered as topology is unknown for most LD proteins and not all LD proteins with known topologies have hydrophobic sequences or amphipathic helices.

LDs are often found in close apposition to other organelles, including peroxisomes (Binns et al., 2006), mitochondria (Pu et al., 2011, Blanchette-Mackie et al., 1983, and Shaw et al., 2008), endosomes (Liu et al., 2007), phagosomes (van Manen et al., 2005), and especially the endoplasmic reticulum (ER) (Jacquier et al., 2011 and Ozeki et al, 2005). In fact, some proteins

that appear to target the LD may actually target ER membranes closely apposed to the LD; this can be difficult to distinguish at the resolution of confocal light microscopy (~300 nm). The functional consequences of these close appositions are not well explored.

Disregulation of LD numbers, both decreases and increases, have been implicated in many diseases including lipodystrophy, cachexia, metabolic syndrome, non-alcoholic fatty liver disease, atherosclerosis, and neutral lipid storage disease (reviewed in Krahmer et al., 2013). There is much work being done to understand the molecular causes of such disregulation as the causation behind correlation is often poorly understood. One such example is in cancer where LDs have been proposed to be pathogenic but may be, in fact, a consequence of cellular stress and it is fatty acids not LDs, per se, that are pathogenic (Currie et al., 2013).

The Yeast Lipid Droplet

Saccharomyces cerevisiae yeast are an important and well characterized model for the study of LDs because they are eukaryotic with highly conserved lipid metabolic pathways, are easy to manipulate biochemically and genetically, and have been used for many large scale studies to identify genetic determinants of LD morphology and LD proteins (Radulovic et al., 2013). While similar in many ways, the yeast LD has notable differences from metazoans. A wild type yeast cell contains LDs that are all roughly the same size and, while their size can be increased genetically or by lipid supplementation (Szymanski et al., 2007), they grow a relatively small amount when compared to the massive potential for size differences in metazoan cells. In metazoan cells there are clear examples of two separate LD populations – those that are able to grow and those that are not (Wilfling et al., 2013) – however in yeast, there has not been an identification of functionally separate populations. In fact, it appears that all LDs are functionally connected to the ER (Jacquier et al., 2011), unlike metazoan cells. There are examples of yeast LD proteins that only localize to some LDs but the functional consequences, if any, have not been explored (Currie et al., 2014).

Yeast LD cores are roughly 50% TG and 50% SE (Leber et al., 1994), although the composition can be altered genetically (e.g. Sandager, 2002) or by lipid supplementation (e.g. Grillitsch et al., 2011). There are four neutral lipid synthetic enzymes in yeast - Dga1 (ortholog of mammalian DGAT2) and Lro1 (ortholog of mammalian LCAT) synthesize TG and Are1 and Are2 (orthologs of mammalian ACAT) synthesize SE. Yeast lacking all four enzymes lack LDs and are viable under laboratory growth conditions (Sandager et al., 2002) although they have impaired growth, especially under oleate supplemented conditions (Petschnigg et al., 2009), and impaired

ergosterol synthesis (Sorger et al., 2004). Yeast LD PLs have a characteristic profile that is distinct from other organelles (Schneiter, et al., 1999), although, unlike TG, the composition does not change much in lipid-supplemented conditions (Grillitsch et al., 2011).

Three previous visual screens have been reported to identify genes that affect LD morphology. One screen used Nile Red to mark LDs and screened the deletion collection, identifying 133 with an altered LD number (Fei et al., 2008a). Another used the deletion collection to identify 56 strains that are sensitive to nystatin, 39 of which show an altered LD number (Fei et al., 2008b). Another group used BODIPY to screen the deletion collection and identified 59 with abnormal morphology (Szymanski et al., 2007). Unfortunately, there was very little overlap between the three screens, suggesting that lipid droplet number is highly sensitive to environmental or screening conditions.

Several proteomes attempting specificity have been reported for the yeast LD although, like the visual screens, there is little overlap between the proteomes. There are technical differences between the various reported proteomes that can account for some of the differences in LD protein lists. The first reported yeast LD proteome was highly specific but identified only 19 proteins in part due to technological limitations of MS at the time (Athendstaedt et al., 1999). Two subsequent yeast LD proteomes took advantage of technological advances and reported highly sensitive proteomes, but had limited confirmation and may include a larger number of contaminants, particularly of high abundance proteins. The differences in overlap between proteomes may partially be due to differences in culture conditions (Binns et al., 2006 cultured cells in minimal media with oleate; Grillitsch et al., 2011, cultured in rich media with and

without oleate; Athendstaedt et al., 1999, cultured in rich media without oleate) or minor technical differences in purification methods, but the non-overlapping proteins are likely to be enriched in contaminants.

Proteomes are complimented by large-scale approaches to GFP-tagged protein localization. Huh et al., 2003, reported GFP-tagged localization of over 4,000 proteins and included LD as a potential localization in their screen, although due to the genomic nature of their screen, many LD proteins were missed. Natter et al., 2005, GFP-tagged 400 proteins with roles in lipid metabolism and analyzed their localization. Because the LD plays a major role in lipid metabolism, it identified many LD proteins.

Sterols and the Yeast Lipid Droplet

Yeast synthesize ergosterol, a sterol whose biosynthetic pathway is identical to cholesterol until the last several enzymatic reactions. De novo ergosterol synthesis starts from acetyl-CoA, a substrate used in many lipid synthetic reactions. Synthesis reaches a branch point at farnesyl pyrophosphate (FPP) which can go toward sterol, polyprenol/dolichol, or ubiquinone synthesis. In yeast, as in mammals, all of the membrane-bound sterol synthesis enzymes (Ergs) are found in the endoplasmic reticulum (ER). However, several Ergs (Erg1, Erg6, Erg7, and Erg27) (Athendstaedt et al., 1999, and Mo et al., 2002) are also found at the lipid droplet (LD). The localization of these proteins to different cellular compartments appears to affect their activity; almost all measurable activities for Erg6 (Zinser et al., 1993), Erg7 (Milla et al., 2002), and Erg27 (Mo et al., 2003) are detected in LD fractions.

In yeast, sterols can be acetylated and that acetylation causes their secretion. It is thought that Atf2 promiscuously acetylates sterols while Say1 deacetylates only sterol molecules that should be in the cell in a general detoxification mechanism (Tiwari et al., 2007). While it does not appear that metazoans acetylate sterols and the human genome has no identifiable homolog of Atf2, Say1 has a human ortholog (AADAC) that can rescue defects in say1Δ cells.

Much of the sterol synthesis pathway is conserved between yeast and mammals. Erg7 and Erg27 have direct mammalian homologues (LSS or lanosterol synthase, and HSD17B7 or 17-beta-hydroxysteroid dehydrogenase, respectively) while Erg6 represents the first yeast-specific enzymatic activity at the branch point between ergosterol and cholesterol synthesis. Little work has been done in a mammalian system to examine the localizations or activities of LSS or

HSD17B7. However, published proteomes have found them in the LD fractions in Chinese hamster ovary K2 cells (Liu et al., 2003), rat tissue hepatocytes (Turró et al., 2006), mouse 3T3-L1 adipocytes (Brasaemle et al., 2004), human epidermoid carcinoma A431 cells (Umlauf et al., 2004), and human monocyte U937 cells (Wan et al., 2007). LSS was also found in human hepatocyte HuH7 cells (Fujimoto et al., 2004). Thus, it appears highly likely that cholesterol synthesis is linked to LD biology.

Chapter 2:
High Confidence Proteomic Analysis of Yeast Lipid Droplets Identifies Additional Droplet Proteins and Reveals Connections to Dolichol Synthesis and Sterol Acetylation

Abstract

Accurate protein inventories are essential for understanding an organelle's functions. The lipid droplet (LD) is a ubiquitous intracellular organelle with major functions in lipid storage and metabolism. LDs differ from other organelles because they are bounded by a surface monolayer, presenting unique features for protein targeting to LDs. Many proteins of varied functions have been found in purified LD fractions by proteomics. While these studies have become increasingly sensitive, it is often unclear which of the identified proteins are specific to LDs. Here we used protein correlation profiling to identify 35 proteins that specifically enrich with LD fractions of *Saccharomyces cerevisiae*. Of these candidates, 30 fluorophore-tagged proteins localize to LDs by microscopy, including six proteins, several with human orthologs linked to diseases, that we newly identify as LD proteins (Cab5, Rer2, Say1, Tsc10, YKL047W, and YPR147C). Two of these proteins, Say1, a sterol deacetylase, and Rer2, a cis-isoprenyltransferase, are enzymes involved in sterol and polyprenol metabolism, respectively, and we show their activities are present in LD fractions. Our results provide a highly specific list of yeast LD proteins and reveal that the vast majority of these proteins are involved in lipid metabolism.

Introduction

The lipid droplet (LD) is a cytoplasmic organelle that is ubiquitous among eukaryotic cells and is also found in some prokaryotic cells (Fujimoto et al., 2011, Walther and Farese, 2012, and Brasaemle and Wolins, 2012). LDs were long thought to be mostly inert but are now recognized as a *bona fide* organelle with dynamic size, number, distribution, and protein composition (Farese and Walther, 2009). LD proteins include a family of structural proteins (Brasaemle, 2007), many enzymes involved in lipid metabolism, and an assortment of proteins with other functions. Protein localization to the LD can be regulated by many factors including development (e.g., histones (Cermelli et al., 2006)) or phospholipid content (e.g., CCT1 in flies (Krahmer et al., 2011)). A thorough understanding of protein composition is an essential step in understanding the functions of the LD.

The LD has a unique architecture of neutral lipid core bounded by a phospholipid monolayer. The surfactant monolayer imposes specific structural requirements on proteins localized to the LD, i.e., prohibiting transmembrane proteins with luminal domains and favoring structures that can localize to the interface by dipping segments into the hydrophobic phase, such as proteins with hydrophobic sequences (Martin and Parton, 2006, and Wilfling et al., 2013) or amphipathic helices (Brasaemle, 2007). LD biogenesis and growth are uniquely dependent on neutral lipid synthesis because the organelle core contains primarily triacylglycerols (TGs) and sterol esters (SEs), with composition varying by cell type and nutritional status. In yeast, the composition of TG and SE is roughly 50% for each (Leber et al., 1994).

LDs are often found in close apposition to other organelles, including peroxisomes (Binns et al., 2006), mitochondria (Pu et al., 2011, Blanchette-Mackie et al., 1983, and Shaw et al., 2008), endosomes (Liu et al., 2007), phagosomes (van Manen et al., 2005), and especially the endoplasmic reticulum (ER) (Jacquier et al., 2011 and Ozeki et al., 2005), which is likely their site of origin (reviewed in Goodman, 2008, and Wilfling et al., 2014). In fact, some proteins that appear to target the LD may actually target ER membranes closely apposed to the LD; this can be difficult to distinguish at the resolution of confocal light microscopy (~300 nm). The close association of LDs with other organelles makes their biochemical purification challenging. Additionally, the hydrophobic nature of the organelle offers a potential sink for non-LD proteins whose topologies are disrupted during the mechanical fractionation process. These artifacts, combined with the high sensitivity of mass spectrometry (MS), often yield LD proteomes with low specificity.

We sought to determine a high-confidence proteome of the yeast *Saccharomyces cerevisiae* LD, an established model for LD studies (Radulovic et al., 2013). Although comprehensive lists of yeast LD proteomes have been reported (Binns et al., 2006 and Grillitsch et al., 2011), there is often little overlap between these lists and it remains unclear which of the candidate proteins identified by proteomics are specific to LDs. We sought to overcome the specificity limitations of LD proteomes by using protein correlation profiling (PCP), a quantitative method of determining purification profiles of proteins compared with organelle markers, based on high-resolution mass spectrometry. PCP was successfully used to create specific inventories of many organelles (Andersen et al., 2003, and Foster et al., 2006), including LDs in *Drosophila melanogaster* cells (Krahmer et al., 2013). We reasoned that *bona fide* LD proteins should fulfill

two criteria: a) enrichment in the LD purification fraction by PCP, and b) localization to LDs by microscopy. We used PCP to generate a high-confidence list of 35 proteins that specifically co-purify with the yeast LD. By cross-referencing with fluorescence microscopy in this study or previous reports, we verified that 30 of these proteins are *bona fide* LD proteins. We showed that two proteins (Faa1 and Hfd1) previously identified in yeast LD proteomes in fact do localize to LDs. Additionally, we identified six new LD proteins (Cab5, Rer2, Say1, Tsc10, YKL047W, and YPR147C), and we assessed enzymatic activities for two of these proteins, Say1 and Rer2, at LDs.

Experimental Procedures

Strains, Media and Materials – S. cerevisiae strain BY4741 (*MAT**a** his3Δ0 leu2Δ0 met15Δ0 ura3Δ0)* was used as wild type. Yeast strains were routinely transformed using lithium acetate. Cells were cultured in synthetic complete media with dextrose (SCD) containing 2% dextrose, 0.67% yeast nitrogen base (BD Biosciences), amino acids (Sunrise Science), and ammonium sulfate. Cells were grown for 2 days at 30°C to stationary growth phase for all experiments.

Protein Localization- C-terminally tagged GFP strains were created using published cloning cassettes (Janke et al., 2004). PCR primers were designed using Primer3 (http://bioinfo.ebc.ee/cgi-bin/primer3/primer3web_results.cgi) and purchased from Elim Biopharm. Yeast were labeled with 1:1000 monodansyl pentane (MDH) (Abgent) for LD identification (Yang et al., 2012) and allowed to settle on concanavalin A coated coverslips for 10 minutes. They were then mounted on slides and images were acquired by using a Nikon ECLIPSE Ti 2000 microscope with Yokogawa CSU-X1 spinning disk and Hamamatsu ImagEM electron multiplier CCD camera with image acquisition and mechanical control by Micro-Manager. Solid-state lasers at excitation/emission of 405/460 nm, 491/520 nm, and 561/595 nm were used. Images were deconvolved (Huygens SVI) and cropped (Image J). The fraction of LDs with GFP was determined manually by counting numbers of LDs with and without GFP signal colocalization. The fraction of GFP colocalizing with LDs was determined by a custom CellProfiler pipeline and Python script that calculated the fraction of total GFP intensity that colocalized with MDH punctae on a per cell basis.

Localization was confirmed by crude cellular fractionation and immunoblotting, using mouse monoclonal anti-PDI (Abcam), anti-GFP (Roche) and rabbit polyclonal anti-HA (Upstate). For crude fractionation (e.g., in experiments of Figures 5A, 5C-E, 6A, 6C), cells were dounce-homogenized and lysates spun at 300*g* for 30 min and then 100,000*g* for 30 min. LDs were collected with a tube slicer (Beckman Coulter) and the remaining supernatant and pellet were collected.

TLC – Lipids were extracted by bead beating cells in water:$CHCl_3$:MeOH (0.3:1:1), collecting the single phase, and drying it under N_2 gas. Lipids were resuspended in chloroform, separated on silica gel TLC plates (Whatman or Analtech) using hexane:ethyl ether:acetic acid (80:20:1) and detected by charring with cuprous sulfate. Bands were identified by comparison to standards.

LD purification – SILAC was performed (Ong et al., 2002 and Frohlich et al., 2013). Cells were pelleted, washed with water and then incubated in 0.1M Tris-Cl pH9, 10 mM DTT at 30C for 10m. They were washed and resuspended in 20mM KH_2PO_4 pH7.4, 1.2M sorbitol to 0.5 g/mL and digested with 4 mg/g zymolyase 100T (MP Biomedicals) at 30°C for 2 hrs. Cells were pelleted, washed, and resuspended in 5 mL 20 mM Hepes, pH7.4, 0.6M sorbitol, 1 mM EDTA, and EDTA-free protease inhibitor pellet (Roche) and homogenized in a dounce homogenizer for 40 strokes. Dounced cells were spun at 300*g* for 30 min, 20,000*g* for 30 min, and then 100,000*g* for 30 min with the pellet collected at every centrifugation step. The supernatant was then floated through a sucrose gradient by centrifuging overnight at maximum speed in a SW41 rotor. The LDs were collected with a tube slicer (Beckman Coulter) and other fractions were collected by

pipette. Six gradient fractions and the three pellets from the initial high-speed spins were analyzed by MS.

Liquid Chromatography MS/MS analysis – Each peptide fraction was separated by reversed-phase chromatography on a Thermo Easy nLC 1000 system connected to a Q Exactive mass spectrometer (Thermo) through a nano-electrospray ion source. Peptides were separated on 15-cm columns (New Objective) with an inner diameter of 75 mm packed in house with 1.9 mm C18 resin (Dr. Maisch GmbH). 120-min chromatographic runs were used and peptides were eluted with a linear gradient of acetonitrile from 5 to 30% in 0.1% formic acid for 95 min at a constant flow rate of 250 nl/min. The column temperature was kept at 35°C. Eluted peptides were directly electrosprayed into the mass spectrometer. Mass spectra were acquired on the Q Exactive in a data-dependent mode to automatically switch between full scan MS and up to 10 data-dependent MS/MS scans. The maximum injection time for full scans was 20 ms with a target value of 3,000,000 at a resolution of 70,000 at m/z = 200. The ten most intense multiple charged ions ($z \geq 2$) from the survey scan were selected with an isolation width of 3Th and fragmented with higher energy collision dissociation (HCD) with normalized collision energies of 25. Target values for MS/MS were set to 1,000,000 with a maximum injection time of 120 ms at a resolution of 17,500 at m/z = 200. To avoid repetitive sequencing, the dynamic exclusion of sequenced peptides was set to 20 s.

The resulting MS and MS/MS spectra were analyzed using MaxQuant (version1.3.0.2), utilizing its integrated ANDROMEDA search algorithms (Cox et al., 2008 and 2011). Peak lists were searched against local databases for S. *cerevisiae* (obtained from the Saccharomyces Genome

Database, Stanford University; 6641 entries, July 26, 2012) with common contaminants added. The search included carbamidomethlyation of cysteine as fixed modification, and methionine oxidation and N-terminal acetylation as variable modifications. Maximum allowed mass deviation for MS peaks was set to 6ppm and 20ppm for MS/MS peaks. Maximum missed cleavages were 2. The false discovery rate was determined by searching a reverse database. Maximum false-discovery rates were 0.01 both on peptide and protein levels. Minimum required peptide length was 6 residues. Proteins with at least two peptides (one of them unique) were considered identified. The "match between runs" option was enabled with a time window of 2 min to match identification between replicates.

Criteria for Defining LD Proteins – To define a high-confidence LD protein set, we applied four criteria to filter candidates. First, we set an arbitrary cutoff point for rank-ordered membership in the LD cluster as the top 136 proteins. We chose this arbitrary point because it included the majority of previously identified LD proteins in two experimental replicates. Second, proteins had to be above the arbitrary cutoff in both experimental replicates. Third, proteins had to have a calculable H/L ratio in at least eight fractions so that we were confident that their cluster membership value was not strongly influenced by missing data points. Finally, proteins were filtered based on a purification profile that closely matched that of 12 well-established LD proteins (Fig. 3A). In the case of our analysis, these stringent criteria used the thresholds of H/L <0.06 in fractions 1–3, <0.16 in fractions 4–6, <0.2 in fraction 3, and <0.371 in fraction 2 (Fig. 1E). By including these selected thresholds, we were able to maximize specificity of the selected LD proteins.

Cis-IPTase Assay – Cells were crudely fractionated as above. To reduce cytoplasm in the LD fraction, LDs in 1.5-mL Eppendorf tubes were rinsed twice by addition of 1 volume buffer, spun at max speed in a tabletop centrifuge, and a needle and syringe were inserted below the floating LDs to remove 1 volume cytoplasm. Pellets were rinsed twice and then resuspended in yeast cis-IPTase reaction buffer (60mM HEPES, pH 8.5, 5mM $MgCl_2$, 2mM DTT, 2mM NaF, 2mM sodium orthovanadate). Yeast reaction mixtures contained 100 μg protein, 50 μM FPP and 45 μM 14C-IPP (American Radiolabeled Chemicals). Reactions were incubated at 30 degrees for 1h and quenched by addition of 2 ml $CHCl_3$:MeOH (2:1). Products were separated from unreacted water-soluble IPP by partition through addition of 0.8 ml of 0.9% NaCl in water. The organic phase was washed three times with $CHCl_3$:MeOH:H_2O (3:48:47) and dried under nitrogen. The dried sample was resuspended in hexane and loaded onto silica gel TLC plates, run in hexane: ethyl acetate (80:20), and dried. Plates were exposed to a phosphor screen for 3–4 days and compared with iodine-labeled standards. The band corresponding to dolichol was scraped from the TLC plate, resuspended in scintillation counting liquid, and counted in a scintillation counter.

Cholesteryl Acetate Deacetylase Assay – Cells were crudely fractionated as described for the *cis*-IPTase assay in lysis buffer of 200mM sorbitol, 10mM Hepes-KOH pH7.5, 100mM NaCl, 5mM $MgCl_2$, and 1mM EDTA. 300 ug of microsome or 300 ug of cytoplasm and LD protein were assayed for cholesteryl acetate deacetylase activity as described in (Tiwari and Schneiter, 2009). Cell fractions were incubated with 0.143 uCi 14C-cholesteryl-acetate (CA, American Radiolabeled Chemicals) in 26nmol total CA for 1 hour at 30C. The assay was stopped by adding 1.5 volumes of $CHCl_3$. 3 volumes of MetOH were added and the reaction was vortexed

until clear. 1.5 volumes 2.8% ortho-phosphoric acid was added and the samples were centrifuged for 2 min. at 13k rpm. The upper aqueous layer was discarded. Samples were re-extracted with 1.5 volumes $CHCl_3$ and 3 volumes acidified water. The lower organic layer was collected and dried under nitrogen. The dried sample was resuspended in $CHCl_3$:MetOH (1:1), loaded onto silica gel TLC plates, run in petroleum ether: diethyl ether: acetic acid (70:30:2), and dried. Plates were exposed to a phosphor screen for 2–3days and compared to iodine-labeled standards.

Results

PCP Yields a Distinct LD Purification Profile

LDs were isolated from wild-type yeast grown at 30°C to stationary phase, where LDs are most abundant. To obtain the fractions for PCP, we purified LDs from cells labeled with heavy, non-radioactive isotope-containing lysine (stable isotope labeling by amino acids in cell culture, SILAC (Ong et al., 2002)) using sequential differential centrifugation and a sucrose density gradient. We collected samples from pellets of each initial centrifugation (fractions 1–3) and six layers of the sucrose density gradient (fractions 4–9). By using peptides identified in the various fractions, we found that the sequential centrifugations pelleted primarily the following: unbroken cells and agglomerated membrane in fraction 1; vacuolar, nuclear, ER, plasma, endosomal, and Golgi membranes in fraction 2; and transport vesicles, endosomal membranes, and Golgi complex in fraction 3. The sucrose density gradient separated the cytoplasm into six additional fractions. We combined each of these samples with equal amounts of protein from the LD fraction (fraction 9) of unlabeled cells and analyzed the combined samples by liquid chromatography coupled online to electrospray ionization and high-resolution tandem mass spectrometry (Fig. 1A). We measured 16,589 peptides and 2,165 proteins were measured in all fractions with 1,377 proteins identified in the LD fraction, 993 of which had calculable heavy:light ratios.

We calculated heavy:light ratios (H/L) for each protein in every fraction. To compare individual proteins, we set the maximum H/L to 1 and normalized the ratios in other fractions to this H/L. To directly compare different organelle purification profiles, we plotted a representative profile for a protein from each of the major cellular organelles, choosing proteins that were only

annotated to a single intracellular compartment in SGD (Fig. 1B). We found that *bona fide* LD proteins peak in fraction 9 with very little representation in other fractions. In contrast, ER proteins, which are especially difficult to separate from LDs, similarly peak in fraction 9, but also have peaks in fractions 2 and 3. Several other organelles have abundant proteins in the LD fraction, highlighting the need for a technique such as PCP to determine specificity.

We used soft clustering to generate clusters of typical purification profiles with each protein assigned a membership value for each cluster (Futschik and Carlisle, 2005). The membership value provides a measurement of the similarity between each protein's purification profile and the cluster, thereby providing a measure of the likelihood that a protein belongs to a certain cluster. Soft clustering identified a group of LD proteins (Fig. 1C, bottom center) as well as clusters containing mostly proteins from other organelles (e.g., mitochondria (center) and ER (center right)).

To assess reproducibility of the LD PCP measurements, we repeated the purification and analysis and compared the membership value for the LD cluster of each identified protein. The results were highly reproducible, with a Pearson's correlation of 0.77 between the two PCP experiments (Fig. 1D). We performed the same comparison with a third biological replicate and found that it correlated well with both previous PCPs ($r = 0.79$ and $r = 0.76$, respectively), again showing the reproducibility of our technique and dataset. Thus, with respect to the high-confidence list, the results were highly reproducible.

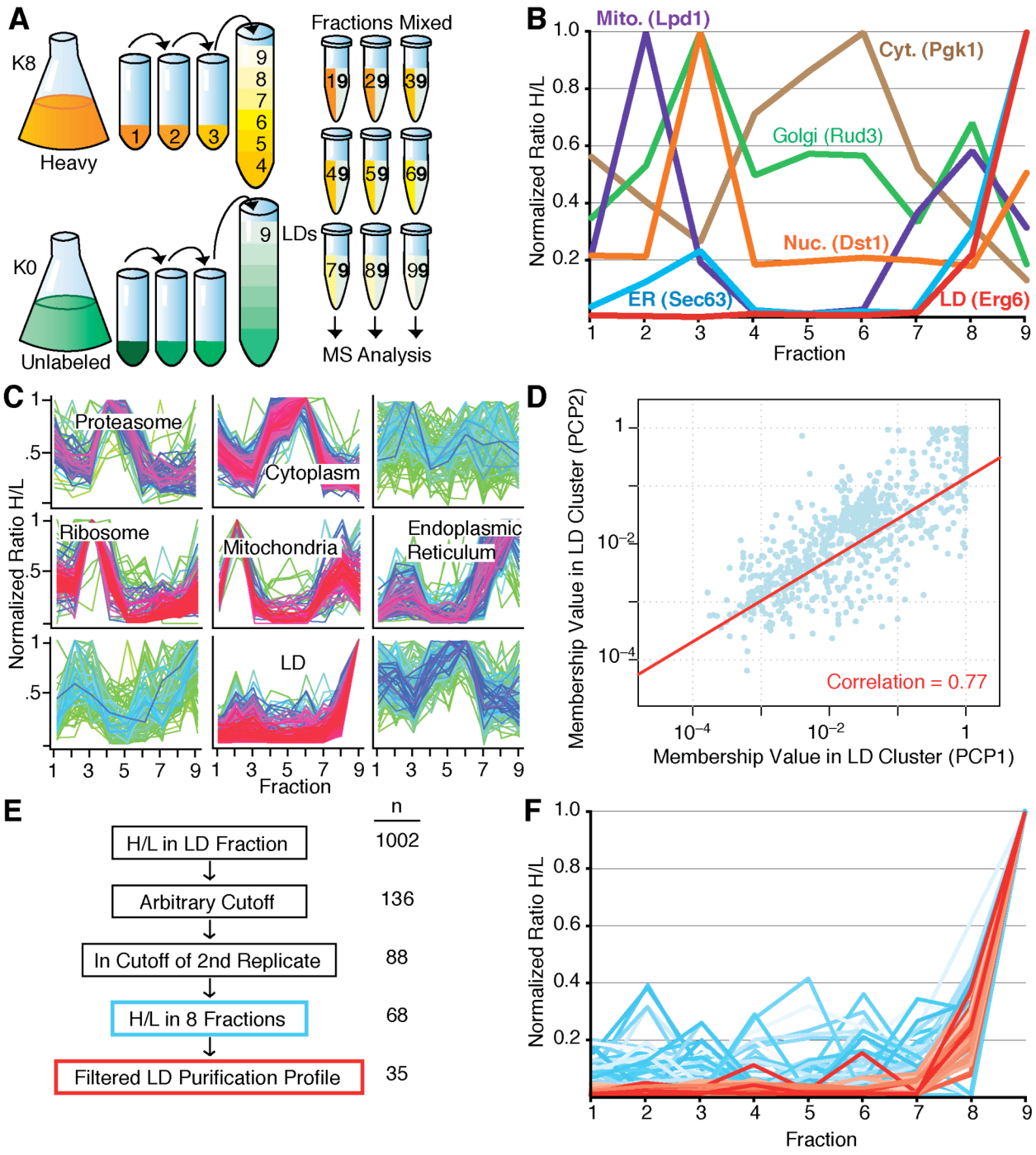

Figure 1. Identification of LD proteins in *S. cerevisiae* using PCP.
A – Schematic of PCP workflow.
B – Purification profiles of representative proteins for different organelles.
C – Analysis of all fractions of a LD purification with Mfuzz in R. Proteins identified in the LD fraction that were identified in at least five of the nine fractions were analyzed. A normalized H/L was used. The cluster number C was set at 9, and cluster stability m = 1.6. Clusters that showed enrichment of proteins of a certain organelle or function are indicated. Proteins with a minimal membership value of 0.1 for LD cluster are shown in supplemental Table S2.

D – Reproducibility of LD proteome data between experiments. Pearson correlation = 0.77
E – Schematic of data filtration to create high-confidence LD protein list.
F – Proteins identified with high confidence in the LD PCP cluster of two biological replicates. Proteins in red passed additional stringent filtration criteria whereas those in blue did not.

We applied an arbitrary cutoff to the LD cluster (as described in Experimental Procedures) and filtered the list to include only proteins that were within this arbitrary cutoff in a biological replicate to generate a cluster of 88 proteins that reproducibly purify in the LD fraction (filtration schematic in Fig. 1 D). To further separate *bona fide* LD proteins from proteins of other cellular localizations, we applied stringent filtration criteria to the cluster to separate it into highest-confidence LD proteins (Fig. 1E, red) and suspected non-LD proteins (Fig. 1E, blue). This analysis yielded a list of 35 highest-confidence LD proteins (Table 1).

Verification of Lipid Droplet Protein Localization

We next tested which proteins in the high-confidence PCP list are *bona fide* LD proteins, as confirmed by localization to LDs by spinning disk live-cell fluorescence microscopy. Of the 35 identified proteins, 19 were previously identified as LD proteins by fluorescence microscopy in published works (annotated in Table 1 and Fig. 2A). Three proteins (Faa1, Hdf1 and Gtt1) were identified in other yeast LD proteomes but were not localized to the LD by fluorescence microscopy. To assess their localization, we tagged these proteins at the C-terminus with GFP to assess LD localization in stationary growth phase by colocalization with monodansylpentene (MDH), a blue LD vital dye. Hfd1-GFP exhibited predominantly LD localization while Faa1-GFP appeared to be visible in additional cellular compartments, likely the ER (representative images shown in Fig. 2B). Gtt1-GFP was predominantly present in other cellular compartments,

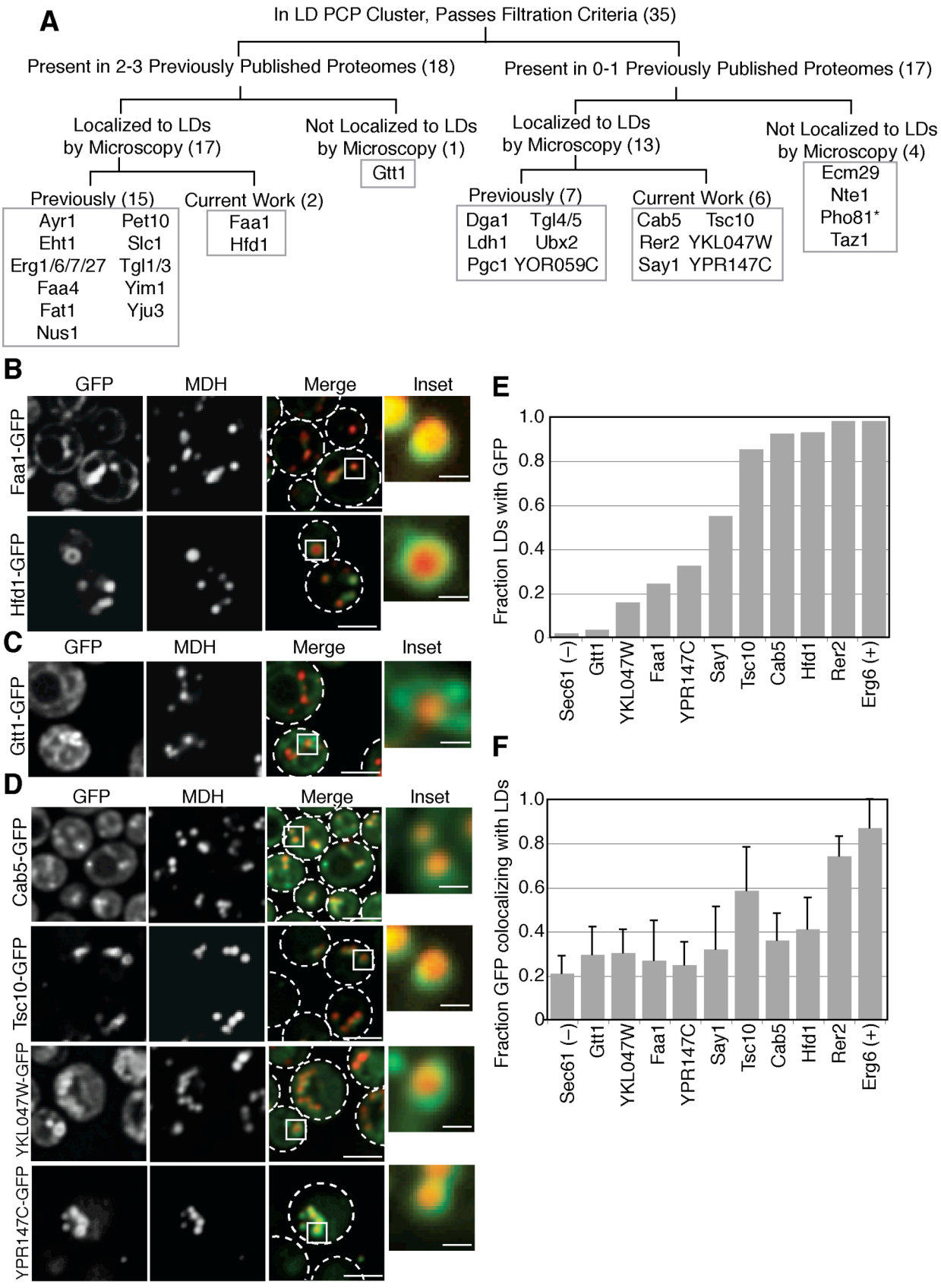
A
In LD PCP Cluster, Passes Filtration Criteria (35)
Present in 2-3 Previously Published Proteomes (18)
Present in 0-1 Previously Published Proteomes (17)
Localized to LDs by Microscopy (17)
Not Localized to LDs by Microscopy (1)
Gtt1
Localized to LDs by Microscopy (13)
Not Localized to LDs by Microscopy (4)
Ecm29
Nte1
Pho81*
Taz1
Previously (15)
Ayr1 Pet10
Eht1 Slc1
Erg1/6/7/27 Tgl1/3
Faa4 Yim1
Fat1 Yju3
Nus1
Current Work (2)
Faa1
Hfd1
Previously (7)
Dga1 Tgl4/5
Ldh1 Ubx2
Pgc1 YOR059C
Current Work (6)
Cab5 Tsc10
Rer2 YKL047W
Say1 YPR147C
B
GFP
MDH
Merge
Inset
Faa1-GFP
Hfd1-GFP
C
Gtt1-GFP
D
Cab5-GFP
Tsc10-GFP
YKL047W-GFP
YPR147C-GFP
E
Fraction LDs with GFP
1.0
0.8
0.6
0.4
0.2
0
Sec61 (–)
Gtt1
YKL047W
Faa1
YPR147C
Say1
Tsc10
Cab5
Hfd1
Rer2
Erg6 (+)
F
Fraction GFP colocalizing with LDs

Figure 2. Identification and verification of LD proteins.
A – Logic flow diagram for identification of LD proteins.
B – Verification of LD localization of 2 proteins previously found in multiple proteomes but not previously localized to the LD by microscopy.
C – Microscopy of a protein that reproducibly purifies with LDs but does not appear to localize to the LD.
D – Microscopy of four newly identified LD proteins.
E – Quantification of the fraction of LDs that colocalize with GFP on a population basis. Sec61 and Erg6 are negative and positive controls, respectively.
F – Quantification of the fraction of GFP signal that colocalizes with LDs on a per cell basis. Sec61 and Erg6 are negative and positive controls, respectively.
GFP tagged proteins were colocalized with monodansyl pentene (MDH), a LD marker vital dye. Cells were grown in SCD media to stationary phase. The scale bar is 3.5um on merged images and 0.7um on inset images.

however we identified some GFP signal that surrounded LD signal, which could explain why Gtt1 biochemically fractionates with LDs (Fig. 2C, 2E-F).

Seventeen proteins identified in our PCP proteome were not previously annotated to the LD or, in some cases, were only found in a single report of the LD proteome. Seven of these proteins were previously localized to the LD by microscopy (Dga1, Ldh1, Pgc1, Tgl4, Tgl5, Ubx2, YOR059C). Of the 10 remaining proteins, three (Ecm29, Nte1, Taz1) did not show LD localization when we examined them by microscopy, suggesting that they purify with the LD fraction but do not localize to this organelle. We were unable to image Pho81 because we could not express the tagged protein. However, we newly identified six proteins (Cab5, Rer2, Say1, Tsc10, YKL047W, and YPR147C) as localizing to LDs (Fig. 2D, 2E-F). Interestingly, of the six, the four proteins with known functions are involved in lipid metabolism. Cab5 is involved in coenzyme A synthesis (Olzhausen et al., 2013), an important cofactor for many lipid synthesis reactions. Tsc10 catalyzes the second step in the synthesis of phytosphingosine, a long-chain base for sphingolipid production (Beeler et al., 1998). Rer2 and Say1 function in dolichol and sterol metabolism, respectively, and are discussed below. YKL047W and YPR147C do not have

known functions in yeast, although the mammalian ortholog of YPR147C was recently reported to have cholesterol esterase activity (Goo et al., 2013).

Comparison of PCP Proteome to Reported Yeast Lipid Droplet Proteomes

Of the 959 proteins with a calculable H/L in the LD fraction, we found 35 (<4%) that specifically purify with the LD according to our filtering criteria (see Experimental Procedures) (Table 1). We compared our LD protein list to other reported proteomes that attempt to threshold their lists and found that the current proteome overlaps most (95%) with the one reported by Athendstaedt et al. (1999), which utilized earlier and less sensitive proteomics technology. In contrast, there was considerably less overlap with LD proteomes generated more recently with more sensitive MS techniques (Grillitsch et al. (2011), 55%; Binns et al. (2006), 30%) (Fig. 2A).

Twelve proteins (Ayr1, Eht1, Erg1, Erg6, Erg7, Faa1, Faa4, Fat1, Pet10, Slc1, Tgl1 and Tgl3), eleven of which are known to be lipid enzymes, were detected in the current work and all reported proteomes.

We also analyzed our results in relationship to protein abundance within cells, using data from Ghaemmaghanmi et al. (2003). Previously reported yeast LD proteomes show an overrepresentation of high abundance proteins, suggesting more contamination of the LD fraction. Our results show substantially fewer high-abundance proteins, consistent with less contamination. As expected with the outstanding sensitivity of current MS instruments, we were able to detect low-abundance proteins with the current proteome.

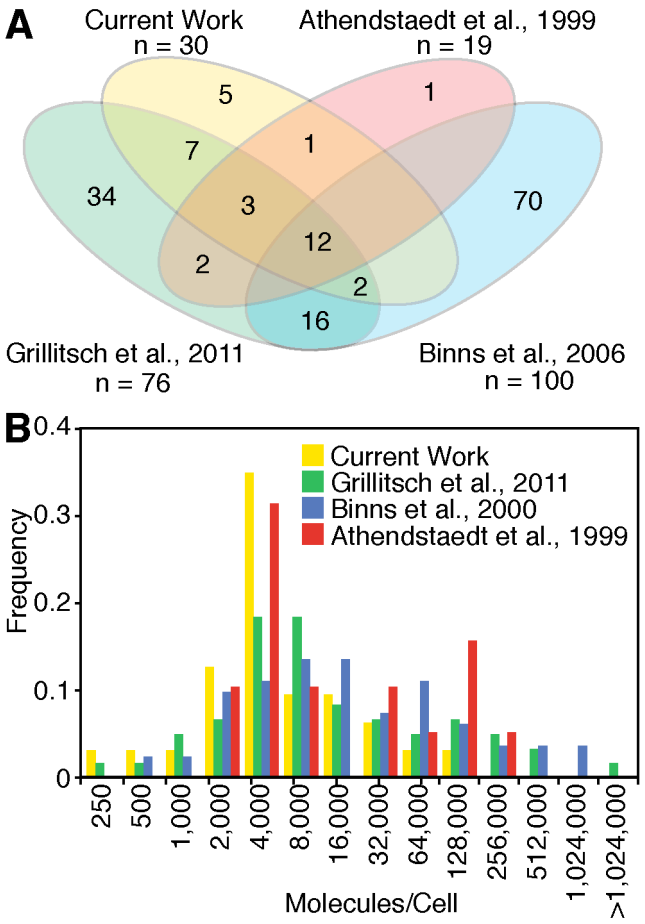

FIGURE 3. Comparison of current LD proteome with previously reported yeast LD proteomes.
A – Venn diagram showing overlap of LD-annotated proteins between the current work and three previously reported LD proteomes that attempted specificity.
B – Current work using PCP for identification of LD proteins has fewer high-abundance proteins than previously reported yeast LD proteomes. Protein abundances were from Ghaemmaghanmi et al. 2003.

Functions of Bona Fide *Lipid Droplet Proteins*

We annotated the functions of the 30 *bona fide* LD proteins based on available data in the literature (Fig. 4A). Interestingly, all proteins with known functions (83%) are involved in lipid metabolism. These included many proteins involved in ergosterol metabolism (Fig. 4B) and fatty-acid esterification and TG metabolism (Fig. 4C). The only *de novo* TG synthetic enzyme that we failed to detect in our LD proteome is Pah1, although it has previously been localized to

the LD (Karansios et al., 2013). Six proteins (Fmp52, Pet10, Yim1, YKL047W, YOR059C, and YPR147C) do not have clear functions (see Table 1).

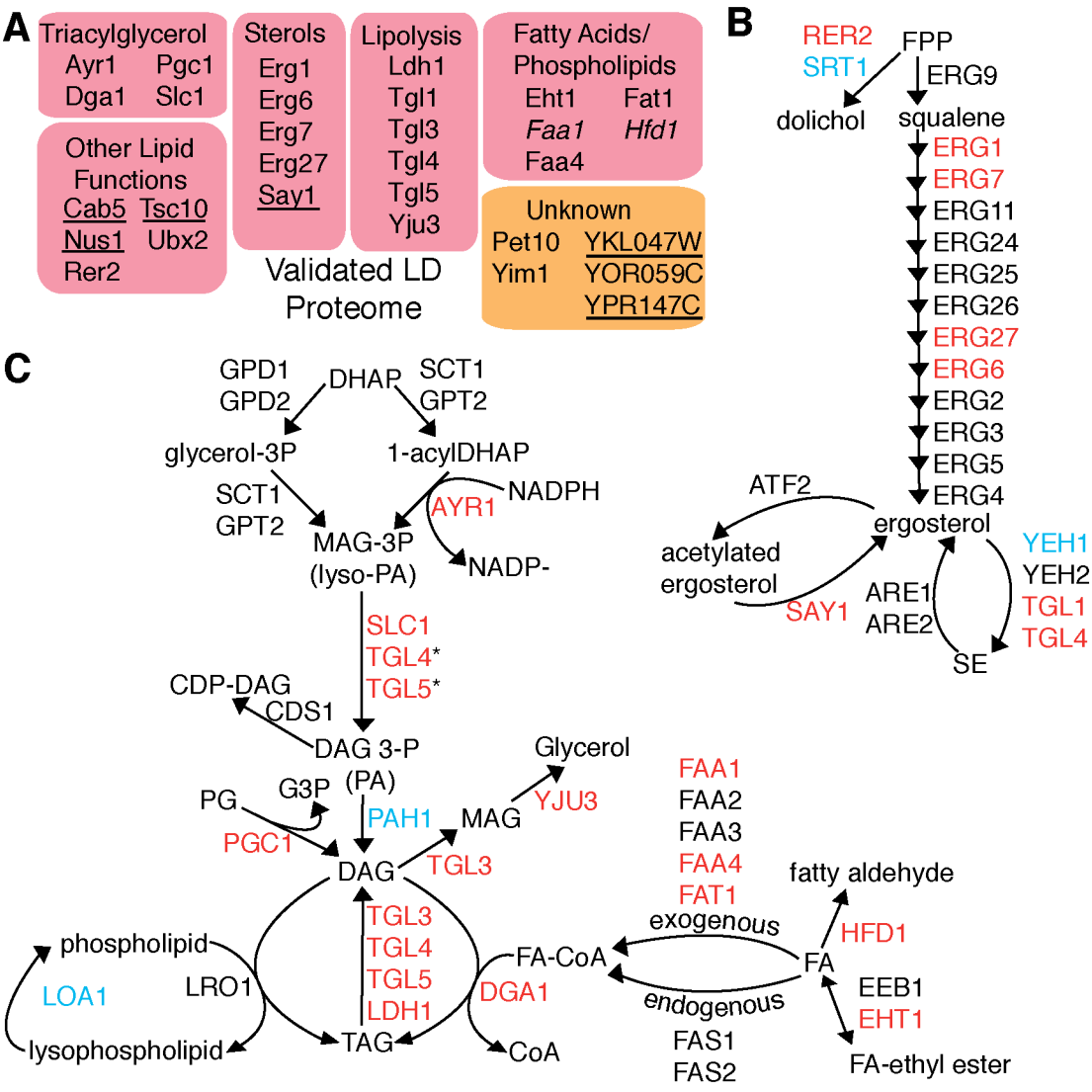

Figure 4. Functional annotation of identified LD localized proteins.
A – All validated LD proteins with known functions are involved in LD metabolism. Newly verified proteins are italic. Newly identified proteins are underlined.
B – Proteins that co-purify with LDs include many enzymes in sterol metabolism. Two are newly identified (Rer2 and Say1).
C – Proteins that co-purify with LDs include most enzymes in TG metabolism.
*activity shown *in vitro*, presumed to be minor function *in vivo*.
Proteins marked in red were identified and microscopically verified in the current work. Proteins marked in blue were not identified in our proteome but have been microscopically verified in other works.

Of the six newly identified LD proteins, we chose to focus our further investigations on Rer2 and Say1 because they have known enzymatic functions in sterol metabolism, and their connections to LDs have not been well explored.

Rer2 Is Active in the LD Fraction

Rer2 is a cis-isoprenyltransferase (cis-IPTase) involved in dolichol synthesis (Sato et al., 1999). It is a 286-amino acid protein with a predicted globular structure. Cis-IPTases condense successive isoprenyl pyrophosphates (IPPs) with farnesyl pyrophosphate (FPP) to create polyprenols, such as dolichol, the lipid anchor for sugars used in N-linked glycosylation. Because many enzymes in N-glycan biosynthesis were recently identified at the *Drosophila* LD (Krahmer et al., 2013), we sought to better understand the LD localization of Rer2.

There are two known cis-IPTases in yeast, Rer2 and Srt1. Another protein, Nus1, has significant homology to Rer2 and Srt1 but does not have cis-IPTase activity (Harrison et al., 2011). Both Srt1 (Sato et al., 2001) and Nus1 (Grillitsch et al., 2011, Athenstaedt et al., 1999, and Prein et al., 2000) have been localized previously to the LD. We found that Rer2 also localizes to the LD as we detected Rer2-GFP in both membrane and LD fractions (Fig. 5A) and saw colocalization of Rer2-GFP with ER marker Sec61-mCherry and MDH (Fig. 5B). The deletion of Rer2 affects neutral lipids as *rer2*Δ cells showed a specific increase (> 2-fold) in SE levels (Fig. 5C) that was rescued by expression of the human Rer2 homolog, DHDDS.

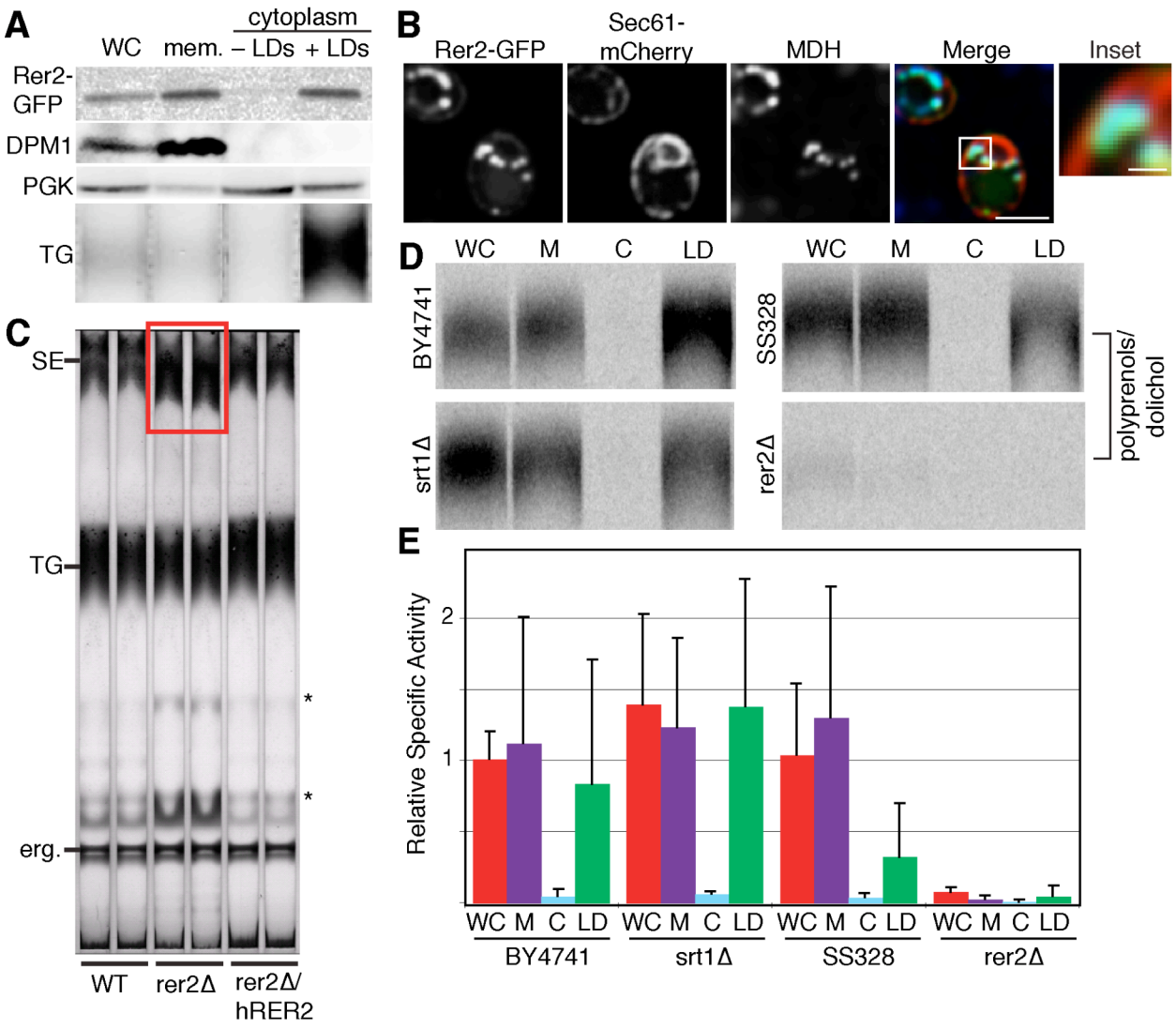

Figure 5. Rer2 is present and active at the LD.

A – Rer2-GFP is present at the LD and in membranes by western blot. Rer2-GFP labeled cells were fractionated by a 100,00 g spin. The centrifuge tubes were sliced. The upper fraction (containing LDs) was rinsed and the rinsed upper fraction, lower fraction (containing cytoplasm), and pellet (containing membranes), were probed with anti-GFP (for Rer2), anti-PGK (for cytoplasm), and anti-DPM1 (for ER) antibodies. The lipids were extracted and separated by TLC. TG was identified by co-migration with a standard.

B – Rer2-GFP is present at the LD and ER by spinning disk confocal microscopy. Rer2-GFP shows a reticular and punctate pattern that colocalizes with ER marker Sec61-mCherry and LD stain MDH.

C – *rer2*Δ have increased levels of sterol esters as determined by TLC. Expression of DHDDS (human homolog of Rer2) rescues the sterol ester accumulation. Unidentified lipids are marked with a *.

D – Rer2 is active at the LD. Cell extracts, as in A, were given FPP and 14C-IPP, which were incorporated into polyprenols by *cis*-IPTases in both the membrane and LD fractions. *cis*-IPTase

activity is nearly wild-type in an *srt1*Δ deletion strain and nearly missing in an *rer2*Δ strain, suggesting that Rer2 is the major *cis*-IPTase in both microsomes and LDs.
E – Quantification of D, normalized to wild type whole cell activity. Error bars represent standard deviation. There are no statistical differences between individual fractions in *srt1*Δ and BY4741. Whole cell and membrane *cis*-IPTase activity is significantly reduced ($p<.05$) in *rer2*Δ when compared to SS328.
WC = whole cell. M or mem. = membrane. C = cytoplasm.

To assess whether Rer2 is active at LDs, we examined cis-IPTase activity in cell extracts by incubating cells with FPP and ^{14}C-IPP and measuring incorporation into polyprenols by TLC. We found that wild-type cells had *cis*-IPTase activity in both membrane and LD fractions (Fig. 5D). *srt1*Δ cells had similar *cis*-IPTase activities, while *rer2*Δ cells had very little *cis*-IPTase activity in either membrane or LD fractions, indicating that Rer2 is the major source of polyprenol synthesis at the ER and the LD in stationary phase yeast.

Say1 Is Active in the LD Fraction

In yeast, sterol metabolism is intricately linked between LDs and the ER. We therefore further investigated Say1, a sterol metabolic enzyme that we newly identified as a LD protein. Say1 de-acetylates acetylated sterols and participates in an apparent cycle of sterol acetylation and de-acetylation, whereas Atf2 promiscuously acetylates sterols so they can be secreted in a detoxification mechanism (Tiwari et al., 2007). In this model, Say1 specifically de-acetylates sterols that should be retained within the cell, like ergosterol and its synthetic intermediates. While Say1 has been previously localized to the ER, we detected Say1-GFP in both the ER and LD fractions (Fig. 6A). Additionally, Say1-GFP colocalized with ER marker Sec61-mCherry and MDH showing that it has both ER and LD localization (Fig. 6B). *say1*Δ yeast do not have grossly altered levels of SE or TG (data not shown).

We detected sterol deacetylase activity in both ER and LD fractions (Fig. 6C and D) when we overexpressed Say1-HA under control of a *GAL1*-promoter. Thus, it appears that Say1-mediated sterol de-acetylation is present at the LD. We did not detect sterol deacetylase activity in either wild-type (cells not overexpressing Say1-HA) or *say1*Δ cells, consistent with a previous report (Tiwari et al., 2007).

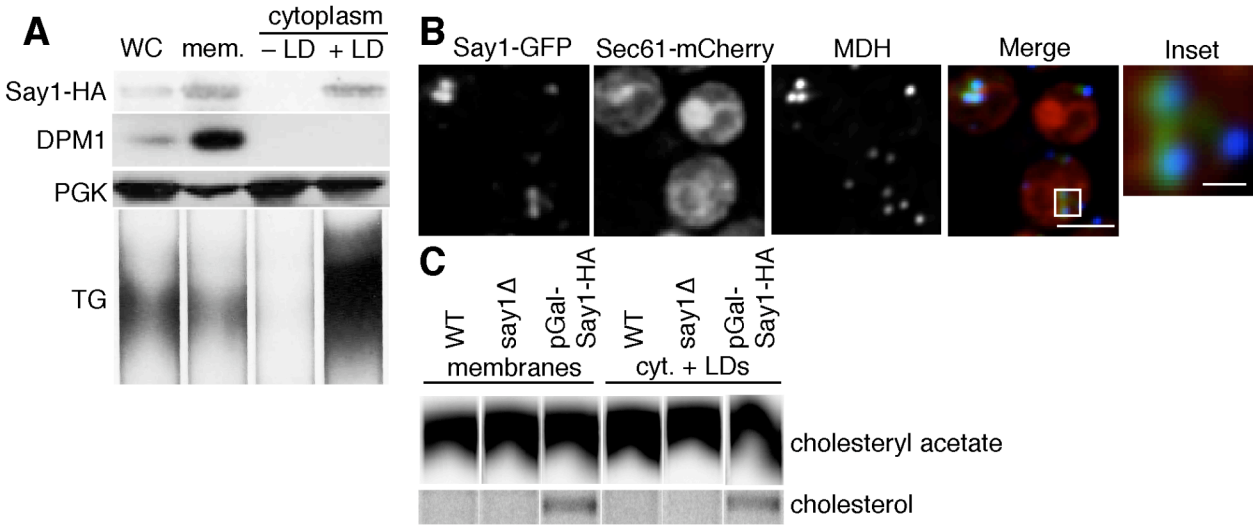

Figure 6. Say1 is present and active at the LD.
A - Say1-GFP is present at the LD and in membranes by western blot. pGal-Say1-GFP cells were fractionated as in Fig. 5 and probed with anti-HA (for Say1), anti-PGK (for cytoplasm), and anti-DPM1 (for ER) antibodies. Lipids were extracted and separated by TLC. TG was identified by co-migration with a standard.
B - Say1-GFP is present at the LD and ER by spinning disk confocal microscopy. Say1-GFP shows a reticular and punctate pattern that colocalizes with ER marker Sec61-mCherry and LD stain MDH.
C - Say1 is active at the LD. Cell extracts were given 14C-Cholesteryl acetate (CA) which was de-acetylated into free cholesterol in both membrane and LD fractions by cells grown in galactose and overexpressing Say1-HA under a GAL1 promoter. CA deacetylase activity was below the limit of detection in wild type or *say1*Δ cells.
WC = whole cell. M or mem. = membrane. C or cyt. = cytoplasm.

Discussion

A yeast lipid droplet proteome generated by protein correlation profiling

LD proteomes are challenging to generate because of the hydrophobic nature of the LD and its close apposition to other organelles. Although LD proteomes have consistently identified a core set of important LD proteins, they are plagued with false positives from co-purifying contaminants. Previous MS-based proteomic examinations of yeast LD proteins yielded lists of candidates ranging in number from 76 (Grillitsch et al., 2011) to 440 (Fei et al., 2011). PCP provides a method to determine a yeast LD proteome that is both highly sensitive and specific (Krahmer et al., 2013). In the current study, we applied PCP to the analysis of yeast LDs and identified 35 proteins that reproducibly and stringently co-purify in the LD fraction. Of the 35 proteins identified, 30 of these proteins localize to the LD by microscopy, in our studies and others (Fig. 2 and Table 1), identifying them as *bona fide* LD proteins. Importantly, we identify six proteins (Cab5, Rer2, Say1, Tsc10, YKL047W, YPR147C) that have not previously been localized to the LD. Further, we show that two of these proteins, Say1 and Rer2, are lipid metabolic enzymes that are active in LD fractions. One of the proteins that we newly identified, Cab5, is involved in coenzyme A biosynthesis, with Cab2, Cab3, and Cab4 (34). By fluorescence microscopy, we were additionally able to detect Cab4-GFP at the LD (data not shown). Using fluorescence microscopy, we also verified stationary-phase LD localization of two proteins previously identified in multiple LD proteomes but never visually shown to be at the LD (Faa1 and Hfd1).

Our results differ somewhat from previous reports of yeast LD proteomes (see Fig. 3). The first reported LD proteome identified only 19 proteins (Athenstaedt et al., 1999), in part due to technological limitations of MS at the time, but was likely highly specific and most closely overlaps with the current results. Two subsequent proteomes benefited from enhanced MS sensitivity, but had limited confirmation and likely included a number of contaminants, particularly of highly abundant proteins. The lack of overlap between the proteomes may also reflect differences in culture conditions (Binns et al. (2006), minimal media with oleate; Grillitsch et al. (2011), rich media with and without oleate; Athendstaedt et al. (1999), rich media without oleate) or differences in purification methods. The twelve proteins identified in all proteomes (Ayr1, Eht1, Erg1, Erg6, Erg7, Faa1, Faa4, Fa1, Pet10, Slc1, Tgl1 and Tgl3) are likely to be constitutive LD proteins, since they were identified regardless of specific growth conditions.

Although our PCP identified 35 proteins that specifically co-purify with the LD, we were unable to verify LD localization by fluorescence microscopy for five proteins (Fig. 2 and Table 1). For some of these proteins, GFP-tagging might interfere with their targeting to the LD. For Gtt1, microscopy revealed that clusters of Gtt1-GFP localize near some LDs, offering an explanation for why Gtt1 biochemically purifies with LDs. Taz1, a cardiolipin remodeling enzyme found primarily in mitochondrial membranes (Brandner et al., 2005), might also co-purify with LDs due to organelle associations.

The stringent filtration criteria we employed resulted in the exclusion of some *bona fide* LD proteins from our results. For example, our list does not include several previously identified LD

proteins (e.g. Atf1 (Verstrepen et al., 2004), Loa1 (Ayciriex et al., 2012), Pah1 (Karanasios et al., 2013), Pdr16 (Schnabl et al., 2003) or Srt1 (Sato et al., 2001)). Our criteria potentially filtered out several proteins that were present in the LD and other cellular fractions, as it did for Pdr16, which localized to the LD and cell periphery (Schnabl et al., 2003). Atf1 and Srt1 were not detected in the LD fraction, whereas Loa1 was only detected in a single replicate. Pah1 was found in the LD fraction but not included because it lacked sufficient H/L ratios in multiple fractions, as our criteria demanded. That we did not identify some proteins may also reflect the dynamic nature of protein localization to the LD (we examined stationary phase only) or limitations of organelle fractionation. For example, nutrient carbon source affects the LD targeting of Osh4, Cpr5, and Ubx2 (Grillitsch et al., 2011).

Our PCP analysis of the yeast LD proteome revealed some notable differences from a PCP analysis of LDs in *Drosophila* S2 cells (Krahmer et al., 2013). Although both PCP studies found that the majority of LD proteins function in lipid metabolism, we found considerably more LD proteins (>100) in *Drosophila* cells. The additional proteins are involved in ER organization, protein degradation, and N-glycan biosynthesis, suggesting additional functions and complexity for LDs in fly versus yeast cells. Other differences might relate to the different relationships between the ER and LDs in these cell types. In yeast, LDs are often more directly connected or exist as a subdomain of the ER (Jacquier et al., 2011), whereas in S2 cells there are distinct LD populations – those that are connected and not connected to the ER (Wilfling et al., 2013). The closer association of LDs and ER in yeast may explain why this study required additional filtration criteria to yield a LD-specific list of proteins.

A specific list of yeast LD proteins presents the opportunity to determine how these proteins target to the LD. For example, of the twelve proteins found in all reported proteomes, six have predicted transmembrane domains (Erg1, Erg7, Fat1, Slc1, Tgl1, and Tgl3), with the topology of Tgl1 experimentally verified (Köffel et al., 2005). It is unclear how a protein with a transmembrane domain can localize to a membrane monolayer at LD surfaces. In yeast, perhaps many of these transmembrane proteins are in an ER microdomain that is closely associated with the LD and indistinguishable by biochemical fractionation or light microscopy. LDs appear to be a subdomain of the ER in yeast, and LD-ER bridges have been found in yeast and a number of other organisms (Willing et al., 2013, Jacquier et al., 2011, Ohsaki et al., 2008, and Wanner et al., 1981).

Most of the newly identified yeast LD proteins (Cab5, Rer2, Say1, Tsc10, and YPR147C) have human orthologs and thus the localization to LDs might also be important for functions of these proteins in humans. The functional homolog of Rer2, dehydrodolichyl diphosphate synthase (DHDDS or hCIT), has been linked to retinitis pigmentosa (Züchner et al., 2011). Human coenzyme A synthase (COASY) is a bifunctional enzyme (phosphopantetheine adenylyltransferase and dephosphocoenzyme A kinase activities) that catalyzes the last step of coenzyme A synthesis, like Cab5 (Daugherty et al., 2002). While sterol acetylation is a yeast specific process, Say1 is orthologous to arylacetamide deacetylase (AADAC) (Tiwari et al., 2007), an enzyme putatively involved in TG hydrolysis (Nourbakhsh et al., 2013). Tsc10 is functionally homologous to FVT1, a 3-ketodihydrosphingosine reductase, known to be active at the cytosolic face of the ER (Kihara et al., 2004) and implicated in tumor processes (Rimokh et al., 1993). YPR147C is a highly conserved protein with a GSXSG lipase motif that has been

shown to affect lipid storage in Drosophila (Thiel et al., 2013) and cholesterol ester storage in macrophages (Goo et al., 2013).

Identification of Rer2 and Say1 as lipid droplet-localized enzymes in yeast

Our findings show that the cis-IPTase Rer2 localizes in part to LDs. Cis-IPTase activity is an essential step in dolichol biosynthesis and in yeast is catalyzed by Rer2 and Srt1, with Nus1 as a potential cofactor (Harrison et al., 2011). Both Srt1 and Nus1 have been previously reported at the LD (Binns et al., 2006, Grillitsch et al., 2011, Sato et al., 2001, and Prein et al., 2000). We found that the cis-IPTase Rer2 localizes to the ER and LDs both biochemically and by fluorescence microscopy and has similar specific activities in each compartment. The major role of ER-localized Rer2 is to generate dolichol for glycosylation, and yeast lacking LDs (lacking all four enzymes of neutral lipid synthesis (Sorger et al., 2004)) still make dolichol (not shown). Therefore, LD-localized Rer2 may be more important for synthesizing dolichol destined for storage pools or other cellular functions.

It is unclear how Rer2 localizes to LDs. Rer2 does not have predicted transmembrane sequences although it behaves as an integral membrane protein (Sato et al., 1999). Thus, there are no theoretical topological problems for its localization to the LD. In our experimental conditions, Rer2 appears to be the major cellular cis-IPTase. A previous report showed that Srt1 was most highly expressed in stationary phase and Srt1-dependent activity was detected in an *rer2*Δ background when Srt1 was overexpressed and only in stationary phase (Sato et al., 2001).

However, we found little cis-IPTase activity in the *rer2*Δ in stationary phase, leaving questions about the cellular role of Srt1.

Yeast cells with Rer2 deletion exhibited an increase in SEs. While stressed or slow-growing yeast cells often accumulate LDs, the accompanying neutral lipid accumulation is usually both SE and TG. We suspect that *rer2*Δ cells likely have a SE-specific accumulation because FPP, a Rer2 substrate, may be channeled into sterol synthesis and SEs. Rechanneling of FPP is consistent with the finding of several unidentified radiolabeled lipid species synthesized by *rer2*Δ cells in cisIPTase activity assays (data not shown).

We also found that an enzyme involved in a sterol detoxification system, Say1, targets to the LD. A current model suggests that Say1 works in concert with Atf2. Atf2 promiscuously acetylates exogenous and endogenous sterol molecules, which are then secreted unless they are recognized and de-acetylated by Say1 (Tiwari et al., 2009). The topology of ER-localized Say1 showed that the enzyme has a single transmembrane domain (Tiwari et al., 2009). Such a topology should not exist at the LD monolayer because it would put a hydrophilic protein domain in the hydrophobic core of the LD. This suggests that LD-localized Say1 is a component of ER that is tightly associated with LDs, a possibility that is the consistent with the apparent connections of ER and LDs in yeast (Jacquier et al., 2011).

Rer2 and Say1 join a list of lipid metabolic enzymes that localize to LDs. While both Say1 and Rer2 are present and active at the LD and ER, similar to Ayr1 (Athenstaedt et al., 2000), Gpt2 (Athenstaedt et al., 1997), and Slc1 (Athenstaedt et al., 1999), not all proteins are active in all

subcellular populations. For example, Dga1 (Sorger et al., 2002), Erg6 (Zinser et al., 1993), Erg7 (Milla et al., 2002), Erg27 (Mo et al., 2003), and Yju3 (Heier et al., 20010) are predominantly active at the LD which may reflect that these proteins have a higher LD:ER localization ratios. In contrast, Erg1 is strongly present in both the ER and LD but only active at the LD (Leber et al., 1998). The significance of some enzymes differing in activity in the ER versus LDs is unclear.

ORF	Gene	Function	Proteomes Present	Microscopically Localized to LD	Biochemically Localized to LD
YIL124W	AYR1	Acyl-DHAP reductase, catalyzes lyso-PA formation	A,B,G	Natter et al., 2005	Athenstaedt et al., 2000
YDR196C	**CAB5**	**Dephospho-CoA kinase involved in coenzyme A synthesis**		**Current Work**	
YOR245C	DGA1	Diacylglycerol acyltransferase, catalyzes DAG to TAG	G	Natter et al., 2005	Athenstaedt et al., 1997
YHL030W	ECM29	Proteasome assembly			
YBR177C	EHT1	Acyl-CoA:ethanol acyltransferase	A,B,G	Natter et al., 2005	
YGR175C	ERG1	Squalene epoxidase, enzyme in ergosterol synthesis	A,B,G	Leber et al., 1998	Leber et al., 1998
YLR100W	ERG27	3-keto sterol reductase, enzyme in ergosterol synthesis	B,G	Leber et al., 1998	Mo et al., 2003
YML008C	ERG6	24-C-sterol methyltransferase, enzyme in ergosterol synthesis	A,B,G	Leber et al., 1998	Zinser et al., 1993
YHR072W	ERG7	Lanosterol synthase, enzyme in ergosterol synthesis	A,B,G	Milla et al., 2002	Milla et al., 2002
YOR317W	FAA1	Fatty acyl-CoA synthetase, activates imported fatty acids	A,B,G	Current Work	
YMR246W	FAA4	Fatty acyl-CoA synthetase, activates imported fatty acids	A,B,G	Natter et al., 2005	
YBR041W	FAT1	Fatty acyl-CoA synthetase, activates imported fatty acids	A,B,G	Natter et al., 2005	
YIR038C	GTT1	Glutathione transferase	B,G		Grillitsch et al., 2011
YMR110C	HFD1	Fatty aldehyde dehydrogenase	B,G	Current work	
YBR204C	LDH1	Serine hydrolase, weak TG lipase activity	G	Thoms et al., 2011	Thoms et al., 2011
YML059C	NTE1	Phospholipase B			
YDL193W	NUS1	Putative prenyltransferase involved in dolichol synthesis	A,G	Prein et al., 2000	
YKR046C	PET10	Unknown	A,B,G	Wang et al., 2014	

YPL206C	PGC1	Phosphatidyl glycerol phospholipase C, catalyzes PG to DAG	G	Beilharz et al., 2003	Simockova et al., 2008
YGR233C	PHO81	Cyclin-dependent kinase inhibitor			
YBR002C	**RER2**	**Prenyltransferase involved in dolichol synthesis**		**Current work**	**Current work**
YGR263C	**SAY1**	**Sterol deacetylase**		**Current work**	**Current work**
YDL052C	SLC1	Acyltransferase, catalyzes lyso-PA to PA	A,B,G	Natter et al., 2005	Rimokh et al., 1993
YPR140W	TAZ1	Lyso-PC acyltranferase, catalyzes lyso-PC to PC			
YKL140W	TGL1	Lipase, catalyzes SE to sterol	A,B,G	Köffel et al., 2005	Jandrositz et al., 2005
YMR313C	TGL3	Lipase, catalyzes TAG to DAG, DAG to MAG, and LPA to PA	A,B,G	Athenstaedt et al., 20013	Athenstaedt et al., 20013
YKR089C	TGL4	Lipase, catalyzes TAG to DAG, LPA to PA, and SE to sterol	G	Athenstaedt and Daum, 2005	
YOR081C	TGL5	Lipase, catalyzes TAG to DAG and LPA to PA	G	Athenstaedt and Daum, 2005	Athenstaedt and Daum, 2005
YBR265W	**TSC10**	**3-ketosphinganine reductase, involved in sphingosine synthesis**	**G**	**Current work**	
YML013W	UBX2	Involved in ER-associated protein degradation, regulates LD homeostasis.	G	Wang et al., 2012	Grillitsch et al., 2011
YMR152W	YIM1	Unknown	A,G	Natter et al., 2005	
YKL094W	YJU3	Monoacylglyceride lipase, catalyzes MAG to glycerol	A,G	Natter et al., 2005	Sorger et al., 2002
YKL047W		**Unknown, putative lipase**		**Current work**	
YOR059C		Unknown, putative lipase.	A	Natter et al., 2005	
YPR147C		**Unknown**		**Current work**	

Table 1. Identification of 35 proteins that specifically purify with the lipid droplet.
Identified proteins were found as described in the results and are annotated are annotated for ORF, gene name, presence in other proteomes, and previous localization to the LD by microscopy or biochemistry. Proteomes are abbreviated as A = Athenstaedt et al., 1999, B =

Binns et al., 2006, and G = Grillitsch et al., 2011. Proteins are considered newly identified if they were not previously manually localized or identified in more than one proteome and are bolded in the table.

Chapter 3:
Insights into Lipid Droplet Biology

In the previous chapter (chapter 2), I highlighted my published primary research. During the course of my graduate research, I started several projects that were not continued to publication because of unexpected technical and biological hurdles. I have highlighted that research here in chapter 4 with the hope that the vignettes will be helpful to others that may wish to follow up the work in the future.

Squalene in Yeast

When I started this project, it was clear that there are connections between lipid metabolism (and hence the LD) and protein degradation although the nature of these connections was unclear. Some observations from the literature that suggested a connection between protein degradation and the LD include the fact that knockdowns of the proteasome affect lipid droplet morphology in *Drosophila* S2 cells (Guo et al., 2008), that protein degradation deficient *Saccharomyces cerevisiae* mutants were sensitive to growth on oleate (Lockshon et al., 2007) and that proteasome subunits and ubiquitinated proteins had been found the LD fraction of biochemically fractionated Huh7 cells (Ohsaki et al., 2006).

To begin to explore this connection, I performed a small screen of genes involved in protein degradation for sensitivity to growth on oleate. I used strains taken from the combined deletion/DAmP library (Giaever et al., 2002 and Breslow et al., 2008) and serially diluted strains of interested on YPD rich media with 1mM oleate. Although I saw dramatically impaired growth of positive control strains, I observed no growth phenotype for many deletions/DAmPs involved in the 26S proteasome, autophagy, and ERAD (Table 4.1).

26S proteasome	
19S proteasome base	rpt2, rpt3, rpt4, rpt6, rpn2
19S proteasome lid	rpn8, rpn5, rpn6, rpn7, rpn11
20S proteasome	pre3, pre5, pre6, pre7, pre8, pup1, scl1
20S proteasome assembly	add66
Autophagy	
Vacuole	atg19, pep1
PI3K complex	atg14, vps30 vps38
ERAD	
Retrotranslocation	cdc48, npl4, ubx2
Ub-receptor proteins	rad23, dsk2
ERAD-C	hlj1, ydj1
ERAD-L	cue1, der1, hrd1, hrd3, jem1, kar2, mnl1, scj1, ubc1, usa1, ubc7, yos9
Other ERAD	dfm1, hul5, ssm4
ER chaperone	cne1, eps1
Glycosylation	pbn1, mns1

Table 4.1: Genes assayed for sensitivity to growth on rich media with 1mM oleate. Genes are grouped into functional classes.

After failing to identify specific genes involved in protein degradation that affected growth on oleate supplemented rich media, we turned to a more direct approach to assay for a gene's connection to lipid metabolism. We purified lipids from a subset of the strains that were used to assay growth and looked for gross lipid metabolic defects using thin layer chromatography (TLC). We were especially interested in the amount of SE and TG, as the major lipid components of LDs, free fatty acids and ergosterol, as the major lipid building blocks of SE and TG, and any accumulation of unidentified lipids, likely representing significantly perturbed lipid metabolism.

We found that the majority of strains had no gross alterations to whole cell neutral lipids as observed by TLC using hexane:diethyl ether:acetic acid (80:20:1) as a solvent. We observed no gross effects for deletion/DAmP strains of pre1, pre2, pre3, pre4, pre5, pre7, pre9, rpn2, rpn4,

rpn5, rpn7, rpn10, rpn11, rpn12, rpn13, rpt1, rpt2, rpt4, rpt6, or sem1. However, we did observe accumulation of unidentified lipids in rpt5-DAmP, pre6-DAmP, and rpn3-DAmP (Fig. 4.1).

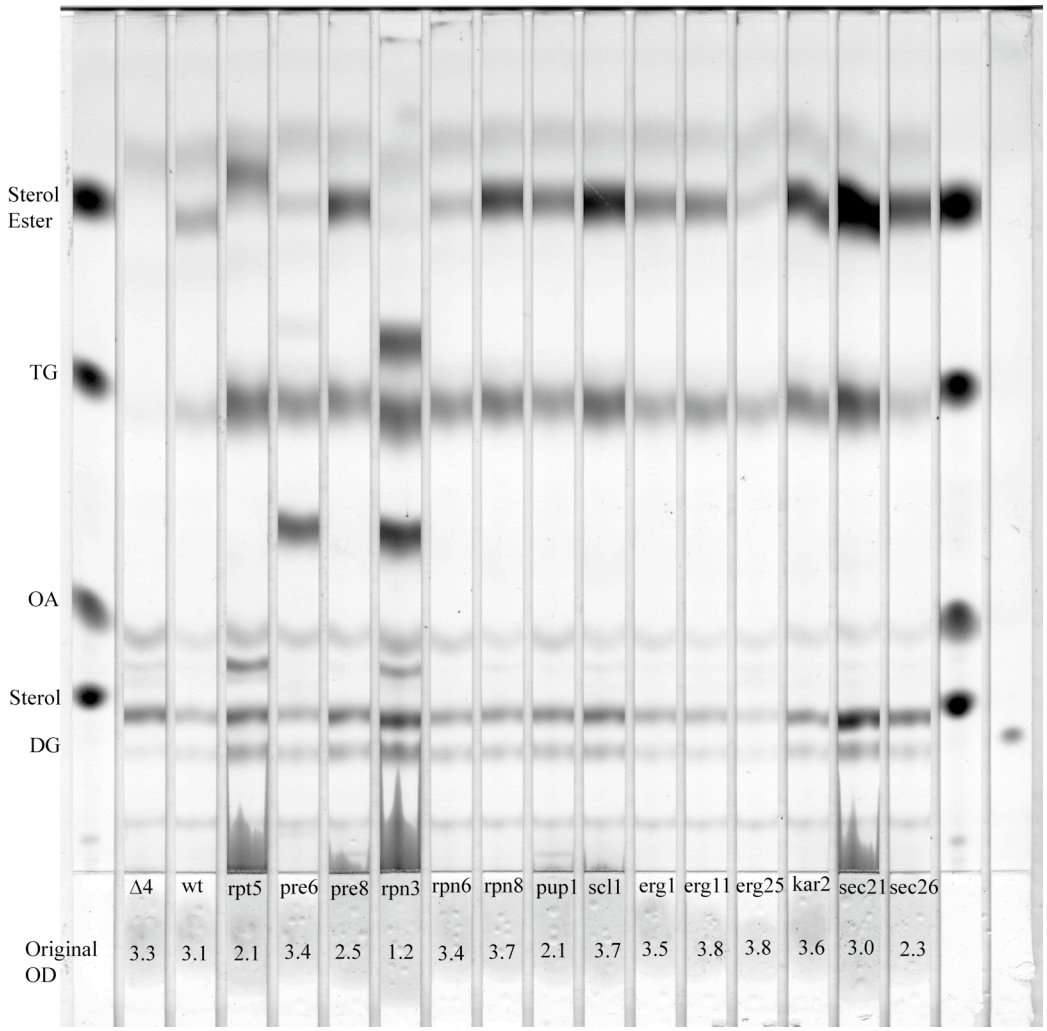

Figure 4.1. Thin layer chromatography for neutral lipids of a subset of deletion/DAmP strains involved in protein degradation. Whole cell extracts separated in hexane:diethyl ether:acetic acid (80:20:1). The first and last 2 lanes are standards, labeled to the left of the plate.

We opted to further explore the unknown accumulated lipid in the rpt5-DAmP strain. Because it migrated farther than TG in a solvent that separates neutral lipids, we knew that it was a particularly hydrophobic molecule. We tested the hypothesis that the lipid is squalene, an early intermediate in sterol synthesis, by comparing rpt5-DAmP lipid profile to cells treated with

terbinafine, an inhibitor of the squalene epoxidase enzyme (Erg1) that causes accumulation of squalene and a squalene standard. We found that rpt5-DAmP behaved similarly to terbinafine treated cells and the unidentified band comigrated with a squalene standard in four separate solvent systems (hexane:diethyl ether:acetic acid (80:20:1), hexane, chloroform, and heptane:benzene (90:10)) (Fig. 4.2), supporting our hypothesis that the rpt5-DAmP strain accumulates squalene. We also found that the rpt5-DAmP strain was sensitive to terbinafine at 5ug/mL, additionally supporting our hypothesis.

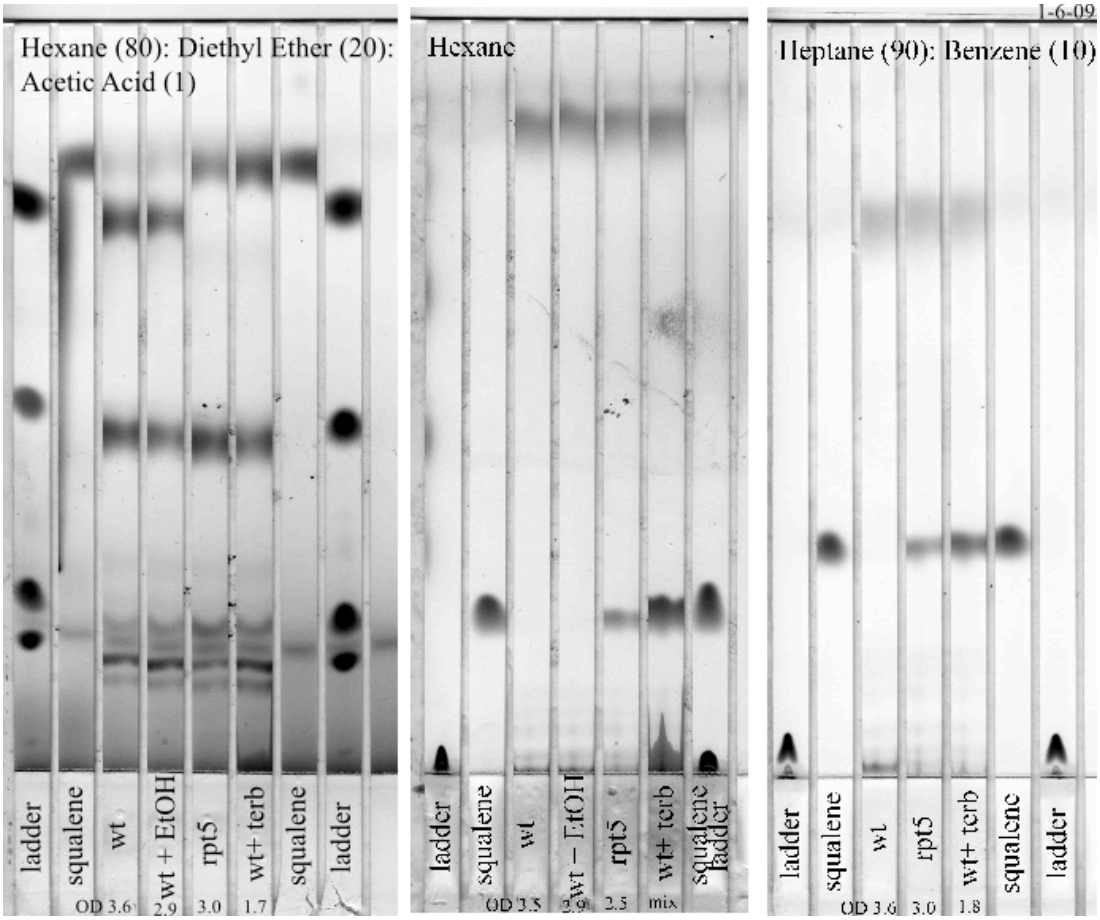

Figure 4.2. Identification of an unidentified lipid in rpt5-DAmP strain as squalene by comparison to squalene standard and terbinafine treated cells by TLC. Shown are neutral lipids separate by hexane:diethyl ether:acetic acid (80:20:10), hexane, and heptane:benzene (90:10).

Before further probing the potential connection between Rpt5 and squalene metabolism, we wanted to confirm that the DAmP cassette at the Rpt5 locus was responsible for the observed

phenotype. Using classical yeast genetics, we dissected rpt5-DAmP/+ tetrads and found that the accumulation of squalene doesn't segregate with KanR cassette from the rpt5-DAmP. Additionally, the lipid phenotypes we observed in the pre6-DAmP and rpn3-DAmP also fail to segregate with the DAmP cassette. We observed that the Rpt5-DAmP/WT diploids had a wild type lipid profile so the squalene accumulation-causing mutation is recessive.

We chose not to further explore the accumulation of squalene as the most likely explanation for the accumulation was an impairment in Erg1 function and our lab was not interested in exploring the function or regulation of this specific enzyme. If there is interest in exploring this mutation or the other non-DAmP-segregating lipid-phenotype-causing mutations in the future, many not-fully-characterized strains were frozen for future work and are summarized in Table 4.2.

Strains	**Diploids**
FYS187	rpt5-DAmP/Rpt5 a/A
FYS188	rpt3-DAmP/Rpt3 b/B
FYS189	pre6-DAmP/Pre6 c/C
FYS190	rpn3-DAmP/Rpn3 d/D
	Haploids
FYS200, FYS202	rpt3-DAmP (B allele unknown)
FYS199, FYS201	Rpt3 (B allele unknown)
FYS203, FYS206	pre6-DAmP C
FYS204, FYS205	Pre6 c
FYS207, FYS208	rpn3-DAmP D
FYS209, FYS210	Rpn3 d
FYS191, FYS192, FYS195	Rpt5 a
FYS193, FYS194, FYS196	rpt5-DAmP A
FYS197	Rpt5 A
FYS198	rpt5-DAmP a

Table 4.2. Summary of uncloned lipid phenotype strains frozen in the Farese yeast strain database. a, b, c, and d represent uncloned lipid-phenotype causing alleles that do not segregate with the DAmP cassettes. Two tetrads derived from FYS187 were saved as FYS191-FYS194 and FYS195-FYS198. A single tetrad derived from FYS188 was saved as FYS199-FYS202. A single tetrad derived from FYS189 was saved as FYS203-FYS206. A single tetrad derived from FYS190 was saved as FYS207-FYS210.

Protein Targeting to the Yeast Lipid Droplet

Little is known about how proteins traffic to the LD in yeast or higher organisms. Compounding a lack of knowledge about LD protein trafficking is the fact that LD biogenesis is also poorly understood. All major models for LD biogenesis involve budding of the LD from the ER (Brasaemle and Wollins, 2012), although it is clear that proteins can target to the LD either at the moment of LD formation or later (e.g. Erg6 and Dga1, respectively, in yeast (Jacquier et al., 2011)). Additionally, some proteins can target subsets of LDs while others appear to target all LDs within a cell.

Three previous visual screens have been done to identify genes that affect LD morphology. One used Nile Red to mark LDs and screened the deletion collection, identifying 133 with an altered LD number, 17 of whom have a loss of LDs (Fei et al., 2008a). Another used the deletion collection to identify 56 strains that are sensitive to nystatin, 17 of which show a loss of LDs (Fei et al., 2008b). Although both papers contain many of the same authors, they found no overlap between their loss of LDs list. Another group used BODIPY to screen the deletion collection and identified 59 with abnormal morphology, 3 of whom were identified by Fei et al. in their first screen (Nem1, Spo7, and Ssd1) and 1 in their second screen (Srv2) (Szymanski et al., 2007).

To identify machinery involved in the targeting of proteins to LDs and/or LD formation, we conducted a genome wide screen for genes whose deletions or knockdown impair targeting of two model LD proteins, Faa4-GFP and Erg6-GFP, to the LD. Faa4 and Erg6 are two of the first identified and major yeast LD proteins (Athendstaedt et al., 1999). Faa4 activates exogenous long chain (C12-C16) fatty acids (Knoll et al., 1995) and plays a role in FA import (Zou et al.,

2003). Erg6 has become the canonical yeast LD protein marker. It is a C4-methyltransferase involved in sterol biosynthesis (Gaber et al., 1999).

We constructed strains that carry genomically tagged Sec61-mCherry (an ER marker) and either Faa4-GFP or Erg6-GFP in the SGA alpha background (FYS255 = SGA alpha Erg6-GFP::Hph Sec61-mCherry::URA. FYS258 = SGA alpha Faa4-GFP::Hph Sec61-mCherry::URA). With the assistance of Florian Frohlich in the laboratory of Tobias Walther (Yale, then at Max Planck in Munich), we used synthetic genetic array (SGA) methodology (Tong et al., 2001, Tong et al., 2006, and Cohen and Schuldiner, 2011) to mate the strains to two different libraries – the yeast deletion collection (Gieaver et al., 2002), ~5000 strains, each with a single deletion in a nonessential gene, and the decreased abundance by mRNA perturbation (DAmP) collection (Schuldiner et al., 2005 and Breslow et al, 2008) ~1000 strains, each with a hypomorph of an essential gene. We selected for haploid MAT A cells with the deletion/DAmP::Kan Erg6/Faa4-GFP::Hph Sec61-mCherry::URA. Two of our plates were duplicated, allowing for multiple identifications of the same gene for a small fraction of our strains.

The constructed strains were sent to the lab of Maya Schuldiner (Weizmann Institute) and were imaged in triplicate by Yael Elbaez. The strains were grown overnight in a 384-well plate. In the morning, they were diluted 1:20 and grown for 3 hrs, transferred to a microscope plate, and visualized. The experiment was calibrated so that the cells would be “mid log” phase, however it takes 2.5-3 hours to image the entire plate so there may be differences in growth phase from the beginning to the end of the plate. Additionally, individual strain fitness could influence the imaged growth phase because of differences in growth rate or exit from stationary phase.

Plate	Plate Coordinate	ORF	Gene	SGD annotated localization
strong loss of GFP punctae				
3	C1	YPL206C	PGC1	LD, M
10	H19	YCR028C	FEN2	PM
17	K11	YNR016C	ACC1	ER, M
18	B5	YDR160W	SSY1	PM
18	E15	YIR010W	DSN1	N
18	M9	YOR232W	MGE1	M
20	B12	YJL125C	GCD14	N
20	B16	YJL195C		
20	D16	YKL189W	HYM1	bud
20	N9	YGR190C		
moderate loss/increased background				
2	H7	YOR328W	PDR10	PM
3	E5	YPL191C		C
4	H22	YCL050C	APA1	C, N
5	N12	YOR245C	DGA1	LD
5	P6	YOR258W	HNT3	C, N
11	P13	YNL107W	YAF9	C, N
18	D17	YDR240C	SNU56	N
18	G14	YBR234C	ARC40	C
18	J3	YDR499W	LCD1	N
18	L14	YJL061W	NUP82	N
20	M14	YMR197C	VTI1	G
distributed punctae/increase background				
1	B17	YML089C		
1	B21	YML087C	AIM33	
1	D7	YML081W	TDA9	N
1	D11	YML079W		C, N
1	D13	YML078W	CPR3	M
1	D19	YML061C	PIF1	M, N
1	P12	YMR245W		
2	J10	YOL081W	IRA2	C, M
4	M13	YGR132C	PHB1	M
4	P19	YHR183W	GND1	C, M
5	B8	YOR141C	ARP8	N
5	C18	YKL085W	MDH1	M
6	L11	YDR207C	UME6	N
6	M14	YLR269C		
6	E23	YJL179W	PFD1	C
8	E8	YDR293C	SSD1	C
8	K3	YKR042W	UTH1	M
8	K6	YIL011W	TIR3	wall
8	L6	YMR075C-A		
8	P6	YNR075W	COS10	C, ER
9	F22	YHR041C	SRB2	N
9	L1	YJL115W	ASF1	N
10	I23	YAL012W	CYS3	C
10	K5	YAL056C-A		
10	P7	YJR011C		
10	P21	YJR024C	MDE1	C
11	B15	YIL121W	QDR2	PM
11	D16	YGR063C	SPT4	N
11	F11	YIL155C	GUT2	M
11	F20	YJL136C	RPS21B	C
11	J5	YIR009W	MSL1	N
11	P21	YNL121C	TOM70	M
12	H17	YDL021W	GPM2	C
14	A7	YGL133W	ITC1	N
15	O18	YKL096C-B		
16	C3	YDL077C	VAM6	V
17	K15	YNR043W	MVD1	C
18	K11	YNR016C	ACC1	M, ER
18	N4	YJL097W	PHS1	ER, V
18	N13	YFR005C	SAD1	N
18	N14	YJR007W	SUI2	C
18	O10	YDR045C	RPC11	N
18	P11	YGL048C	RPT6	N
19	B13	YKL122C	SRP21	N
19	D6	YMR235C	RNA1	C, N
19	M3	YLR397C	AFG2	C
19	O17	YMR047C	NUP116	NP
19	P17	YMR047C	NUP116	NP
20	E13	YPL063W	TIM50	M
20	O9	YOR256C	TRE2	
increased background				
1	M21	YLL019C	KNS1	
4	K1	YER074W	RPS24A	C, M
10	K17	YCL058C	FYV5	
16	I22	YCR063W	BUD31	N
large GFP punctae				
2	F10	YOL052C	SPE2	C, N
2	I16	YOR039W	CKB2	
6	E24	YLR404W	FLD1	ER
7	P9	YGL019W	CKB1	
9	O21	YMR313C	TGL3	LD
14	G10	YDR477W	SNF1	M,N,V,C
16	H10	YDR477W	SNF1	M,N,V,C
17	B11	YDR168W	CDC37	C
20	P17	YIR015W	RPR2	
small cells with no GFP punctae				
4	H15	YHR108W	GGA2	G
4	H17	YHR109W	CTM1	C
4	N17	YHR157W	REC104	N
5	C13	YLR179C		C, N
5	K2	YKL136W		
5	M17	YKL041W	VPS24	C
8	H7	YFL023W	BUD27	C
10	A17	YLR431C	ATG23	
12	C18	YFL019C		
12	D20	YDR456W	NHX1	end
12	H10	YDR484W	VPS52	G
12	H14	YDR486C	VPS60	C
12	H15	YDL020C	RPN4	N
12	I7	YMR135W-A		
12	I9	YMR137C	PSO2	N
12	I16	YOL147C	PEX11	ER, P
12	J15	YDL035C	GPR1	PM
14	A10	YER179W	DMC1	N
17	C6	YBL076C	ILS1	C
17	F2	YGR264C	MES1	C
17	I7	YMR005W	TAF4	N
18	A7	YDL132W	CDC53	
18	K15	YNR043W	MVD1	C
heterogenous				
7	I14	YFR035C		
8	B15	YIL090W	ICE2	ER
9	J3	YJL127C	SPT10	N
10	H7	YCR020W-B	HTL1	N
11	F24	YJL139C	YUR1	G
12	A9	YCR030C	SYP1	bud
14	O5	YER161C	SPT2	N
17	E15	YIR010W	DSN1	N
18	A4	YAL043C	PTA1	
18	H4	YHR197W	RIX1	N
19	H3	YLR033W	RSC58	
19	O13	YMR013C	SEC59	ER
19	P13	YMR013C	SEC59	ER
20	P21	YJL015C		

Table 4.3. Strains identified as having non-wild type distribution of Faa4-GFP. Duplicates represent strains that were duplicated in the screened collection and identified phenotypically both times. All hits were roughly grouped into phenotypic classes. SGD annotated localization are reported localizations for the annotated proteins as documented at yeastgenome.org as of the time of screening. C=cytoplasm, ER=endoplasmic reticulum, G=Golgi, LD=lipid droplet, M=membrane, N=nucleus, PM=plasma membrane, and V=vacuole.

We manually viewed 3 images/well of Faa4-GFP, annotating any strain that had a non-wild type appearance. We identified 121 clones (171 unique genes) that had altered Faa4-GFP morphology and roughly clustered these into 7 phenotypic classes (Table 4.3) – strong loss of GFP punctae (n=10), moderate loss/increased background (n=11), distributed punctae/increased background (n=50), increased background (n=4), large LDs (n=9), small cells with no GFP punctae (n=23), and heterogenous (n=14).

We combined the 20 of these hits that had a strong or moderate loss of Faa4-GFP punctae (discarding YJL195C as being a dubious ORF) for further phenotypic examination. Only one of these 20 had been found in previous visual screen for reduced LDs (Dga1 in Fei, et al. 2008a). We also included several genes from other phenotypic classes, selected as being of interest because they had functions in lipid metabolism or ER function (Acc1, Ice2, Mvd1, Nup116, Sec59, Srp21). We pulled these strains from the deletion/DAmP collections and visually screened live cells for LD phenotypes using BODIPY. We identified 5 with a strong loss of LDs (acc1-DAmP, Δfen2, hym1-DAmP, nup82-DAmP, ssy1-DAmP) (Figure 4.3).

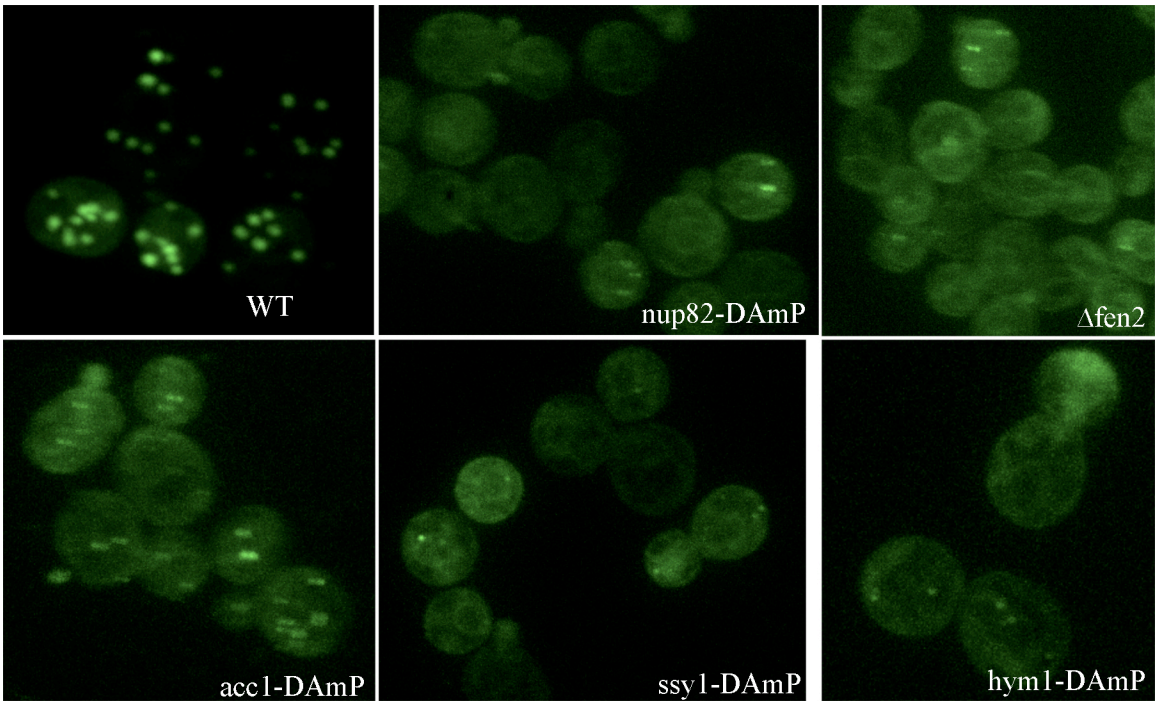

Figure 4.3. Positive hits from secondary screen of 20 hits from the genome wide screen to identify genes that affect Faa4-GFP targeting to the LD. Z-projections of spinning disk confocal images of live yeast labeled with vital dye BODIPY.

The five genes with the strongest phenotypes in our secondary screen represent a variety of functions. Fen2 is a plasma membrane proton-pantothenate symporter (Stolz and Sauer, 1999). Pantothenic acid (Vitamin B5) eventually is metabolized to CoA, an essential component of many aspects of lipid synthesis. Acc1 catalyzes the carboxylation of acetyl-CoA to malonyl-CoA (Mishinia et al., 1980) which is required for de novo biosynthesis of long-chain fatty acids. Nup82 is nucleoporin, a subunit of the nuclear pore complex (Grandi et al., 1995). Ssy1 is a component of the SPS plasma membrane amino acid sensor system (Klasson et al., 1999 and Forsberg and Ljungdahl, 2001). Hym1 is a component of the RAM signaling network that is involved in the regulation of Ace2 activity and cellular morphogenesis (Nelson et al., 2003). We added Pgc1 to our list for further examination because it has a lipid function (as a phosphatidyl glycerol phospholipase C)(Simockova et al., 2008) and is localized to the LD (Beilharz, 2003).

We examined the deletions/DAmPs of Fen2, Acc1, Nup82, Ssy1, and Hym1 for phenotypes that may explain their loss of LDs. We found no gross changes to phospholipids, ER morphology, LD-ER association, mitochondrial morphology, or LD-mitochondrial association. When examining neutral lipids by thin layer chromatography, we did observe a specific loss of SE in all 5 strains. This was unexpected as altered LD numbers are usually attributable to equal modulation of TG and SE or to alterations to TG alone. TG, free fatty acid, and ergosterol levels were similar between strains.

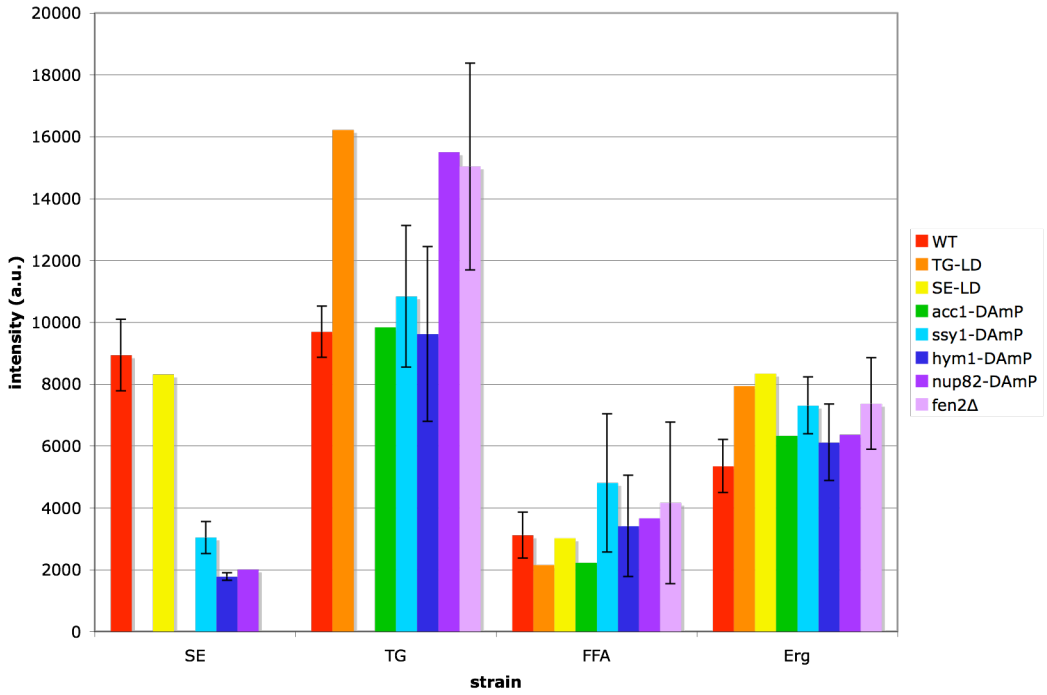

Figure 4.4. Neutral lipid content of strains identified by visual screening to have a loss of LDs. Measurements were made from quantifying intensity of TLC bands. Error bars are standard deviation, shown only on conditions where n>3.

Before continuing in our studies, we wanted to verify that the observed phenotypes were due to the known genotypes and not from background mutations or mislabeled strains caused by maintenance in 384-well format. Additionally, we wanted to know if the phenotypes were strain specific. We remade acc1-DAmP [frozen as FYS550 and FYS551], fen2Δ [FYS557 and

FYS558], Δhym1 [FYS552 and FYS553], nup82-DAmP [FYS555 and FYS556], Δpgc1 [FYS554] in the W303 background and none had a LD phenotype by BODIPY. We next remade acc1-DAmP [FYS566 and FYS567], fen2Δ [FYS559 and FYS565], nup82-DAmP [FYS563 and FYS564], Δpgc1 [FYS561 and FYS562] in the original BY4741 (S288C) background. acc1-DAmP, nup82-DAmP, and Δpgc1 did not have a LD phenotype by BODIPY. Δfen2 appeared to have a defect in uptake of BODIPY as it did not label any internal structures, but we did not follow up on this phenotype.

We additionally tried to use genetic means to confirm the genetic cause of the phenotypes in the original strains used in the screen. We mated acc1-DAmP to a wild type strain, sporulated, and found that the Kan selection cassette (used to create acc1-DAmP allele) did not segregate with the loss of LD phenotype. We transformed Hym1-DAmP with MOBY-ORF (**Mo**lecular **B**arcoded **Y**east **ORF** database) plasmid of ~900bp upstream through ~250bp downstream of YKL189C (Hym1) on plasmid backbone p5472 and found that it did not rescue the loss of LD phenotype.

Because we were not able to verify a single hit from our screen, we opted to not continue work on this project. Yuan Xue in the Walther lab has manually examined all of the images generated in the screen and was not able to craft a research project out of her results, having similar problems verifying phenotypes. All of the images are available on the Farese lab server in the event that there is further interest in the original data.

Erg Protein Targeting to the Yeast Lipid Droplet

Because an unbiased approach failed to identify machinery necessary for protein targeting to the LD (see previous section), we decided to approach this question with a targeted approach. An observation was reported that Erg27-GFP doesn't traffic to the LD in a strain lacking TG (dga1Δlro1Δ) but its trafficking is not affected in a strain lacking SE (are1Δare2Δ) (Garbarino et al., 2009). Since I worked on this project, the same observation was made for Erg6-GFP (Jacquier et al., 2011). The authors proposed that the lipid content of the LD affected targeting of Erg7. We wanted to investigate that hypothesis.

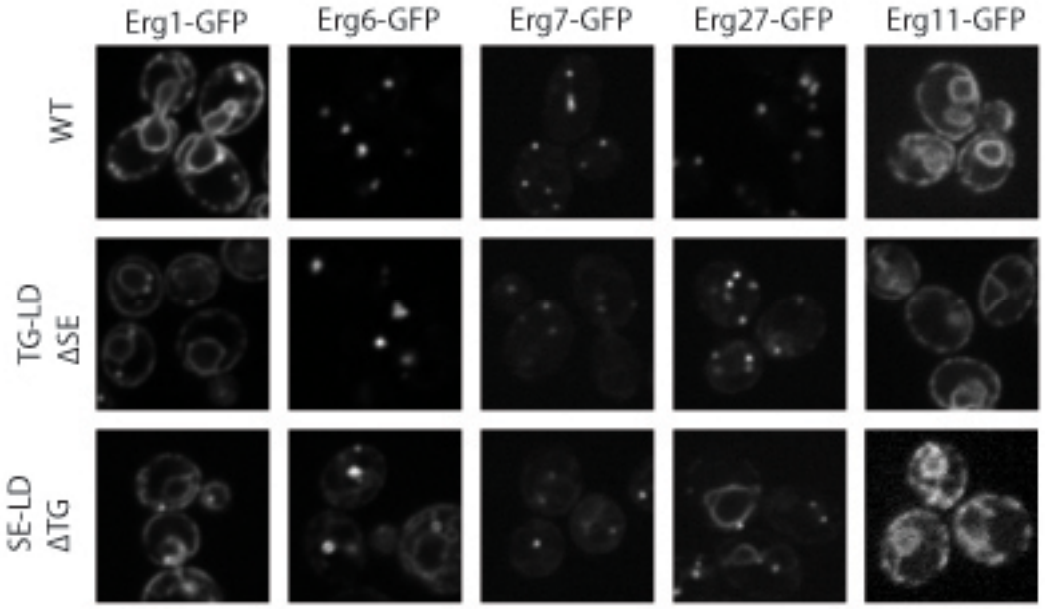

Figure 4.5. Erg protein localization in TG and SE deficient strains. Erg genes were tagged at the genomic locus and visualized by spinning disk microscopy. Single Z slices are shown.

We first asked if we could replicate the Erg27 findings and if they extended to other LD Erg proteins. We made TG deficient (dga1Δlro1Δ) and SE deficient (are1Δare2Δ) strains and tagged Erg1, Erg6, Erg7, and Erg27 in both deficiency strains and in a wild type background. We additionally tagged Erg11 as a negative control as it is an ER localized protein. We were able to

replicate the published findings that Erg7 (and Erg6) had more ER localization in a TG deficient strain and were able to extend the finding to Erg27 (Fig. 4.5). Unsurprisingly, Erg11 localization did not appear to be affected, and, potentially interestingly, Erg1 localization also was not affected.

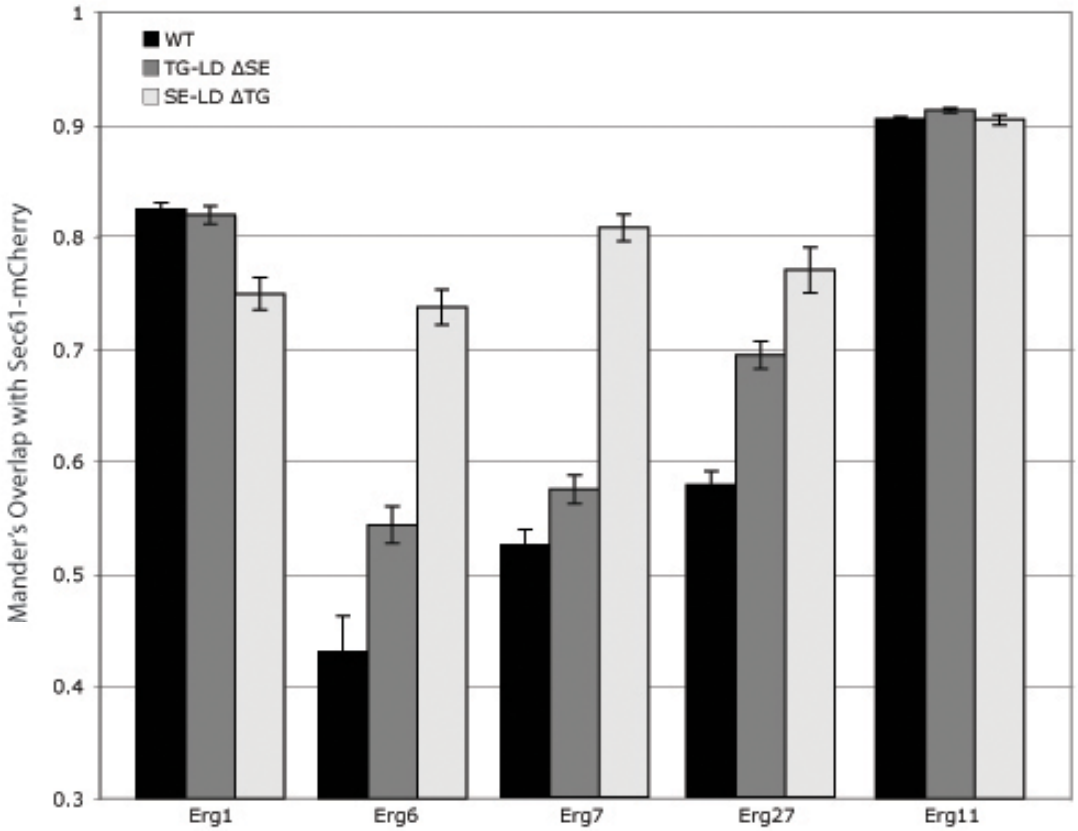

Figure 4.6. Quantification of GFP localization to the ER by overlap between Erg-GFP and Sec61-mCherry as calculated by Mander's Overlap coefficient.

We quantified our GFP imaging results by calculating a Mander's coefficient of overlap between green (GFP) and red (mCherry) channels after expressing Sec61-mCherry on a CEN/ARS plasmid in all strains. The quantified results were consistent without our visual observation of the differences in localization between wild type and TG deficient backgrounds (Fig. 4.6). Interestingly, we also observed a slight increase in GFP localization to the ER for Erg6, Erg7,

and Erg27 in the SE deficient background as well. Erg1 and Erg11 did not change localization between conditions, consistent with visual observations.

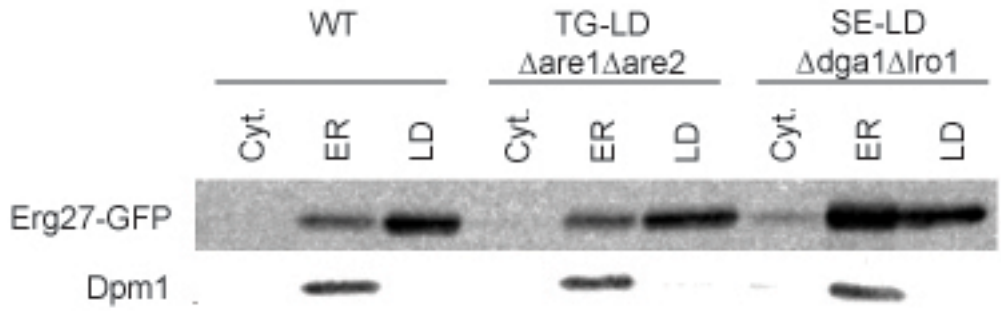

Figure 4.7. Localization of Erg27-GFP to the ER by western blot. Cells were crudely fractionated as described in Currie et al., 2014.

We were additionally able to verify our results by western blot. We crudely fractionated cells expressing Erg27-GFP at the genomic locus with a 100k x g spin, collecting membrane pellet, and slicing the cytoplasm into upper (containing floating LDs) and lower (cytoplasm only) fractions. We observed that Erg27-GFP had a higher ratio of ER to LD localization in dga1Δlro1Δ cells than wild type or are1Δare2Δ (Fig. 4.7).

GFP/Background	WT BY4742	FYS252 are1Δ are2Δ	FYS242 dga1Δ lro1Δ	Size (with GFP)
Erg1	268	266	594	82 kD
Erg6	585	595	593	70 kD
Erg7	570	267	572	110 kD
Erg27	571	275	459	67 kD
Erg11	675	596	703	89 kD
Tgl3	589		801	104 kD

Table 4.4 FYS numbers of strains generated for analysis of Erg protein localization.

All strains generated for analysis of Erg localization were frozen in the Farese yeast library. Strain numbers are given in table 4.4. Tgl3-GFP strains were made for use as a non-Erg LD protein control but were never analyzed.

There are many differences between dga1Δlro1Δ and are1Δare2Δ strains that could be responsible for the differences in Erg protein localization to the LD. We first hypothesized that differences in lipid content of the LD affect Erg targeting. To explore this hypothesis, we collaborated with Christer Ejsing, to analyze the lipidome of the wild type, TG deficient, and SE deficient strains (e860). As expected, TG-LD strains completely lacked SE. In accordance with published literature, we were able to detect some TG in SE-LD strains, because Are1 and Are2 are able to esterify DG to TG in small amounts (Sandager et al. 2002). We found altered TG species, as well as changes in amounts and species of PC, PE, and PI in dga1Δlro1Δ cells. Very few alterations were observed in are1Δare2Δ cells. Additional changes are summarized in Fig. 4.8 and Fig. 4.9.

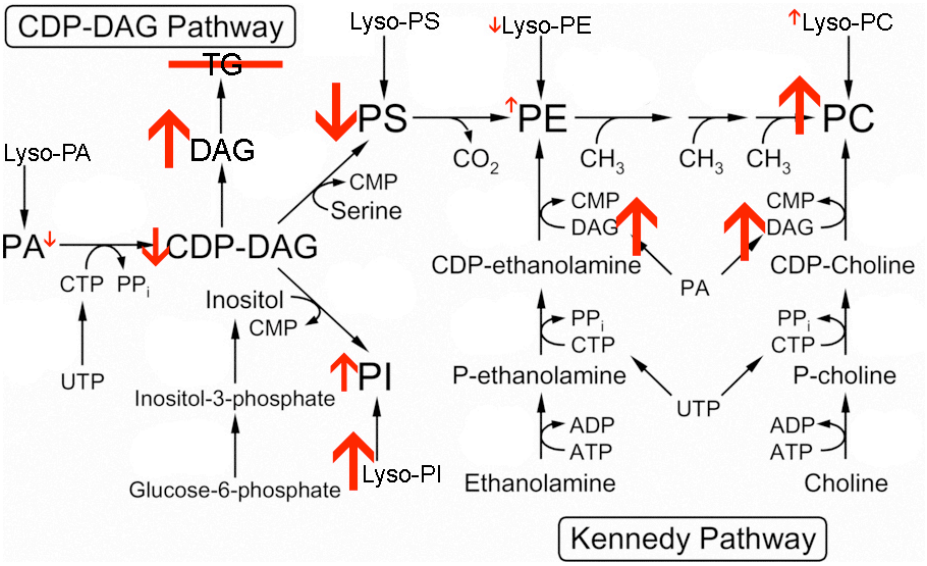

Figure 4.8. Summary of changes in the lipidome of Δdga1Δlro1 (SE-LD) strains. Figure adapted from Choi et al., 2004.

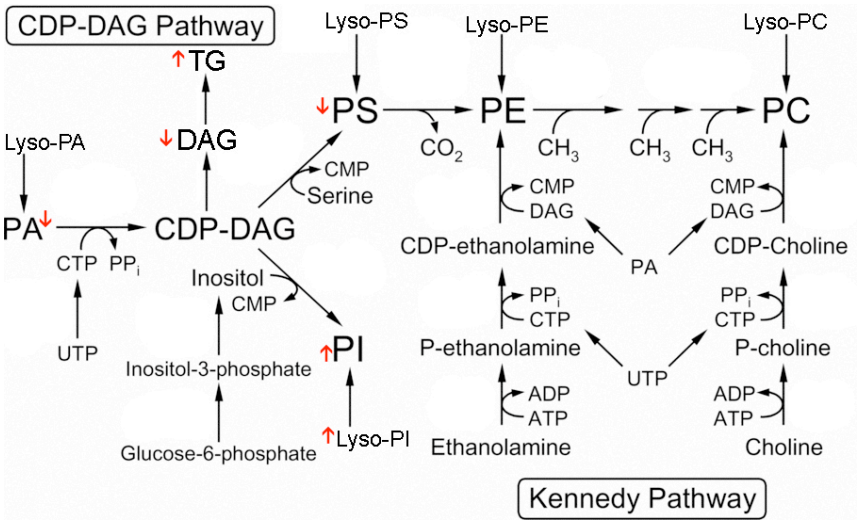

Figure 4.9. Summary of changes in the lipidome of Δare1Δare2 (TG-LD) strains. Figure adapted from Choi et al., 2004.

To better understand whether the whole cell lipid alterations affect LD lipids, we isolated lipid droplets and analyzed the lipidome of the lipid droplets, again in collaboration with Christer Ejsing (e909). The data generated is calculated as the mol percent of monitored species. Because the strains are missing major classes of lipids (TG or SE), it is hard to get an overview of changes to lipid classes using the dataset generated. In order to generate a more interpretable dataset, the experiment needs to be run with an absolute which could come from repeating the data using protein measurements or spiked lipid standards. We did observe some minor alterations that could merit further investigation with a more interpretable dataset. There were minor changes in PE in are1Δare2Δ and differences in SE species in dga1Δlro1Δ. TG species were quite similar between the three strains (although the mass of TG greatly reduced in dga1Δlro1Δ), however there are 2 species each with roughly 2% intensity of TG species that are detectable in dga1Δlro1Δ and not the other strains – TAG 48:1 mg/z 822.7524 and TAG 50:1 m/z 850.7837. These likely reflect differences in substrate specificities for TG synthesis between the major TG synthetic enzymes (dga1 and lro1) and are1 and are2.

Because our lipidomic data did not show differences large enough to generate testable hypotheses about lipid derived differences affecting LD protein targeting, we considered other differences between dga1Δlro1Δ and are1Δare2Δ. A major difference that we noticed by microscopy is that dga1Δlro1Δ cells have fewer LDs than are1Δare2Δ. We quantified the average LD number/cell by visualizing LDs with BODIPY and manually counting LDs, and found that are1Δare2Δ have slightly fewer LDs than WT (WT = 8.0 +/- 3.8, are1Δare2Δ = 7.1 +/- 2.8, dga1Δlro1Δ = 1.9 +/- 1.5). Student's T-test between WT and are1Δare2 = .01 showing that the slight difference is significant. Interestingly, these differences in LD number correlate with the observed differences in Erg localization as quantified by Mander's coefficient, leading us to the hypothesis that LD number controls Erg localization to the LD.

Genotype	Reported phenotype	Observed phenotype
ssd1Δ	fld	sick, full of vacuoles
nem1Δ	fld	fld
ltv1Δ	fld	wt
vp53Δ	mld	wt/fld
est1Δ	mld	mld
gon7Δ	mld	wt

Table 4.5. Genomic deletion of genes reported to have LD phenotypes fails to replicate most published results.

To explore the connection between LD number and Erg localization, we wanted to quantify Erg localization to the LD in strains with increased (mld) and decreased (fld) numbers of LDs. We sought to alter the number of LDs without dramatically altering the lipid composition of the cell and chose to freshly make candidates based on phenotypes reported in Fei et al., 2008a. We found that only 2 of 6 genetic deletions replicated published results (Table 4.5) and so continued our explorations with nem1Δ and est1Δ for our fld and mld strains, respectively.

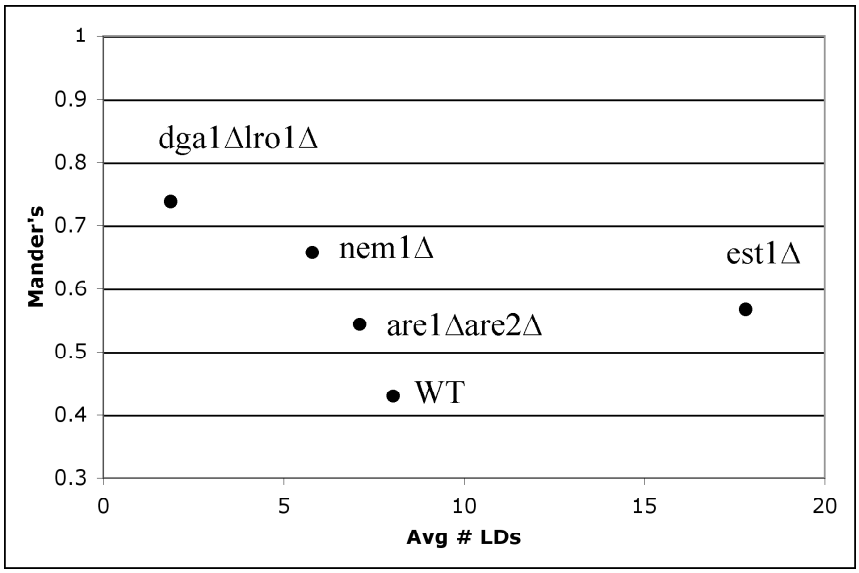

Figure 4.10. Correlation between LD number and LD localization of Erg6-GFP. Mander's correlation coefficient was calculated by overlap between Green (genomic Erg6-GFP) and Red (Sec61-mCherry on a CEN-ARS plasmid) channels. Lipid droplet number was manually counted in non-GFP tagged strains by visualization of LDs with BODIPY.

We quantified the number of LDs and the Mander's coefficient as previously described in nem1Δ and est1Δ. Plotting these and the WT, dga1Δlro1Δ and are1Δare2Δ results, we see an anti-correlation between LD number and ER localization of Erg6-GFP, consistent with our hypothesis (Fig. 4.10). To further explore whether lipid content of the LD affects LD protein targeting, we started testing stress conditions that increase the number of LDs without significantly changing their composition (i.e. are1Δare2Δ cells synthesize more LDs when stressed but are still unable to make SE). We did not further pursue this avenue of research because we did not have a method for simple and sensitive quantification of cellular lipids.

Although there are some Erg enzymes that localize to the ER and some to the LD, LD localization is not necessary for these enzymes as yeast lacking LDs are able to synthesize ergosterol, albeit with a defect due to Erg1 instability (Sorger et al., 2004). We sought to explore the importance of Erg targeting to the LD in a wild type cell by tethering Erg6 to the ER and then

testing efficiency of Erg6 activity and ergosterol synthesis activity. To tether Erg6 to the ER, we sought to follow the work of Ho Yi Mak who showed that a LD protein could be tethered to the ER in *Caenorhabditis elegans* with the addition of a segment of cytochrome b5 and unaffected by the addition of a mutant form of this segment (Xu et al., 2012). Ken Harrison was able to show that this same strategy works in yeast on the protein Nus1 (unpublished). Unfortunately, Erg6 did not have wild type localization when tagged with the mutant cytochrome b5 segment so we could not continue with this strategy.

Chapter 4:
Cellular Fatty Acid Metabolism and Cancer

During the course of graduate school, I became interested in science writing as a career. Accordingly, I jumped on an opportunity that presented itself to write a review. What follows is a review on the connections between cellular lipid metabolism and cancer. While it may seem distant from my primary research interest of proteins at the lipid droplet in yeast, there are in fact many reasons that I thought it was a relevant and appropriate detour. My research on proteins at the lipid droplet in yeast is essentially a focus on cellular lipid metabolism in yeast. Writing a review on cellular lipid metabolism in mammalian cells was an exciting opportunity to build upon my knowledge base and expand it to include other cell systems. Additionally, I believe that as a lipid biochemist, I have a unique perspective on a whole class of molecules (i.e. lipids) that are often poorly understood by other scientists, even those that often think on the cellular level. By surveying the cancer literature for connections to cellular lipid metabolism, I was able to create and explain a framework for other scientists, especially cancer researchers, to think about the problem of cancer in a novel way.

Introduction

Although cancers are hugely diverse in type and etiology, cancer cells frequently share the attribute of metabolic abnormalities. For example, glucose metabolism is commonly altered to decouple glycolysis from pyruvate oxidation (the Warburg effect) so that carbohydrates are not used for maximal ATP generation via mitochondrial respiration, despite high oxygen availability. A better understanding of these metabolic changes has prompted new approaches toward cancer therapy (reviewed in Hsu and Sabatini, 2008; Schulze and Harris, 2012).

Alterations in fatty acid (FA) metabolism in cancer cells have received less attention but are increasingly being recognized. FAs consist of a terminal carboxyl group and a hydrocarbon chain, mostly occurring in even numbers of carbons, that can be either saturated or unsaturated. They are required for energy storage, membrane proliferation, and the generation of signaling molecules. Here, we provide a brief review of metabolism in cancer cells, focusing on pathways of FA synthesis and storage. Furthermore, we examine a model for attenuating cancer cell proliferation and metastasis by manipulating FA metabolism to diminish FA availability. Due to the great diversity of cancer cells, our perspective is meant to be provocative, not universal. Nevertheless, our intention is to provide a framework for the generation of new ideas on how to manipulate fatty acid metabolism in cancer cells.

Alterations in Energy Metabolism in Cancer Cells

Cancer is fundamentally a disorder of cell growth and proliferation, which requires cellular building blocks, such as nucleic acids, proteins, and lipids. Cancer cells often have perturbed metabolism that allows them to accumulate metabolic intermediates as sources of these building blocks.

The most understood metabolic perturbation in cancer cells is the Warburg effect, an energetically wasteful alteration to glucose metabolism in which cancer cells use carbon from glucose to build other molecules instead of completely oxidizing them to carbon dioxide (Warburg, 1956). During normal cellular metabolism in the presence of oxygen, glucose undergoes glycolysis in the cytoplasm to produce pyruvate. After import into mitochondria, pyruvate is oxidized to acetyl-CoA, which then enters the Krebs cycle to produce reducing equivalents for oxidative phosphorylation (**Figure 2.1**). When oxygen is limiting, excess pyruvate is fermented to lactate in the cytoplasm. Differentiated cells typically use oxidative phosphorylation because of its efficiency, with one glucose molecule undergoing complete oxidation to yield ~36 ATP molecules versus 2 ATP that are obtained from anaerobic glycolysis. The Warburg effect is the use of fermentation even in the presence of oxygen and is characterized by an increase in glucose uptake and consumption, a decrease in oxidative phosphorylation, and the production of lactate[1].

Another commonly observed metabolic alteration in cancer is increased glutamine metabolism. In mammalian cells, glutamine is a major energy substrate through its metabolism to produce α-ketoglutarate, which feeds into the Krebs cycle. Glutamine-derived α-ketoglutarate contributes to the production of citrate by forward-flux through the Krebs cycle and malic

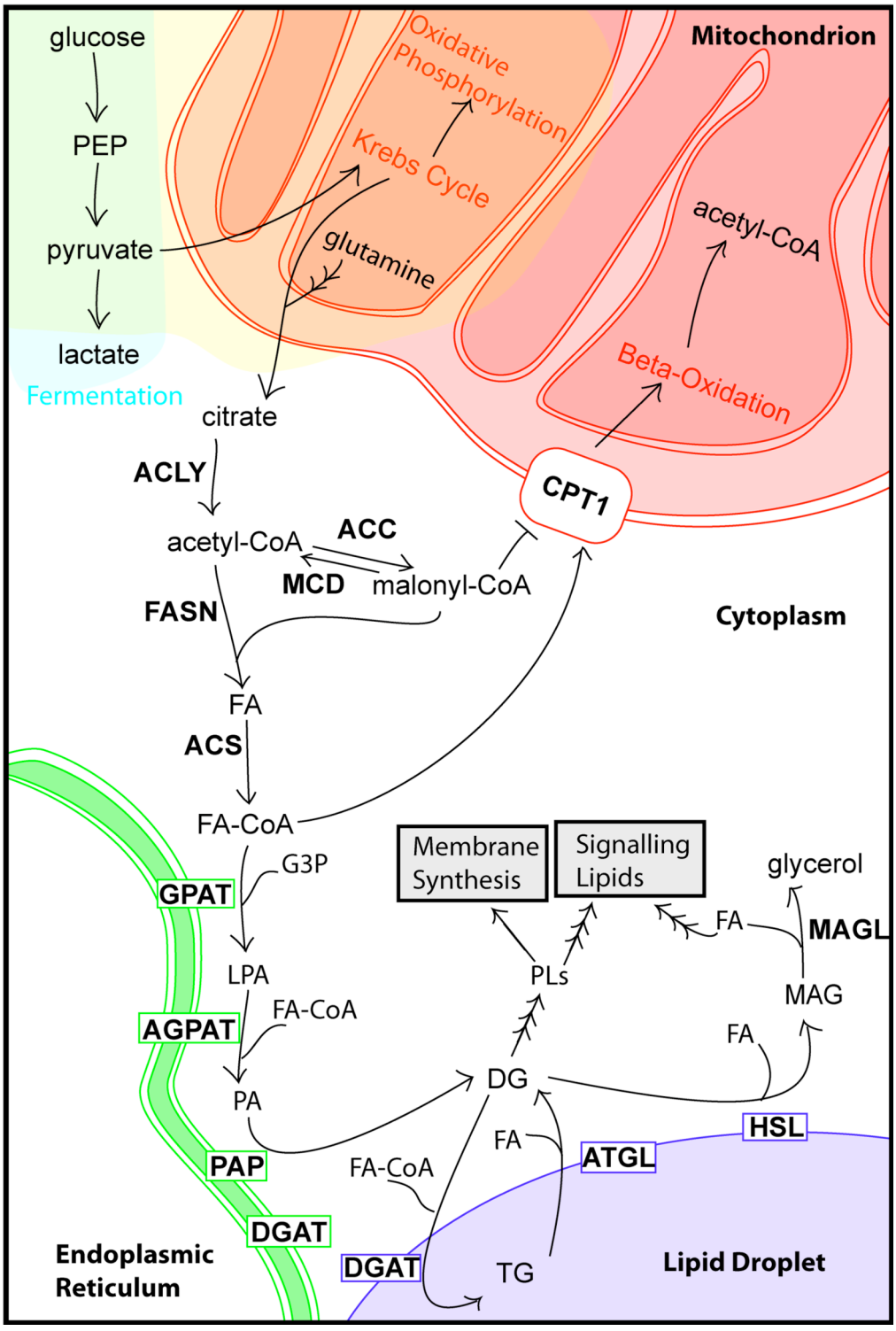

Figure 2.1. **Overview of cellular fatty acid metabolism**. See text for description of depicted pathways. Enzymes are in bold. Enzymes with boxes around them are membrane localized.

enzyme-dependent production of pyruvate (DeBerardinis et al., 2007). Glutamine can also be converted to citrate by the reversal of the Krebs cycle reactions catalyzed by isocitrate dehydrogenase and aconitase (Wise et al., 2008; Mullen et al., 2012; Metallo et al., 2012). Citrate can then be used for the production of acetyl-groups for FA synthesis (see below).

Lipid metabolism is also altered in rapidly proliferating cells (for general reviews, see Swinnen et al., 2006; DeBerardinis and Thompson, 2012; Santos and Schulze, 2012). Here we focus on cancer and FA metabolism. In cancer cells, carbon must be diverted from energy production to FAs for biosynthesis of membranes and signaling molecules. The bulk of cell membrane lipids are phospholipids (PLs), such as phosphatidylcholine (PC) and phosphatidylethanolamine (PE), in addition to other lipids, such as sterols, sphingolipids, and lyso-PLs. All of these lipids are derived in part from acetyl CoA, and many contain FAs. The FA building blocks come from either exogenous sources or from *de novo* FA synthesis. While most normal human cells prefer exogenous sources, tumors synthesize FA *de novo* (Medes et al., 1953) and often exhibit a shift toward FA synthesis (Ookhtens et al., 1984). To enter the bioactive pool, FAs require "activation" by covalent modification by CoA via fatty acyl CoA synthetases. Once in the active pool, FAs can be esterified with glycerol or sterol backbones, generating triacylglycerols (TGs) or sterol esters (SEs), respectively, and then stored in lipid droplets (LDs) (See **Figure 2.1**). Within cells, FAs can have many fates, including being incorporated into membrane, storage, or signaling lipids, or oxidized to carbon dioxide as an energy source.

Although this review focuses on *de novo* FA synthesis pathways, some tumors scavenge lipids from their environment, rendering FA uptake pathways as a potential target. For example, fatty acid binding protein 4 (FABP4), a lipid chaperone, is implicated in providing FAs from

surrounding adipocytes for ovarian tumors (Nieman et al., 2011). Also, prostate cancer cells show reduced viability in the presence of FASN (C75) or ACLY (SB-204990) inhibitors only when cultured in the absence of lipoproteins, an exogenous lipid source (Ros et al., 2012). CD36, a widely expressed transmembrane protein with diverse functions that include fatty acid uptake, has been implicated in breast cancer, and decreased levels of CD36 in stromal tissue are correlated with early steps in tumorigenesis (Defilippis et al., 2012). It is noteworthy that *in vitro* conditions for cell culture experiments are likely to be different than *in vivo* conditions, where exogenous uptake may be more important in some cancers.

Limiting Supplies of Fatty Acids to Limit Cancer Cell Proliferation

Since FAs are essential for cancer cell proliferation, limiting their availability could provide a therapeutic strategy. From the perspective of lipid metabolism, limiting FA availability could be achieved in several ways: 1) blocking FA synthesis, 2) increasing FA degradation via oxidation, 3) diverting FAs to storage, or 4) decreasing FA release from storage (**Figure 2.2**). Limiting FAs through these mechanisms could be accomplished in isolation or in a combinatorial manner. Using this as a framework, we review evidence relevant to this model.

Blocking Fatty Acid Synthesis

The simplest way to reduce FA levels is to block their synthesis. Glucose metabolism feeds into FA metabolism at the point of citrate, an intermediate in the Krebs cycle (see **Figure 2.1**). Several steps are required to convert carbons from citrate to bioactive fatty acids. These steps involve ATP citrate lyase (ACLY, ACL, or ATPCL), acetyl-CoA carboxylase (ACC), fatty acid synthase (FASN or FAS), and acyl-CoA synthetase also known as fatty acid-CoA ligase (ACS,ACSL or FACL). In the model of decreasing FA availability, inhibiting these enzymes would limit cancer cell growth. Important for the clinical significance of these strategies, many inhibitors of these enzymes have minimal effects on non-cancer cells.

The subcellular localization of citrate determines its metabolic fate: mitochondrial citrate feeds into the Krebs cycle, and cytoplasmic citrate feeds into FA synthesis. Citrate is transported across the inner mitochondrial membrane for use in the cytoplasm in a regulated fashion by the transport protein CIC (**ci**trate **c**arrier). CIC levels are elevated in various cancer cell lines and tumors in a manner correlated with poor outcomes, and the inhibition of transport by benzene-tricarboxylate analog (BTA) shows anti-tumor effects in various tumor types and *in vivo* in xenograft mice (Catalina-Rodriguez et al., 2012).

ACLY: ACLY bridges glucose metabolism and FA metabolism by converting six-carbon citrate to oxaloacetate and two-carbon acetyl-CoA, the precursor for FA synthesis. Knockdown of ACLY reduces the ability of cells to metabolize glucose to lipid as shown by shRNA in murine lymphoid cells (Bauer et al., 2005) and siRNA in human adenocarcinoma cells (Hatzivassiliou et al., 2005). This alteration in metabolism impairs murine tumorigenesis and prevents xenograft tumor formation by human cancer cells when ACLY is knocked down by shRNA (Bauer et al., 2005; Hatzivassiliou et al., 2005) or siRNA (Migita et al., 2008) or

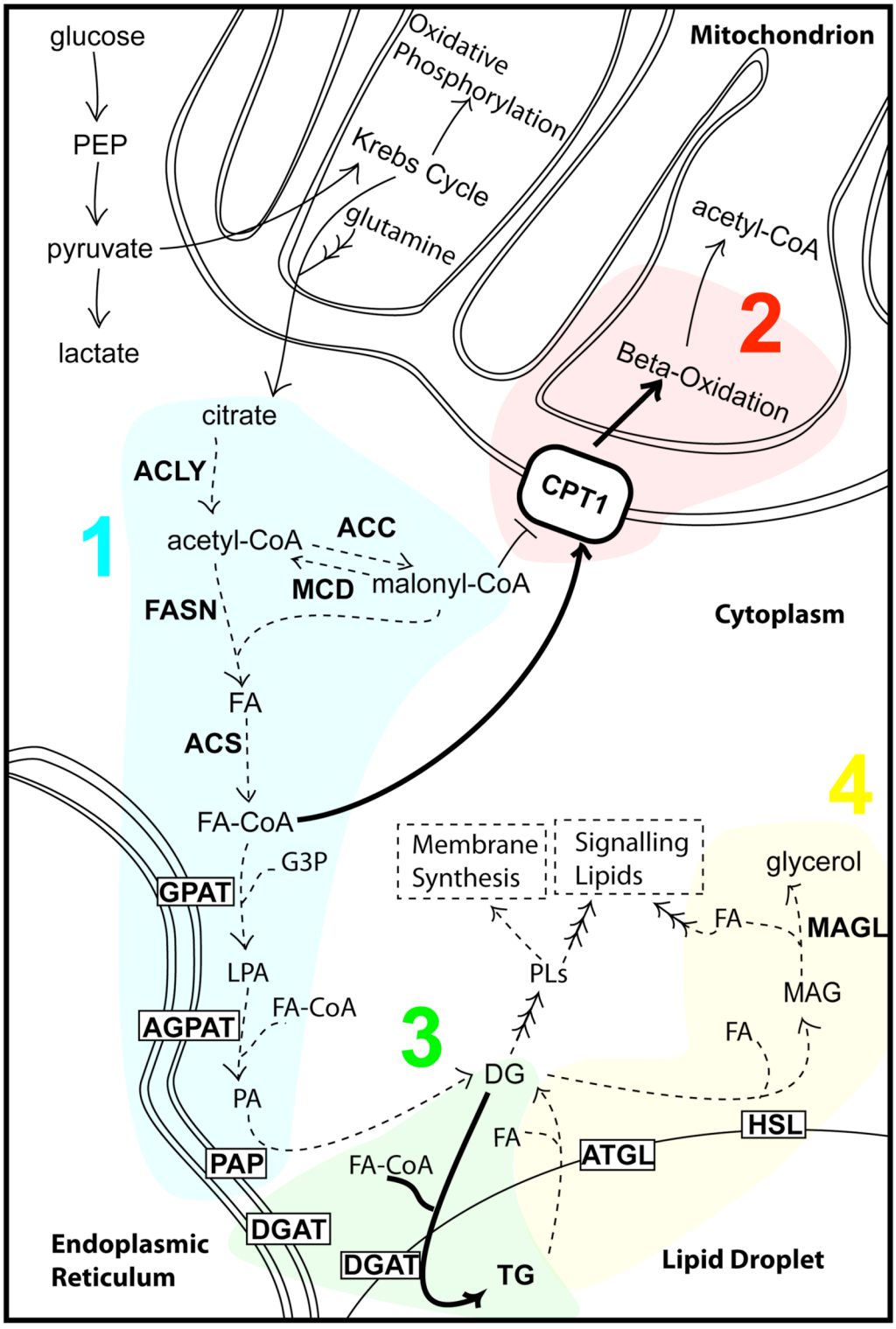

Figure 2. **Model showing how limiting FAs in the cell might limit cancer cell proliferation.** This may be done by 1) blocking the synthesis of fatty, 2) increasing the rate of FA degradation, 3) increasing FA storage in neutral TG, and/or 4) decreasing FA release from storage.

chemically inhibited by SB-204990 (Hatzivassiliou et al., 2005). While ACLY is a promising therapeutic target, its product acetyl-CoA is an important metabolite for many molecules and a substrate for the acetylation of proteins and nucleic acids (Wellen et al., 2009). Thus, inhibiting its production may have consequences for other metabolic pathways as well.

ACC: ACC carboxylates acetyl-CoA to form malonyl-CoA, catalyzes the committed step, and is the most highly regulated enzyme in the fatty acid synthesis pathway (reviewed in Wakil and Abu-Elheiga, 2008). ACC is positively and allosterically regulated by citrate and glutamate and negatively and allosterically regulated by long- and short-chain fatty acyl CoAs such as palmitoyl-CoA. ACC is inactivated by phosphorylation by AMP-activated protein kinase (AMPK) and potentially regulated by many other kinases. There are two ACCs in the human genome, ACC1 (ACCα or ACACA) and ACC2 (ACCß or ACACB). ACC1 is highly enriched in lipogenic tissues, and ACC2 occurs in oxidative tissues. Because they are primarily found in different specialized tissues, ACC1 and ACC2 have different metabolic roles. Malonyl-CoA made by ACC1 is thought to serve as a substrate for FA synthesis, whereas the malonyl-CoA made by ACC2 serves to inhibit CPT1 (see next section), thus preventing FA degradation.

Knockdown of ACC1 by siRNA induces apoptosis in prostate cancer (Brusselmans et al., 2005) and breast tumor (Chajès et al., 2006) cells but not in control non-malignant cells. Chemical inhibition of ACC1 and ACC2 by soraphen-A showed similar results in prostate cancer cells (Beckers et al., 2007). However, a contradictory result was observed with ACC inhibition by TOFA (5-(tetradecyloxy)-2-furoic acid) in breast cancer cells (Pizer et al., 2000). This may be attributable to epidermal growth factor receptor (EGFR) activation, as TOFA was observed by another group to block the growth of EGFR-activated human glioblastoma cell lines while not affecting non-EGFR activated cell lines (Guo et al., 2009a). The situation is further

complicated by the observation that silencing of ACC1 or ACC2 accelerated tumor growth in lung cancer cells by promoting NADPH-dependent redox balance (Jeon et al., 2012).

While some aspects of the role of ACC in cancer cells still need to be elucidated, ACC activity might be controlled by promoting ACC phosphorylation. AMPK is activated by drugs, such as metformin, already widely used to treat diabetes. There is experimental evidence *in vitro* and *in vivo* in mice and humans, mainly in solid tumor models, that metformin treatment has anti-tumor activity, and clinical trials to further explore efficacy are underway (Pollak, 2012).

MCD: Malonyl-CoA decarboxylase (MCD) decarboxylates malonyl-CoA to acetyl-CoA, essentially reversing the reaction catalyzed by ACC. Thus, it is surprising that MCD inhibition yields similar data as ACC. siRNA against MCD and MPA treatment, a small-molecule inhibitor of MCD, are cytotoxic to breast cancer lines but not fibroblasts (Zhou et al., 2009).

FASN: FASN catalyzes successive condensation reactions to form a fatty acid from malonyl-CoA and acetyl-CoA substrates, producing mainly 16-carbon palmitate. It is perhaps the most studied FA metabolic enzyme with respect to cancer. Increased fatty acid synthesis due to increased levels of FASN has been observed in a multitude of cancers and is strongly correlated with a poor prognosis in many instances (reviewed in Menendez and Lupu, 2007). RNAi against FASN decreases levels of TG and phospholipids and inhibits cell growth and apoptosis in cells derived from a lymph node metastasis of prostate carcinoma (LNCaP) cells with no effects on growth rate or viability of non-malignant cultured skin fibroblasts (DeSchrijver et al., 2003). In many reports, chemical inhibitors of FASN preferentially killed cancer cells (reviewed in Lupu and Menendez, 2006). FASN is a particularly appealing therapeutic target because most cancer cells depend upon FASN-mediated *de novo* FA synthesis, whereas most non-cancer cells prefer exogenous FA. However, cell death induced after FASN inhibition might be due to the toxic

accumulation of malonyl-CoA rather than a lack of FA (Pizer et al., 2000). Moreover, some inhibitors of FASN show severe side effects in animal models, including dramatic weight loss (Loftus et al., 2000), and FASN is required for adult neuronal stem cell function (Knobloch et al., 2012).

ACS: For FAs to enter bioactive pools, they must be activated by ACS enzymes, which generate FA-CoA. Bioactive FAs also contribute to protein palmitoylation, a post-translational modification that is important in certain cancers (Resh, 2012). Mammals have five ACS isoforms (ACSL1, 3, 4, 5, and 6) and also have fatty acid transport proteins with acyl CoA synthetase activity. ACSL4 is upregulated in some colon adenocarcinomas (Cao et al., 2000), and ACSL5 levels are increased in glioblastomas (Yamashita et al., 2000). Overexpression of ACSL4 promotes tumor cell survival by preventing apoptosis, likely through depletion of unesterified arachidonic acid (AA), which yields a pro-apoptotic signal (Cao et al., 2000). Chemical inhibition of ACS by Triacsin C (inhibitor of ACSL1, 3, and 4 but not 5 or 6 (Van Horn et al., 2005; Kim et al., 2001) preferentially induces apoptotic cell death in lung, colon, and brain cancer cells (Mashima et al., 2005). Several thiazolidinediones (TZDs) directly bind and inhibit rat ACSL4 (but not ACSL1 or ACSL5) *in vitro* (Kim et al., 2001). TZDs activate peroxisome proliferator-activated receptors (PPARs), particularly PPARγ, and are already in wide use for the treatment of diabetes. TZD use is correlated with decrease incidence of certain cancers in diabetics in what is likely to be a PPARγ-independent manner (Weng et al., 2006). When considering treatment through inactivation of ACS, it is important to note that different drugs have different isoform specificities so they may have differential effects, as the various isoforms have different tissue specificities, responses to nutritional state (Mashek et al., 2006), and preferred substrates (notably, ACSL4 prefers AA).

SCD: SCD catalyzes the introduction of double bonds into short-chain FAs in the C9 position (mainly converting stearoyl-CoA to oleoyl-CoA) (Paton and Ntambi, 2009). This alters the physical properties of FAs and has profound effects on lipid function. There are two isoforms of SCD in human cells (SCD1 and SCD5). SCD expression and activity is upregulated in some cancers, and its importance for cancer biology is increasingly recognized (Igal, 2010). Inhibition of SCD function causes cell death in cancer cells, probably by inducing the accumulation of unsaturated fatty acids (Ariyamo et al., 2010). Pharmacological inhibition of SCD limits tumor growth in pre-clinical cancer models (Fritz et al., 2010) without affecting overall body weight (Roongta et al., 2011). Since cancer cells rely considerably on de novo FA synthesis, SCD inhibition will likely show some degree of selectivity.

FAs are also substrates for sphingolipid synthesis. While sphingolipid metabolism is not a focus of this review, it is noteworthy that specific sphingolipids, such as ceramides and sphingosine-1-phosphate, are bioactive signaling molecules that generally suppress or promote tumors, respectively (Ogretmen and Hannun, 2004). Moreover, accumulation of ceramides is implicated in the therapeutic effects of various chemotherapeutic treatments of cancer.

Blocking Expression of Fatty Acid Synthesis Genes

In addition to directly targeting enzymes of fatty acid synthesis, their activities could be reduced by reducing transcription levels. The master transcriptional regulators of FA synthesis are sterol regulatory element-binding protein 1 (SREBP-1) transcription factors (Horton et al., 2002). SREBP-1 has two isoforms: SREBP-1a is the predominant isoform in most cultured cell lines and SREBP-1c is predominant in liver and most tissues. At normal levels, SREBP-1c activates the FA biosynthetic pathway with responsive genes including ACLY, ACC, FAS, SCD-1, and GPAT. Therefore, inhibiting SREBP-1 in cancer cells could decrease fatty acid synthesis gene expression and possibly prevent cancer cell proliferation. Indeed, shRNA knockdown of SREBP-1 decreases abundance of ACC and FAS and promotes tumor cell death of glioblastoma cells that overexpress SREBP-1 because of constitutively active EGFR, and 25-hydroxycholesterol (25-HC), an inhibitor of activation of SREBP-1 and -2, causes cell death in high EGFR (and therefore high SREBP-1) expressing cancer cell lines (Guo et al., 2009b). Additionally, higher levels of SREBP-1 are seen in prostate cancer tissue and both SREBP-1 and -2 play a role in the prostate cancer progression to androgen independence (Ettinger et al., 2004). Interestingly, recent work suggests that a mechanism for SREBP-1 repression preventing cancer cell proliferation is through loss of SCD-1 and FA desaturation, thereby causing lipotoxicity due to abnormally high levels of saturated FAs (Williams et al., 2013; Griffiths et al., 2013). Inhibition of SREBP by 25-HC, fatostatin, and FGH10019 all cause a decrease in expression of SREBP-1 and -2 target genes and significantly reduce cellular growth in a variety of cancer cell lines (Williams et al., 2013) and SREBP1 knockdown by shRNA reduces tumor growth *in vivo* in nude mice (Griffiths et al., 2013).

Further upstream, SREBP transcription factors and FA synthesis can be regulated by many

signaling pathways, including growth factor signaling, which is reviewed in depth elsewhere (Shao and Espenshade, 2012; Kumar-Sinha et al., 2003; Peterson et al., 2011; Laplante and Sabatini, 2009; Lewis et al., 2011). Another transcription factor, liver X-activated receptor (LXR), activates fatty acid synthesis by inducing SREBP-1c (Liang et al., 2002). Therefore, cancer cell proliferation might be attenuated by preventing LXR activation. However, activation of LXR, particularly through T0901317, inhibits cancer cell proliferation in breast, colon, and prostate cancers (Viennois et al., 2012). These findings likely reflect functions of LXR other than regulating FA synthesis.

Increasing Fatty Acid Degradation

FA levels might be decreased in cancer cells by increasing the rate at which they are degraded. Activated FAs are broken by mitochondrial β-oxidation. FA-CoAs are transported from the cytosol across the outer mitochondrial membrane after they are converted to FA carnitines by carnitine palmitoyl transferase 1 (CPT1). Within the mitochondria, FAs are then repeatedly cleaved to produce acetyl-CoAs that feed into the Krebs cycle and produce reducing equivalents for oxidative phosphorylation. Increasing FA oxidation to limit FA abundance could in theory be beneficial, but data from experiments testing this idea are mixed.

CPT1: CPT1 is the first and rate-limiting step of fatty acid transport into mitochondria for oxidation to carbon dioxide. It is inhibited by malonyl-CoA. β-Oxidation of FAs is increased when ACC2 is inhibited because of the depletion of malonyl-CoA, the direct product of ACC. Therefore, the attenuation of cancer cell proliferation by inhibiting ACC (discussed previously) may also be due in part to an increase in degradation of FAs.

It is yet unclear whether increased FA oxidation in cancer cells will block proliferation. Cancer types likely differ in their clinical response to increasing FA oxidation, depending upon their energy requirements and ACC isoform expression patterns. In some types, increased FA oxidation may diminish FA availability and be beneficial. On the other hand, etomoxir, an inhibitor of CPT1, and ranolazine, an indirect inhibitor of FA oxidation, may kill cancer cells (Samudio et al., 2010; Pike et al., 2011). A further caveat of increasing the FA oxidation rate is that it could increase cellular ATP levels, thus providing energy for further cellular proliferation. Indeed, CPT1C, the brain isoform of CPT1, is important for the survival of cancer cells under energy stress (Zaugg et al, 2011).

It has long been known that PPARα is a major transcriptional regulator of FA oxidation with

activation inducing oxidation. In keeping with the uncertainty regarding the role of FA oxidation in cancer cell proliferation, extended PPARα activation causes hepatocellular carcinoma in mice and rats by an unclear mechanism that involves perturbation of the cell cycle and production of reactive oxygen species (reviewed by Michalik et al., 2004). However, humans taking PPARα agonists do not develop similar cancers, and in fact, PPARα activation inhibits tumor growth in several models (reviewed in Yokoyama and Mizunuma, 2010).

Diverting Fatty Acids to Storage

Once made, FAs can be used for membrane lipid synthesis, degraded, or stored. Conceivably, increased storage of FAs in neutral lipids, such as TGs or sterol esters, could lead to a reduction in FAs available for use as membrane building blocks or signaling lipids and inhibit cellular proliferation. Most cells store FAs in TGs in the cytosolic lipid droplet (LD), an organelle whose major function is lipid storage (see Farese and Walther, 2009). The role of LDs in cancer cells is unclear. While increased numbers of LDs have been reported in many cancer cells (reviewed in Bozza and Viola, 2010), and this accumulation has been proposed to be pathogenic, the accumulation of LDs per se, might not be the culprit. The readily available pool of FAs that they represent might be pathogenic. LD accumulation might also reflect a cellular response to stress (Hapala et al., 2011). Future studies should also carefully delineate whether LD accumulation occurs within cancer cells or in surrounding cells.

The major TG synthesis pathway is known as the Kennedy or glycerol-phosphate pathway. It condenses FAs with glycerol 3-phosphate using the enzymes glycerol-3-phosphate acyltransferase (GPAT), acylglycerolphosphate acyltransferase (AGPAT), phosphatidic acid phosphohydrolase (Lipin or PAP), and diacylglycerol acyltransferase (DGAT). The products of all but the most distal enzyme (DGAT) feed into PL synthesis. Therefore, GPAT, AGPAT and Lipin might be inhibited to limit PL production, while efforts to increase FA storage would be focused on activating DGAT. Additionally, the potential benefits of increasing FA storage may only be realized while concomitantly inhibiting the release of FA from storage.

AGPAT: AGPAT esterifies lysophosphatidic acid (LPA) and a FA-CoA to form phosphatidic acid (PA). There may be as many as 11 human AGPATs. Elevated AGPAT2 expression is associated with poor prognosis of ovarian cancers, and AGPAT2 inhibitors have antitumor

activity in xenograft mice (reviewed in Takeuchi and Reue, 2009). Additionally, AGPAT9 and AGPAT11 are upregulated in a variety of cancers (reviewed in Agarwal, 2012). As with any enzyme with multiple isoforms, differences in expression patterns of the isoforms may have a profound influence on the effectiveness of inhibition/activation of a particular isoform in a particular cancer.

PAP: Lipin removes a phosphate group from PA to form diacylglycerol (DG). It is one of the least-studied enzymes in the lipid storage pathway with respect to cancer, and little is known about how blocking or overexpressing this step of lipid synthesis affects cancer progression. However, lipin is involved in the regulation of the activity of sterol regulatory element binding proteins (SREBP), a family of transcription factors that regulate the expression of many enzymes involved in fatty acid and cholesterol biosynthesis (Ishimoto et al., 2009). Lipin is phosphorylated and inhibited by the mammalian target of rapamycin complex 1, resulting in activation of SREBP transcriptional activity (Peterson, et al., 2011). Modulating lipin activity may therefore have significant effects on cellular lipid homeostasis.

DGAT: DGAT enzymes esterify DG and a FA-CoA to form TG. Mammals have two DGATs (DGAT1 and DGAT2). DGAT catalyzes the only dedicated step in TG formation and thus provides a key target for decreasing available lipids by increasing lipid storage. Transformed human fibroblasts overexpressing DGAT1 had increased TG and decreased phospholipids, as well as reduced proliferation and invasiveness (Bagnato and Igal, 2003). Unpublished data from the Farese laboratory suggests that DGAT1-deficient mice have increased levels of LPA and PGE2 in mammary fat and develop some breast cancers more rapidly (Sylvaine Cases, unpublished). DGAT1 inhibition might also favor the accumulation of its substrate diacylglycerol in cells, which might have signaling effects. These findings would suggest

caution, from a cancer standpoint, for the use of DGAT1 inhibitors, which are being explored clinically for use in metabolic diseases.

PLs are the other major products of glycerolipid synthesis and are important for membrane expansion in rapidly proliferating cells. The major mammalian membrane phospholipid is PC. Many cancers have increased PC levels and increased activity of any of several enzymes in the PC synthesis pathway, while inhibition or knockdown of many of the enzymes decrease cancer phenotypes (Glunde et al., 2011). An inhibitor of choline kinase alpha (CKα), the first step of choline activation for PC synthesis, is currently in Phase I trials for use against advanced solid tumors (http://clinicaltrials.gov/show/NCT01215864).

Blocking Fatty Acid Release From Storage

Once stored, FAs can be released for use by specific lipases. By preventing lipolysis, the active FA pool available for cancer cell proliferation might be decreased. FAs derived from lipolysis can also serve as precursors for important signaling lipids (see Wymann and Schneiter, 2008). Most knowledge on lipolysis is derived from work on adipocytes where each TG molecule in the LD can be fully hydrolyzed to release three FAs by the sequential action of adipose triglyceride lipase (ATGL), hormone sensitive lipase (HSL) and monoacylglycerol lipase (MAGL). Although each of these lipases also has important functions in other tissues, it is yet unclear whether other lipases might operate in other cell types. Currently, most data addressing lipases and cancer are for MAGL.

MAGL: MAGL hydrolyzes the final FA from MG leaving the glycerol backbone. MAGL expression and activity are increased in several aggressive cancer cell lines and primary tumors (Nomura et al., 2010). Knockdown and chemical inhibition of MAGL by JZL184 lowered free FA levels and reduced pathogenicity of melanoma and ovarian cancer cells in vitro and in vivo, while overexpression showed the opposite phenotype. Interestingly, a high-fat diet in mice reversed the reduced tumor growth of MAGL-inhibited tumors in mice. This observation raises the question of whether targeting lipid metabolism for cancer therapy may only be effective in combination with specific dietary regimes. Additionally, MAGL has a role in the regulation of signaling lipids: more invasive tumors have increased LPA and PGE_2 levels, and those are decreased in the presence of MAGL inhibitors.

ATGL and HSL: Although their roles in cancer cell proliferation are unclear, ATGL and HSL play an important role in cancer cachexia, a wasting syndrome that is an adverse prognostic factor in cancer. Cancer patients with cachexia show increased HSL and ATGL activity when

compared to non-cancer patients, and genetic ablation of ATGL (and HSL to a lesser extent) protects mice from cancer-associated loss of adipose tissue and skeletal muscle (Das et al., 2011). Therefore, pharmacological inhibition of ATGL and/or HSL may help to prevent cancer-associated cachexia.

Conclusion and Perspective

Cancer cells rely on FAs as cellular building blocks for membrane formation, energy storage, and the production of signaling molecules. Our review highlights this requirement and provides a framework for the investigation of limiting the supply of FAs. If the model that FAs are required for cancer cell proliferation is correct, cancer cells might be targeted at multiple points within the pathway of FA metabolism to subvert rapid proliferation, and many chemical inhibitors for specific steps already exist (Table 1). Much like glucose metabolism, targeting FA metabolism might be more selective for highly proliferative cells. Alternatively, delivery of FA metabolism inhibitors might be done in a cell-specific and targeted manner.

Cancers are diverse in type and underlying genetic alterations. Lipid metabolism is complex, with many different feedback mechanisms and points of regulation. Additionally, most of the lipid metabolic enzymes have multiple isoforms, and these may be coupled to different lipid metabolic processes and can have different cellular localization or tissue distribution. Therefore, successful therapies may be dependent upon understanding the specific metabolic abnormalities for a particular type of cancer.

Enzyme	Inhibitor	Comments	Selected References
ACC	Soraphen-A		(Beckers et al., 2007)
	TOFA (5-(tetradecyloxy)-2-furoic acid)		(Pizer et al., 2000), (Guo et al., 2009a)
	A-769662		(Göransson et al., 2007)
	Metformin	Indirect, activates AMPK	(Pollak, 2012)
	AICAR	Indirect, activates AMPK	(Jose et al., 2011)(Swinnen et al., 2005)
ACLY	SB-204990		(Hatzivassiliou et al., 2005), (Ros et al., 2012)
	LY294002	Indirect, PI3K inhibitor	(Migita et al., 2008)
ACS	Triacscin C		(Mashima et al., 2005)
	Thiazolidinediones (TZDs)	ACSL4 specific, also activates PPARγ, FDA approved	(Kim et al, 2001)
AGPAT	CT-32501	AGPAT2 specific	(Takeuchi and Reue, 2009)
CKα	TCD-717	Currently in phase I trials	http://clinicaltrials.gov/show/NCT01215864
	MN58B		(Glunde et al., 2011)
CIC	Benzene-tricarboxylate analog (BTA)		(Catalina-Rodriguez et al., 2012)
CPT1	Etomoxir		(Samudio et al., 2010) (Pike et al., 2011)
	Ranolazine	FDA approved	(Samudio et al., 2010)
FASN	Cerulenin and its derivative C75		(Lupu and Menendez, 2006) (Ros et al., 2012)
	Orlistat	FDA approved	(Lupu and Menendez, 2006)
	Flavonoids	Naturally occurring	(Lupu and Menendez, 2006)
	Epigallocatechin-3-gallate (EGCG)	Found in green tea	(Lupu and Menendez, 2006)
MAGL	JZL184		(Nomura et al., 2010)
SCD	BZ36		(Fritz et al., 2010)
	A939572		(Roongta et al., 2011)
SREBP	Fatostatin	Inhibits processing of SREBP-1 and -2	(Williams et al, 2013)
	FGH10019	Inhibits processing of SREBP-1 and -2	(Williams et al, 2013) (Kamisuki et al, 2011)

Table 2.1. **Examples of chemical inhibitors of lipid enzymes that could reduce fatty acid availability**. Shown are selected inhibitors for enzymes mentioned in text.

Chapter 5:
Summary and Future Directions

Summary

My work has focused on proteins at the yeast *Saccharomyces cerevisiae* LD – understanding what proteins are present at the LD, how they target the LD, how they affect LD formation, and what functions proteins have at the LDs. In my published work, I generated a high confidence LD proteome in which I verified the LD targeting of 30 proteins, 6 of which were newly identified. I also showed that at least two of the newly identified LD proteins (Rer2 and Say1) are active at the LD, connecting the LD to dolichol synthesis and sterol acetylation. In my unpublished work, I performed a visual screen for genetic requirements of protein targeting to the LD and LD formation. I explored the mechanism of targeting to the LD of proteins involved in ergosterol synthesis. I also explored a potential functional role of LDs in protein degradation.

Future Directions

Many questions that guided my research still remain unanswered, with many potential avenues of exploration for better understanding.

What proteins are present at the lipid droplet?

What is the stationary phase yeast LD proteome? - Although I published a high-confidence LD proteome of yeast at stationary growth phase grown in defined media, it is quite possible that there are further yeast LD proteins that remain to be discovered in the same conditions. Although several yeast LD proteomes have been published, some in the same conditions, the fact that our proteome was able to identify and verify 6 new proteins suggests that there has not been saturation.

What is the complete yeast LD proteome? It is clear that many variables (e.g. nutrient source, growth phase, genetic background, etc.) affect protein targeting to the LD and there is a need for high confidence proteomes in different conditions in order to understand the dynamic nature of the LD proteome. One comparative proteome was reported comparing rich growth conditions with and without oleate supplementation (Grillitsch et al., 2011), however it was not a high-confidence proteome nor was it validated. There have not been reports of other comparative yeast LD proteomes. The SILAC technique that we used in our high-confidence proteome is a perfect tool for the future generation of comparative proteomes.

What is the LD proteome of other cell types? Although the high-confidence PCP technique has now been reported for LDs in yeast (Currie et al., 2014) and *Drosophila* (Krahmer et al., 2013), there are many other cell types that lack proteomes, much less high-confidence proteomes. LDs in different cell types have different functions and roles in disease (e.g. fat storage in adipocytes, atherosclerosis in foam cells) so it will be informative to have high

confidence proteomes of varied cell types. Not only will high-confidence proteomes be important for research on cell-type specific functions but having many high-confidence proteomes will allow comparisons between cell types to aid in the discovery of universal LD characteristics.

How do proteins affect lipid droplet formation?

What is the structure of the yeast LD? Relatively little is known about how LDs are formed. It is commonly accepted that LDs arise from the endoplasmic reticulum (ER) because the TG synthetic enzymes (e.g. mammalian DGAT1 and DGAT2, yeast Dga1 and Lro1) are ER localized (reviewed in Goodman, 2008 and Walther and Farese, 2012), although it is clear that proteins can target to the LD either at the moment of LD formation or later (e.g. Erg6 and Dga1, respectively, in yeast (Jacquier et al., 2011)). My work and the recently published work of others (Jacquier et al., 2011) supports the hypothesis that LDs in yeast are different from LDs in other cell types and we need to be approaching the questions of LD formation and LD protein targeting differently in this model system. In yeast, LDs appear to be a subdomain of the ER that is closely associated with the LD (Jacquier et al., 2011). This is different from other cell types, like S2 cells where there are distinct LD populations – those that are connected and not connected to the ER (Wilfling et al., 2013). More research is needed to explore this hypothesis not only to answer the question of how LDs are formed in yeast but because the LD topology affects other major questions such as how proteins target to the LD.

What proteins affect yeast LD formation? Several studies have explored the genetic requirements of LD formation and morphology (Fei et al., 2008a, 2008b, and Szymanski et al., 2007), including a genetic screen that I completed but did not publish (Chapter 3). However, there is little overlap between the many studies and few of the strongest hits have these studies have been confirmed, suggesting that the experimental designs have been prone to false positives and/or that LD formation is either incredibly sensitive or surprisingly insensitive to experimental

conditions. I suggest that the question of what proteins affect LD formation is better addressed by a mechanistic understanding of the few known determinants (e.g seipin) rather than further variations on the same screen.

How do proteins target the LD?

What are the topologies of yeast LD proteins? The PL monolayer imposes unique structural requirements upon proteins that target to the LD, for example, prohibiting transmembrane proteins and favoring structures that can localize to the interface by dipping segments into the hydrophobic phase, such as proteins with hydrophobic sequences (Martin and Partin, 2006, Wilfling et al., 2013) or amphipathic helices (Brasaemle et al., 2007). How and why proteins target to the LD is a major question that remains unanswered as topology is unknown for most LD proteins and not all LD proteins with known topologies have hydrophobic sequences or amphipathic helices. Additionally, protein topology is always experimentally determined in the microsomal fraction and it is possible that the same protein could have different topologies in the ER than the LD, analogous to ApoE and its different tertiary structure upon binding lipids (Lu et al., 2000)

Are LD proteins really at the LD in yeast? Twelve proteins (Ayr1, Eht1, Erg1, Erg6, Erg7, Faa1, Faa4, Fa1, Pet10, Slc1, Tgl1 and Tgl3) have been identified in all published yeast proteomes (Athendstaedt et al., 1999, Binns et al., 2006, Currie et al., 2014, and Grillitsch et al., 2011), suggesting that they constitutively target the LD. Six of these proteins have predicted transmembrane domains (Erg1, Erg7, Fat1, Slc1, Tgl1, and Tgl3), with the topology of Tgl1 experimentally verified (Köffel et al., 2005). It is unclear how a protein with a transmembrane domain can localize to a membrane monolayer at LD surfaces. Likely, these proteins are targeting to ER membrane that is closely associated with LD membrane, a hypothesis which

merits testing. A complementary hypothesis is that the proteins have different topologies in the ER than the LD fractions, discussed above.

What functions do LDs have?

What proteins are active at the yeast LD? While we experimentally determined that Say1 and Rer2 are active at the LD (Currie et al., 2014), there are many proteins that have been localized to the LD by microscopy or cellular fractionation whose biochemical activities have not been tested at the LD. As there are examples of proteins localized to the LD but not active at the LD (e.g. Erg1, Leber et al., 1998), to ascribe a function to the LD it is important to biochemically test that function.

Why are LD proteins active (or not) at the LD and/or elsewhere? Of the proteins that have been shown at the yeast LD, there is variability as to whether they are active at the LD. While we showed that both Say1 and Rer2 are present and active at the LD and ER (Currie et al., 2014), similar to Ayr1 (Athenstaedt et al., 2000), Gpt2 (Athenstaedt et al., 1997), and Slc1 (Athenstaedt et al., 1999), not all proteins are active in all subcellular populations. For example, Dga1 (Sorger et al., 2002), Erg6 (Zinser et al., 1993), Erg7 (Milla et al., 2002), Erg27 (Mo et al., 2003), and Yju3 (Heier et al., 20010) are predominantly active at the LD which may reflect that these proteins have higher LD:ER localization ratios. In contrast, Erg1 is strongly present in both the ER and LD but only active at the LD (Leber et al., 1998). The significance of some enzymes differing in activity at the ER versus LDs is unclear and merits further exploration.

Is protein localization to the LD a regulatory mechanism? There are many examples of some proteins but not others in a complex or pathway being found at the LD. The most well-described is the Erg pathway where Erg1, Erg6, Erg7, and Erg27 but not the other 8 Ergs in the pathway

are found at the LD. One of the proteins that we newly identified, Cab5, is involved in coenzyme A biosynthesis, with Cab2, Cab3, and Cab4 (Olzhausen et al., 2013). By fluorescence microscopy, we were additionally able to detect Cab4-GFP at the LD (data not shown) but not the other Cabs, and we didn't find any of them in the LD fraction in our proteome. The data merit a careful examination of this pathway and its connection to the LD. Additionally, the role of LD localization of some enzymes but not others in a pathway should be explored as localization may be a regulatory mechanism.

What is the functional role of association with other organelles? LDs are clearly connected to other organelles both functionally and physically, although those connections have not been thoroughly explored. In yeast, there has been some exploration of the connections between LDs and peroxisomes (Binns et al., 2006) but little exploration of the connections to other organelles. In our proteome we found that Taz1, a cardiolipin remodeling enzyme found primarily in mitochondrial membranes (Brandner et al., 2005), reproducibly fractionates with the LD and this might be due to organelle associations. Additionally, microscopy revealed that clusters of Gtt1-GFP localize near some LDs, offering an explanation for why Gtt1 biochemically purifies with LDs. Again, the mechanism is unclear and may have to do with organelle association.

What are the functions of LD proteins whose functions are unknown? Our proteome identified five proteins at the LD whose functions are unknown (Pet10, Yim1, YKL047W, YOR059C, YPR147C). While YPR147C and YOR059C contain potential lipase motifs, they have not been experimentally shown to be lipases. However, it is highly likely that all five

proteins are involved in lipid metabolism as all other verified yeast LD proteins are involved in lipid metabolism.

What proteins are active at the LD of other cell types? Our lab's high-confidence *Drosophila* S2 proteome (Krahmer et al., 2013) revealed many proteins involved in ER organization, protein degradation, and N-glycan biosynthesis, suggesting additional functions and complexity for LDs in fly versus yeast cells. Following high confidence proteomes in other cell types (discussed above) should be the functional exploration of protein activities at the LD for the same reasons discussed for the functional exploration of yeast protein activities at the LD.

Works Cited

Agarwal, A.K. (2012). Lysophospholipid acyltransferases: 1-acylglycerol-3-phosphate O-acyltransferases. From discovery to disease. Curr Opin Lipidol *23*, 290-302.

Andersen, J.S., Wilkinson, C.J., Mayor, T., Mortensen, P., Nigg, E.A., and Mann, M. (2003) Proteomic characterization of the human centrosome by protein correlation profiling. Nature **426**, 570-574

Ashrafi, K., Chang, F.Y., Watts, J.L., Fraser, A.G., Kamath, R.S., Ahringer, J., Ruvkun, G. (2003). Genome-wide RNAi analysis of Caenorhabditis elegans fat regulatory genes. Nature *421*, 268-272.

Ariyama, H., Kono, N., Matsuda, S., Inoue, T., and Arai, H. (2010). Decrease in membrane phospholipid unsaturation induces unfolded protein response. J Biol Chem *285*, 22027-22035.

Athenstaedt, K., and Daum, G. (1997) Biosynthesis of phosphatidic acid in lipid particles and endoplasmic reticulum of *Saccharomyces cerevisiae*. J. Bacteriol. **179**, 7611-761

Athenstaedt, K., Weys, S., Paltauf, F., and Daum, G. (1999) Redundant systems of phosphatidic acid biosynthesis via acylation of glycerol-3-phosphate or dihydroxyacetone phosphate in the yeast *Saccharomyces cerevisiae*. J. Bacteriol. **181**, 1458-1463

Athenstaedt, K., D. Zweytick, A. Jandrositz, S.D. Kohlwein, and Daum, G. (1999). Identification and characterization of major lipid particle proteins of the yeast *Saccharomyces cerevisiae*. J Bacteriol *181*, 6441-6448.

Athenstaedt, K., and Daum, G. (2000) 1-Acyldihydroxyacetone-phosphate reductase (Ayr1p) of the yeast *Saccharomyces cerevisiae* encoded by the open reading frame YIL124w is a major component of lipid particles. J. Biol. Chem. **275**, 235-240

Athenstaedt, K., and Daum, G. (2003) YMR313c/TGL3 encodes a novel triacylglycerol lipase located in lipid particles of Saccharomyces cerevisiae. J. Biol. Chem. **278**, 23317-23323

Athenstaedt, K., and Daum, G. (2005) Tgl4p and Tgl5p, two triacylglycerol lipases of the yeast Saccharomyces cerevisiae are localized to lipid particles. J. Biol. Chem. **280**, 37301-37309

Ayciriex, S., Le Guedard, M., Camougrand, N., Velours, G., Schoene, M., Leon, S., Wattelet-Boyer, V., Dupuy, J., Shevchenko, A., Schmitter, J., Lessire, R., Bessoule, J., and Testet, E. (2012) YPR139c/LOA1 encodes a novel lysophosphatidic acid acyltransferase associated with lipid droplets and involved in TAG homeostasis. Mol. Biol. Cell **23**, 233-246

Bagnato, C., and Igal, R.A. (2003). Overexpression of diacylglycerol acyltransferase-1 reduces phospholipid synthesis, proliferation, and invasiveness in simian virus 40-transformed human lung fibroblasts. J Biol Chem *278*, 52203-52211.

Bauer, D.E., Hatzivassiliou, G., Zhao, F., Andreadis, C., and Thompson, C.B. (2005). ATP citrate lyase is an important component of cell growth and transformation. Oncogene *24*, 6314-6322.

Beckers, A., Organe, S., Timmermans, L, Scheys, K., Peeters, A., Brusselmans, K., Verhoeven, G., and Swinnen, J.V. (2007). Chemical inhibition of acetyl-CoA carboxylase induces growth arrest and cytotoxicity selectively in cancer cells. Cancer Res *67,* 8180-8187.

Beeler, T., Bacikova, D., Gable, K., Hopkins, L., Johnson, C., Slife, H., and Dunn, T. (1998) The *Saccharomyces cerevisiae* TSC10/YBR265w gene encoding 3-ketosphinganine reductase is

identified in a screen for temperature-sensitive suppressors of the Ca2+-sensitive csg2Delta mutant. J. Biol. Chem. **273**, 30688-30694

Beilharz, T., Egan, B., Silver, P.A., Hofmann, K., and Lithgow, T. (2003). Bipartite signals mediate subcellular targeting of tail-anchored membrane proteins in *Saccharomyces cerevisiae*. J Biol Chem *278*, 8219-8223.

Binns, D., Januszewski, T., Chen, Y., Hill, J., Markin, V.S., Zhao, Y., Gilpin, C., Chapman, K.D., Anderson, R.G., and Goodman, J.M. (2006) An intimate collaboration between peroxisomes and lipid bodies. J. Cell Biol. **173**, 719-731

Blanchette-Mackie, E.J., and Scow, R.O. (1983) Movement of lipolytic products to mitochondria in brown adipose tissue of young rats: an electron microscope study. J. Lipid Res. **24**, 229-244

Bozza, P.T., and Viola, J.P. (2010). Lipid droplets in inflammation and cancer. Prostag Leukotr Ess *82*, 243-250.

Brandner, K., Mick, D.U., Frazier, A.E., Taylor, R.D., Meisinger, C., and Rehling, P. (2005) Taz1, an outer mitochondrial membrane protein, affects stability and assembly of inner membrane protein complexes: implications for Barth Syndrome. Mol. Biol. Cell **16**, 5202-5214

Brasaemle, D.L., G. Dolios, L. Shapiro, and R. Wang. (2004). Proteomic analysis of proteins associated with lipid droplets of basal and lipolytically stimulated 3T3-L1 adipocytes. J Biol Chem *279*, 46835-42.

Brasaemle, D. (2007) Thematic review series: adipocyte biology. The perilipin family of structural lipid droplet proteins: stabilization of lipid droplets and control of lipolysis. J. Lipid Res. **48**, 2547-2559

Brasaemle and Wolins. (2012). Packaging of Fat: An Evolving Model of Lipid Droplet Assembly and Expansion. J Biol Chem *287*, 2273-2279.

Breslow, D., Cameron, D., Collins, S., Schuldiner, M., Stewart-Ornstein, J., Newman, H., Braun, S., Madhani, H., Krogan, N., and Weissman, J. (2008). A comprehensive strategy enabling high-resolution functional analysis of the yeast genome. Nat Methods *5*, 711-718.

Brusselmans, K., De Schrijver, E., Verhoeven, G., and Swinnen, J.V., (2005). RNA interference-mediated silencing of the acetyl-CoA-carboxylase-alpha gene induces growth inhibition and apoptosis of prostate cancer cells. Cancer Res *65*, 6719-6725.

Cao, Y., Pearman, A.T., Zimmerman, G.A., McIntyre, T.M., and Prescott, S.M. (2000). Intracellular unesterified arachidonic acid signals apoptosis. Proc Natl Acad Sci *97*, 11280-11285.

Catalina-Rodriguez, O., Kolukula, V.K., Tomita, Y., Preet, A., Palmieri, F., Wellstein, A., Byers, S., Giaccia, A.J., Glasgow, E., Albanese, C., and Avantaggiati, M.L. (2012). The mitochondrial citrate transporter, CIC, is essential for mitochondrial homeostasis. Oncotarget *3,* 1220-1235.

Cermelli, S., Guo, Y., Gross, S., and Welte, M.A. (2006) The lipid-droplet proteome reveals that droplets are a protein-storage depot. Curr. Biol. **16**, 1783-1795

Chajès, V., Cambot, M., Moreau, K., Lenoir, G.M., and Joulin, V. (2006). Acetyl-CoA carboxylase alpha is essential to breast cancer cell survival. Cancer Res *66*, 5287-5294.

Choi, H.S., Sreenivas, A., Han, G.S., and Carman, G.M. (2004). Regulation of phospholipid synthesis in the yeast cki1Δeki1Δ mutant defective in the Kennedy pathway. The Cho1-encoded phosphatidylserine synthase is regulated by mRNA stability. J Biol Chem *279*, 12081-12087.

Cohen, Y., and Schuldiner, M. (2011). Cell biology in the 21st century—the revolution of high throughput microscopy methods. In: Network Biology: Methods and Applications (Methods in Molecular Biology), ed. A Emili and G Cagney, Totowa, NJ: Humana Press.

Cox, J., and Mann, M. (2008) MaxQuant enables high peptide identification rates, individualized p.p.b.-range mass accuracies and proteome-wide protein quantification. Nat. Biotechnol.,**26**, 1367

Cox, J., Neuhauser, N., Michalski, A., Scheltema, R. A., Olsen, J. V., and Mann, M. (2011) Andromeda - a peptide search engine integrated into the MaxQuant environment. J Proteome Res. **10**, 1794

Das, S.K., Eder, S., Schauer, S., Diwoky, C., Temmel, H., Guerti, B., Gorkiewicz, G., Tamilarasan, K.P., Kumari, P., Trauner, M., Zimmerman, R., Vesely, P., Haemmerle, G., Zechner, R., and Hoefler, G. (2011). Adipose triglyceride lipase contributes to cancer-associated cachexia. Science *333*, 233-238.

Daugherty, M., Polanuyer, B., Farrell, M., Scholle, M, Lykidis, A., de Crecy-Lagard, V., and Osterman, A. (2002) Complete reconstitution of the human coenzyme A biosynthetic pathway via comparative genomics. J. Biol. Chem. **277**, 21431-21439

DeBerardinis, R.J., Mancuso, A., Daikhin, E., Nissim, I., Yudkoff, M., Wehrli, S., and Thompson, C.B. (2007). Beyond aerobic glycolysis: transformed cells can engage in

glutamine metabolism that exceeds the requirement for protein and nucleotide synthesis. Proc Natl Acad Sci USA *104*, 19345-19350.

DeBerardinis, R.J., and Thompson, C.B. (2012). Cellular Metabolism and Disease: What Do Metabolic Outliers Teach Us?. Cell *148*, 1132-1144.

Defilippis, R., Chang, H., Dumont, N., Rabban, J., Chen, Y., Fontenay, G., Berman, H., Gauthier, M., Zhao, J., Hu, D., Marx, J., Tjoe, J., Ziv, E., Febbraio, M., Kerlikowske, K., Parvin, B., and Tlsty, T. (2012). CD36 Repression Activates a Multicellular Stromal Program Shared by High Mammographic Density and Tumor Tissues. Cancer Discov *2*, 826-839.

De Schrijver, E., Brusselmans, K., Heyns, W., Verhoeven, G., and Swinnen, J.V. (2003). RNA interference-mediated silencing of the fatty acid synthase gene attenuates growth and induces morphological changes and apoptosis of LNCaP prostate cancer cells. Cancer Res *63*, 3799-3804.

Ettinger, S.L., Sobel, R., Whitmore, T.G., Akbari, M., Bradley, D.R., Gleave, M.E., and Nelson, C.C. (2004). Dysregulation of sterol response element-binding proteins and downstream effectors in prostate cancer during progression to androgen independence. Cancer Res *64*, 2212-2221.

Farese, R.V. and Walther, T.C. (2009). Lipid droplets finally get a little R-E-S-P-E-C-T. Cell *139*, 855-860.

Fei, W., Shui, G., Gaeta, B., Du, X., Kuerschner, L., Li, P., Brown., A.J., Wenk, M.R., Parton, R.G., and Yang, H. (2008a). Fld1p, a functional homologue of human seipin, regulates the size of lipid droplets in yeast. J Cell Biol *180*, 473-482.

Fei, W., Alfaro, G., Muthusamy, B.P., Klaassen, Z., Graham, T.R., Yang, H., and Beh, C.T. (2008b) Genome-wide analysis of sterol-lipid storage and trafficking in Saccharomyces cerevisiae. Euk Cell *7*, 401-414.

Fei, W., Zhong, L., Ta, M.T., Shui, G., Wenk, M.R., and Yang, H. (2011) The size and phospholipid composition of lipid droplets can influence their proteome. Biochem. Biophys. Res. Commun. **415**, 455-462

Forsberg, H., and Ljungdahl, P.O. (2001). Genetic and biochemical analysis of the yeast plasma membrane Ssy1p-Ptr3p-Ssy5p sensor of extracellular amino acids. Mol Cell Biol *21*, 814-826.

Foster, L.J., de Hoog, C.L., Zhang, Y., Zhang, Y., Xie, X., Mootha, V.K., and Mann, M. (2006) A mammalian organelle map by protein correlation profiling. Cell **125**, 187-199

Fritz, V., Benfodda, Z., Rodier, G., Henriquet, C., Iborra, F., Avances, C., Allory, Y., de la Taille, A., Culine, S., Blancou, H., Cristol, J.P., Michel, F., Sardet, C., and Fajas, L. (2010). Abrogation of *de novo* lipogenesis by stearoyl-CoA desaturase 1 inhibition interferes with oncogenic signaling and blocks prostate cancer progression in mice. Mol Cancer Ther *9*, 1740-1754.

Frohlich, F., Christiano, R., and Walther, T. (2013) Native SILAC: metabolic labeling of proteins in prototroph microorganisms based on lysine synthesis regulation. Mol. Cell. Proteomics **12**, 1995-2005

Fujimoto, Y., H. Itabe, J. Sakai, M. Makita, J. Noda, M. Mori, Y. Higashi, S. Kojima, and T. Takano. (2004). Identification of major proteins in the lipid droplet-enriched fraction isolated from the human hepatocyte cell line HuH7. Biochim Biophys Acta *1644*, 47-59.

Fujimoto, T., and Parton, R.G. (2011) Not just fat: the structure and function of the lipid droplet. Cold Spring Harb. Perspect. Biol. **3**, a004838

Futschik, M.E., and Carlisle, B. (2005) Noise-robust soft clustering of gene expression time-course data. J Bioinfom. Comput. Biol. **3**, 965-988

Gaber, R.F., Copple, D.M., Kennedy, B.K., Vidal, M., and Bard. M. (1989). The yeast gene ERG6 is required for normal membrane function but is not essential for biosynthesis of the cell-cycle-sparking sterol. Mol Cell Biol *9*, 3447-3456.

Garbarino, J., Padamsee, M., Wilcox, L., Oelkers, P., D'Ambrosio, D., Ruggles, K., Ramsey, N., Jabado, O., Turkish, A., and Sturley, S. (2009). Sterol and aiacylglycerol acyltransferase deficiency triggers fatty acid-mediated cell death. J Biol Chem *284,* 30994-31005.

Ghaemmaghami, S., Huh, W., Bower, K., Howson, R.W., Belle, A., Dephoure, N., O'Shea, E., and Weissman, J. (2003) Global analysis of protein expression in yeast. Nature **425**, 737-741

Giaever, G., Chu, A.M., Ni, L., Connelly, C., Riles, L., Veronneau, S., Dow, S., Lucau-Danila, A., Anderson, K., Andre, B., Arkin, A.P., Astromoff, A., El-Bakkoury, M., Bangham, R., Benito, R., Brachat, S., Campanaro, S., Curtiss, M., Davis, K., Deutschbauer, A., Entian, K.D., Flaherty, P., Foury, F., Garfinkel, D.J., Gerstein, M., Gotte, D., Guldener, U., Hegemann, J.H., Hempel, S., Herman, Z., Jaramillo, D.F., Kelly, D.E., Kelly, S.L., Kotter, P., LaBonte, D., Lamb, D.C., Lan, N., Liang, H., Liao, H., Liu, L., Luo, C., Lussier, M., Mao, R., Menard, p., Ooi, S.L., Reveulta, J.S., Roberts, C.J., Rose, M., Ross-Macdonald, P., Scherens, B., Schimmack, G., Shafer, B., Shoemaker, D.D., Sookhai-Mahadeo, S., Storms, R.K., Stathern, J.N., Valle, G., Voet, M., Volckaert, G., Wang, C.Y., Ward, T.R., Wilhelmy, J., Winzeler, E.A., Yang, Y., Yen, G., Youngman, E., Yu, K., Bussey, H., Boeke, J.D.,

Snyder, M., Philippsen, P., Davis, R.W., and Johnston, M. (2002). Functional profiling of the Saccharomyces cerevisiae genome. Nature *418*, 387–391.

Glunde, K., Bhujwalla, Z.M., Ronen, S.M. (2011). Choline metabolism in malignant transformation. Nat Rev Cancer *11*, 835-848.

Goo, Y.H., Son, S.H., Kreienberg, P.B., and Paul, A. (2013) Novel lipid droplet-associated serine hydrolase regulates macrophage cholesterol mobilization. Arterioscler. Thromb. Vasc. Biol. 10.1161/ATVBAHA.113.302448

Goodman, J. (2008) The gregarious lipid droplet. J. Biol. Chem. **283**, 28005-28009

Göransson, O., McBride, A., Hawley, S.A., Foss, F.A., Shpiro, N., Foretz, M., Viollet, B., Hardie, D.G., and Sakamoto, K. (2007) Mechanism of action of A-769662, a valuable tool for activation of AMP-activated protein kinase. J Biol Chem *282*, 32549-32560.

Grandi, P., Emig, S., Weise, C., Hucho., F., Pohl., T., and Hurt, E.C. (1995). A novel nuclear pore protein Nup82p which specifically binds to a fraction of Nsp1p. J Cell Biol *130*, 1263-1273.

Griffiths, B., Lewis, C.A., Bensaad, K., Ros, S., Zhang, Q., Ferber, E.C., Konisti, S., Peck, B., Miess, H., East, P., Wakelam, M., Harris, A.L., and Schulze, A. (2013). Sterol regulatory element binding protein-dependent regulation of lipid synthesis supports cell survival and tumor growth. Cancer & Metabolism *1*.

Grillitsch, K., Connerth, M., Kofeler, H., Arrey, T.N., Rietschel, B., Wagner, B., Karas, M., and Daum, G. (2011) Lipid particles/droplets of the yeast *Saccharomyces cerevisiae* revisited: lipidome meets proteome. Biochim. Biophys. Acta – Mol. Cell Biol. of Lipids **1811**, 1165-1176

Guo, D., Hildebrandt, I.J., Prins, R.M., Soto, H., Mazzotta, M.M., Dang, J., Czernin, J., Shyy, J.Y., Watson, A.D., Phelps, M., Radu, C.G., Cloughesy, T.F., and Mischel, P.S. (2009a). The AMPK agonist AICAR inhibits the growth of EGFRvIII-expressing glioblastomas by inhibiting lipogenesis. Proc Natl Acad Sci *106*, 12932-12937.

Guo, D., Prins, R.M., Dang, J., Kuga, D., Iwanami, A., Soto, H., Lin, K.Y., Huang, T.T., Akhavan, D., Hock, M.B., Zhu, S., Kofman, A.A., Bensinger, S.J., Yong, W.H., Vinters, H.V., Horvath, S., WatsonA.D., Kuhn, J.G., Robins, H.,I., Mehta, M.P., Wen, P.Y., DeAngelis, L.M., Prados, M.D., Mellinghoff, I.K., Cloughesy, T.F., and Mischel, P.S. (2009b). EGFR signaling through an Akt-SREBP-1-dependent, rapamycin-resistant pathway sensitizes glioblastomas to antilipogenic therapy. Sci Signal *2*, ra82.

Guo, Y., Walther, T.C., Rao, M., Stuurman, N., Goshima, G., Terayama, K., Wong, J.S., Vale, R.D., Walter, P., and Farese, R.V. (2008). Functional genomic screen reveals genes involved in lipid-droplet formation and utilization. Nature *453,* 657-61.

Hapala, I., Marza, E., and Ferreira, T. (2011). Is fat so bad? Modulation of endoplasmic reticulum stress by lipid droplet formation. Biol Cell *103*, 271-285.

Harris, C.A., Haas, J., Streeper, R.S., Stone, S.J., Kumar, M., Yang, K., Han, X., Brownell, N., Gross, R.W., Zechner, R., Farese, R.V. (2011). DGAT enzymes are required for triacylglycerol synthesis and lipid droplets in adipocytes. J Lipid Res *52*, 657-667.

Harrison, K.D., Park, E.J., Gao, N., Kuo, A., Rush, J.S., Waechter, C.J., Lehrman, M.A., Sessa, W.C. (2011) Nogo-B receptor is necessary for cellular dolichol biosynthesis and protein N-glycosylation. EMBO J. **30**, 2490-2500

Hatzivassiliou, G., Zhao, F., Bauer, D.E., Andreadis, C., Shaw, A.N., Dhanak, D., Hingorani, S.R., Tuveson, D.A., and Thompson, C.B. (2005). ATP citrate lyase inhibition can suppress tumor cell growth. Cancer Cell *8,* 311-321.

Heier, C., Taschler, U., Rengachari, S., Oberer, M., Wolinski, H., Natter, K., Kohlwein, S.D., Leber, R., and Zimmermann, R. (2010) Identification of Yju3p as functional orthologue of mammalian monoglyceride lipase in the yeast *Saccharomyces cerevisiae*. Biochim. Biophys. Acta **1801**, 1063-1071

Horton, J., Goldstein, J.L., and Brown, M.S. (2002). SREBPs: activators of the complete program of cholesterol and fatty acid synthesis in the liver. J Clin Invest *109*, 1125-1131.

Hsu, P.P., and Sabatini, D.M. (2008). Cancer cell metabolism: Warburg and beyond. Cell *134*, 703-707.

Huh, W., Falvo, J., Gerke, L.C., Carroll, A.S., Howson, R.W., Weissman, J., and O'Shea, E. (2003). Global analysis of protein localization in budding yeast. Nature *425*, 686-691.

Igal, R.A. (2010). Stearoyl-CoA desaturase-1: a novel key player in the mechanisms of cell proliferation, programmed cell death and transformation to cancer. Carcinogenesis *31*, 1509-1515.

Ishimoto, K., Nakamura, H., Tachibana, K., Yamasaki, D., Ota, A., Hirano, K., Tanaka, T., Hamakubo, T., Sakai, J., Kodama, T., and Doi, T. (2009). Sterol-mediated Regulation of Human Lipin 1 Gene Expression in Hepatoblastoma Cells. J Biol Chem *284*, 22195-22205.

Jacquier, N., Choudhary, V., Mari, M., Toulmay, A., Reggiori, F., and Schneiter, R. (2011). Lipid droplets are functionally connected to the endoplasmic reticulum in *Saccharomyces cerevisiae*. J Cell Sci *124*, 2424-2437.

Jandrositz, A., Petschnigg, J., Zimmermann, R., Natter, K., Scholze, H., Hermetter, A., Kohlwein, S.D., and Leber, R. (2005) The lipid droplet enzyme Tgl1p hydrolyzes both steryl esters and triglycerides in the yeast, *Saccharomyces cerevisiae*. Biochim. Biophys. Acta **1735**, 50-58

Janke, c., Magiera, M.M., Rathfelder, N., Taxis, C., Reber, S., Maekawa, H., Moreno-Borchart, A., Doenges, G., Schwob, E., Schiebel, E., and Knop, M. (2004) A versatile toolbox for PCR-based tagging of yeast genes: new fluorescent proteins, more markers and promoter substitution cassettes. Yeast **21**, 947-962

Jeon, S.M., Chandel, N.S., and Hay, N. (2012). AMPK regulates NADPH homeostasis to promote tumour cell survival during energy stress. Nature *485*, 661-665.

Jose, C, Hebert-Chatelain, E., Bellance, N., Larendra, A., Su., M., Nouette-Gaulain, K., and Rossignol, R. (2011) AICAR inhibits cancer cell growth and triggers cell-type distinct effects on OXPHOS biogenesis, oxidative stress and Akt activation. BBA - Bioenergetics 1807, 707-718.

Kamisuki, S., Shirakawa, T., Kugimiya, A., Abu-Elheiga, L., Choo, H.Y., Yamada, K., Shimogawa, H., Wakil, S.J., and Uesugi, M. (2011). Synthesis and evaluation of diarylthiazole derivatives that inhibit activation of sterol regulatory element-binding proteins. J Med Chem *54*, 4923-4927.

Karanasios, E., Barbosa, A.D., Sembongi, H., Mari, M., Han, G.S., Reggiori, F., Carman, G.M., Siniossoglou, S. (May 8, 2013) Regulation of lipid droplet and membrane biogenesis by the acidic tail of the phosphatidate phosphatase Pah1p. Mol. Biol. Cell 10.1091/mbc.E13-01-0021

Kihara, A., and Igarashi, Y. (2004) FVT-1 is a mammalian 3-ketodihydrosphingosine reductase with an active site that faces the cytosolic side of the endoplasmic reticulum membrane. J. Biol. Chem. **279**, 49243-49250

Kim, J.H., Lewin, T.M., and Coleman, R.A. (2001). Expression and characterization of recombinant rat Acyl-CoA synthetases 1, 4, and 5. Selective inhibition by triacsin C and thiazolidinediones. J Biol Chem *276*, 24667-24673.

Klasson, H., Fink, G.R., and Ljungdahl, P.O. (1999). Ssy1p and Ptr3p are plasma membrane components of a yeast system that senses extracellular amino acids. Mol Cell Biol *19*, 5405-5416.

Knobloch, M., Braun, S.M., Zurkirchen, L., von Schoultz, C., Zamboni, N., Arauzo-Bravo, M.J., Kovacs, W.J., Karalay, O., Suter, U., Machado, R.A., Roccio, M., Lutolf, M.P., Semenkovich, C.F., and Jessberger, S. (2012). Metabolic control of adult neural stem cell activity by Fasn-dependent lipogenesis. Nature *493*, 226-230.

Knoll, L.J., Schall, O.R., Suzuki, I., Gokel, G.W., and Gordon, J.I. (1995). Comparison of the reactivity of tetradecenoic acids, a triacsin, and unsaturated oximes with four purified Saccharomyces cerevisiae fatty acid activation proteins. J Biol Chem *270*, 20090-20097.

Köffel et al. The *Saccharomyces cerevisiae* YLL012/YEH1, YLR020/YEH2, and TGL1 genes encode a novel family of membrane-anchored lipases that are required for steryl ester hydrolysis. Mol Cell Biol (2005) vol. 25 (5) pp. 1655-68

Krahmer, N., Guo, Y., Wilfling, F., Hilger, M., Lingrell, S., Heger, K., Newman, H., Schmidt-Supprian, M., Vance, D., Mann, M., Farese, R.F., and Walther, T. (2011)

Phosphatidylcholine synthesis for lipid droplet expansion is mediated by localized activation of CTP:phosphocholine cytidylyltransferase. Cell Metab. **14**, 504-515

Krahmer, N., Hilger, M., Kory, N., Wilfling, F., Stoehr, G., Mann, M., Farese, R.V., and Walther, T. (2013) Protein correlation profiles identify lipid droplet proteins with high confidence. Mol. Cell. Proteomics **12**, 1115-1126

Krahmer, N., Farese, R.V., and Walther, T.C. (2013). Balancing the fat: lipid droplets and human disease. EMBO Mol Med *5*, 973-983.

Kumar-Sinha, C., Ignatoski, K.W., Lippman, M.E., Ethier, S.P., and Chinnaiyan, A.M. (2003). Transcriptome analysis of HER2 reveals a molecular connection to fatty acid synthesis. Cancer Res *63*, 132-139.

Laplante, M. and Sabatini, D.M. (2009). An Emerging Role of mTOR in Lipid Biosynthesis. Curr Biol *19*, R1046-R1052.

Leber, R., E. Zinser, G. Zellnig, F. Paltauf, and G. Daum. (1994). Characterization of lipid particles of the yeast, *Saccharomyces cerevisiae*. Yeast *10*, 1421-1428.

Leber, R., Landl, K., Zinser, E., Ahorn, H., Spok, A., Kolwein, S.D., Turnowsky, F., Daum, G. (1998) Dual localization of squalene epoxidase, Erg1p, in yeast reflects a relationship between the endoplasmic reticulum and lipid particles. Mol. Biol. Cell **9**, 375-386

Lewis, C., Griffiths, B., Santos, C., Pende, M., and Schulze, A. (2011). Regulation of the SREBP transcription factors by mTORC1. Biochem Soc Trans *39*, 495-499.

Liang, G., Yang, J., Horton, J., Hammer, R.E., Goldstein, J.L., and Brown, M.S. (2002). Diminished hepatic response to fasting/refeeding and liver X receptor agonists in mice with

selective deficiency of sterol regulatory element-binding protein-1c. J Biol Chem *277*, 9520-9528.

Liu, P., Y. Ying, Y. Zhao, D.I. Mundy, M. Zhu, and Anderson, R.G. (2003). Chinese hamster ovary K2 cell lipid droplets appear to be metabolic organelles involved in membrane traffic. J Biol Chem *279*, 3787-3792.

Liu, P., Bartz, R., Zehmer, J.K., Ying, Y.S., Zhu, M., Serrero, G., and Anderson, R.G. (2007) Rab-regulated interaction of early endosomes with lipid droplets. Biochim. Biophys. Acta **1773**, 784-793

Lockshon, D, Surface, L.E., Kerr, E.O., Kaeberlein, M., and Kennedy, B.K. (2007). The sensitivity of yeast mutants to oleic acid implicates the peroxisome and other processes in membrane function. Genetics *175*, 77-91.

Loftus, T. M., Jaworsky, D. E., Frehywot, G. L., Townsend, C. A., Ronnett, G. V., Lane, M. D. and Kuhajda, F. P. (2000). Reduced food intake and body weight in mice treated with fatty acid synthase inhibitors. Science *288*, 2379-2381.

Lu, B., Morrow, J.A., and Weisgraber, K.H. (2000) Conformational reorganization of the four-helix bundle of human apolipoprotein E in binding to phospholipid. J Biol Chem *275*, 20775-81

Lupu, R. and Menendez, J.A. (2006). Pharmacological inhibitors of fatty acid synthase (FASN)-catalyzed endogenous fatty acid biogenesis: a new family of anti-cancer agents?. Curr Pharm Biotechnol *7*, 483-493.

Martin, S., and Parton, R.G. (2006) Lipid droplets: a unified view of a dynamic organelle. Nat. Rev. Mol. Cell. Biol. **7**, 373-378

Mashek, D.G., Li, L.O., and Coleman, R.A. (2006). Rat long-chain acyl-CoA synthetase mRNA, protein, and activity vary in tissue distribution and in response to diet. J Lipid Res *47*, 2004-2010.

Mashima, T., Oh-hara, T., Sato, S., Mochizuki, M., Sugimoto, Y., Yamazaki, K., Hamada, J., Tada, M., Moriuchi, T., Ishikawa, Y., Kato, Y., Tomoda, H., Yamori, T., and Tsuruo, T. (2005). p53-defective tumors with a functional apoptosome-mediated pathway: a new therapeutic target. J Natl Cancer Inst *97*, 765-777.

McGookey, D.J., and R.G. Anderson. (1983). Morphological characterization of the cholesteryl ester cycle in cultured mouse macrophage foam cells. The Journal of Cell Biology 97, 1156-1168.

Medes, G., Thomas, A., and Weinhouse, S. (1953). Metabolism of neoplastic tissue. IV. A study of lipid synthesis in neoplastic tissue slices in vitro. Cancer Res *13,* 27-29.

Menendez, J.A., and Lupu, R. (2007). Fatty acid synthase and the lipogenic phenotype in cancer pathogenesis. Nat Rev Cancer *7*, 763-777.

Metallo, C.M., Gameiro, P.A., Bell, E.L., Mattaini, K.R., Yang, J., Hiller, K., Jewell, C.M., Johnson, Z.R., Irvine, D.J., Guarente, L., Kelleher, J.K., Vander Heiden, M., Iliopoulos, O., and Stephanopoulos, G. (2012). Reductive glutamine metabolism by IDH1 mediates lipogenesis under hypoxia. Nature *481*, 380-384.

Michalik, L., Desvergne, B., and Wahli, W. (2004). Peroxisome-proliferator-activated receptors and cancers: complex stories. Nat Rev Cancer *4*, 61-70.

Migita, T., Narita, T., Nomura, K., Miyagi, E., Inazuka, F., matsuura, M., Ushijima, M., Mashima, T., Seimiya, H., Satoh, Y., Okumura, S., Nakagawa, K., and Ishikawa, Y. (2008).

ATP citrate lyase: Activation and therapeutic implications in non-small cell lung cancer. Cancer Res *68*, 8547-8554.

Milla, P., K. Athenstaedt, F. Viola, S. Oliaro-Bosso, S.D. Kohlwein, G. Daum, and Balliano, G. (2002).Yeast oxidosqualene cyclase (Erg7p) is a major component of lipid particles. J Biol Chem *277*, 2406-2412.

Mishina, M., Roggenkamp, R., and Schweizer, E. (1980). Yeast mutants defective in acetyl-coenzyme A carboxylase and biotin: apocarboxylase ligase. Eur J Biochem *111*, 79-87.

Mo, C., M. Valachovic, S.K. Randall, J.T. Nickels, and Bard, M. (2002). Protein-protein interactions among C-4 demethylation enzymes involved in yeast sterol biosynthesis. Proc Natl Acad Sci USA *99*, 9739-9744.

Mo, C., P. Milla, K. Athenstaedt, R. Ott, G. Balliano, G. Daum, and Bard, M. (2003). In yeast sterol biosynthesis the 3-keto reductase protein (Erg27p) is required for oxidosqualene cyclase (Erg7p) activity. Biochim Biophys Acta *1633*, 68-74.

Mullen, A.R., Wheaton, W.W., Jin, E.S., Chen, P.H., Sullivan, L.B., Cheng, T., Yang, Y., Linehan, W.M., Chandel, N.S., and DeBerardinis, R.J. (2012). Reductive carboxylation supports growth in tumour cells with defective mitochondria. Nature *481,* 385-388.

Natter, K., Leitner, P., Faschinger, A., Wolinski, H., McCraith, S., Fields, S., and Kohlwein, S.D. (2005). The spatial organization of lipid synthesis in the yeast *Saccharomyces cerevisiae* derived from large scale green fluorescent protein tagging and high resolution microscopy. Mol Cell Proteomics *4,* 662-672.

Nelson, B., Kurischko, C., Horecka, J., Mody, M., Nair, P., Pratt, L., Zougman, A., McBroom, L.D., Hughes, T., Boones, C., and Luca, F.C. (2003). RAM: a conserved signaling network

that regulates Ace2p transcriptional activity and polarized morphogenesis. Mol Biol Cell *14*, 3782-3803.

Nieman, K.M., Kenny, H.A., Penicka, C.V., Ladanyi, A., Buell-Gutbrod, R., Zillhardt, M.R., Romero, I.L., Carey, M.S., Mills, G.B., Hotamisligil, G.S., Yamada, S.D., Peter, M.E., Gwin, K., and Lengyel, E. (2011). Adipocytes promote ovarian cancer metastasis and provide energy for rapid tumor growth. Nat Med *17*, 1498-1503.

Nomura, D.K., Long, J.Z., Niessen, S., Hoover, H.S., Ng, S., and Cravatt, B.F. (2010). Monoacylglycerol lipase regulates a fatty acid network that promotes cancer pathogenesis. Cell *140*, 49-61.

Nourbakhsh, M., Douglas, D.N., Pu, C.H., Lewis, J.T., Kawahara, T., Lisboa, L.F., Wei, E., Asthana, S., Quiroga, A.D., Law, L.M.J., Chen, C., Addison, W.R., Nelson, R., Houghton, M., Lehner, R., and Kneteman, N.M. (2013) Arylacetamide deacetylase: A novel host factor with important roles in the lipolysis of cellular triacylglycerol stores, VLDL assembly and HCV production. J Hepatology *59*, 336-343.

Ogretmen, B. and Hannun, Y. (2004). Biologically active sphingolipids in cancer pathogenesis and treatment. Nat Rev Cancer *4*, 604-616.

Ohsaki, Y., Cheng, J., Fujita, A., Tokumoto, T., Fujimoto, T. (2006). Cytoplasmic lipid droplets are sites of convergence of proteasomal and autophagic degradation of apolipoprotein B. Mol Biol Cell *17*, 2674-2683.

Ohsaki, Y., Cheng, J., Suzuki, M., Fujita, A., Fujimoto, T. (2008) Lipid droplets are arrested in the ER membrane by tight binding of lipidated apolipoprotein B-100. J Cell Sci *121*, 2415-2422

Olzhausen, J., Moritz, T., Neetz, T., and Schuller, H. (2013) Molecular characterization of the heteromeric coenzyme A-synthesizing protein complex (CoA-SPC) in the yeast *Saccharomyces cerevisiae*. FEMS Yeast Res. **13**, 565-573

Ong, S.E., Blagoev, B., Kratchmarova, I., Kristensen, D.B., Steen, H., Pandey, A., and Mann, M. (2002) Stable isotope labeling by amino acids in cell culture, SILAC, as a simple and accurate approach to expression proteomics. Mol. Cell. Proteomics **1**, 376-386

Ookhtens, M., Kannan, R., Lyon, I., and Baker, N. (1984). Liver and adipose tissue contributions to newly formed fatty acids in an ascites tumor. Am J Physiol *247,* R146-R153.

Ozeki, S., Cheng, J., Tauchi-Sato, K., Hatano, N., Taniguchi, H., and Fujimoto, T. (2005) Rab18 localizes to lipid droplets and induces their close apposition to the endoplasmic reticulum-derived membrane. J. Cell Sci. **118,** 2601-2611

Paton, C.M., and Ntambi, J.M. (2009). Biochemical and physiological function of stearoyl-CoA desaturase. Am J Physiol Endocrinol Metab *297*, E28-E37.

Peet, D.J., Turley, S.D., Ma, W., Janowski, B.A., Lobaccaro, J.M., Hammer, R.E., and Mangelsdorf, D.J. (1998). Cholesterol and bile acid metabolism are impaired in mice lacking the nuclear oxysterol receptor LXR alpha. Cell *93*, 693-704.

Peterson, T.R., Sengupta, S.S., Harris, T.E., Carmack, A.E., Kang, S.A., Balderas, E., Guertin, D.A., Madden, K.L., Carpenter, A.E., Finck, B.N., and Sabatini, D.M. (2011). mTOR complex 1 regulates lipin 1 localization to control the SREBP pathway. Cell *146*, 408-420.

Petschnigg, J., Wolinski, H., Kolb, D., Zellnig, G., Kurat, C., Natter, K., and Kohlwein, S. (2009). Good fat - essential cellular requirements for triacylglycerol synthesis to maintain membrane homeostasis in yeast. J Biol Chem *284*, 30981-30993.

Pike, L.S., Smift, A.L., Croteau, N.J., Ferrick, D.A., and Wu, M. (2011). Inhibition of fatty acid oxidation by etomoxir impairs NADPH production and increases reactive oxygen species resulting in ATP depletion and cell death in human glioblastoma cells. Biochim Biophys Acta *1807*, 726-734.

Pizer, E.S., Thupari, J., Han., W.F., Pinn, M.L., Chrest, F.J., Frehywot, G.L., Townsend, C.A., and Kuhajda, F.P. (2000). Malonyl-coenzyme-A is a potential mediator of cytotoxicity induced by fatty-acid synthase inhibition in human breast cancer cells and xenografts. Cancer Res *60*, 213-218.

Pollak, M.N. (2012). Investigating metformin for cancer prevention and treatment: the end of the beginning. Cancer Discov *2*, 778-790.

Prein, B., Natter, K., and Kohlwein, S.D. (2000) A novel strategy for constructing N-terminal chromosomal fusions to green fluorescent protein in the yeast *Saccharomyces cerevisiae*. FEBS Letters **485**, 29-34

Pu, J., Ha, C., Zhang, S., Jung, J., Huh, W., and Liu, P. (2011) Interactomic study on interaction between lipid droplets and mitochondria. Protein Cell **2** 487-496

Radulovic, M., Knittelfelder, O., Cristobal-Sarramian, A., Kolb, D., Wolinski, H., and Kohlwein, SD. (2013). The emergence of lipid droplets in yeast: current status and experimental approaches. Curr Genet *59*, 231-242.

Resh, M.D. (2012). Targeting protein lipidation in disease. Trends Mol Med *18*, 206-214.

Rimokh, R., Gadoux, M., Bertheas, M.F., Berger, F., Garoscio, M., Deleage, G., Germain, D., and Magaud, J.P. (1993) FVT-1, a novel human transcription unit affected by variant translocation t(2;18)(p11;q21) of follicular lymphoma. Blood **81**, 136-142

Roongta, U.V., Pabalan, J.G., Wang, X., Ryseck, R.P., Fargnoli, J., Henley, B.J., Yang, W.P., Zhu, J., Madireddi, M.T., Lawrence, R.M., Wong, T.W., and Rupnow, B.A. (2011). Cancer cell dependence on unsaturated fatty acids implicates stearoyl-CoA desaturase as a target for cancer therapy. Mol Cancer Res *9,* 1551-1561.

Ros, S., Santos, C.R., Moco, S., Baenke, F., Kelly, G., Howell, M., Zamboni, N., and Schulze, A. (2012). Functional metabolic screen identifies 6-phosphofructo-2-kinase/fructose-2,6-biphosphatase 4 as an important regulator of prostate cancer cell survival. Cancer Discov *2*, 328-343.

Samudio, I., Harmancey, R., Fiegl, M., Kantarjian, H., Konopleva, M., Korchin, B., Kaluarachchi, K., Bornmann, W., Duvvuri, S., Taegtmeyer, H., and Andreeff, M. (2010). Pharmacologic inhibition of fatty acid oxidation sensitizes human leukemia cells to apoptosis induction. J Clin Invest *120*, 142-156.

Sandager, L., Gustavsson, M.H., Stahl, U., Dahlqvist, A., Wiberg, E., Banas, A., Lenman, M., Ronne, H., Stymne, S. (2002). Storage lipid synthesis is non-essential in yeast. J Biol Chem *277*, 6478-6482.

Santos, C.R., and Schulze, A. (2012). Lipid metabolism in cancer. FEBS J *279*, 2610-2623

Sato, M., Sato, K., Nishikawa, S., Hirata, A., Kato, J., and Nakano, A. (1999) The yeast RER2 gene, identified by endoplasmic reticulum protein localization mutations, encodes cis-prenyltransferase, a key enzyme in dolichol synthesis. Mol. Cell. Biol. **19**, 471-483

Sato, M., Fujisaki, S., Sato, K., Nishimura, Y., and Nakano, A. Yeast (2001) *Saccharomyces cerevisiae* has two cis-prenyltransferases with different properties and localizations. Implication for their distinct physiological roles in dolichol synthesis. Genes Cells **6**, 495-506

Schnabl, M., Oskolkova, O.V., Holic, R., Brezna, B., Pichler, H., Zagorsek, M., Kohlwein, S.D., Paltauf, F., Daum, G., and Griac, P. (2003) Subcellular localization of yeast Sec14 homologues and their involvement in regulation of phospholipid turnover. Eur. J. Biochem. **270**, 3133-3145

Schneiter, R., Brugerr, B., Sandhoff, R., Zellnig, G., Leber, A., Lampl, M., Athenstaedt, K., Hrastnik, C., Eder, S., Daumg, G., Paltauf, F., Wieland, F.T., Kohlwein, S.D. (1999). Electrospray ionization tandem mass spectrometry (ESI-MS/MS) analysis of the lipid molecular species composition of yeast subcellular membranes reveals acyl chain-based sorting/remodeling of distinct molecular species en route to the plasma membrane. J Cell Biol *146*, 741-754.

Schuldiner, M., Collins, S., Thompson, N.J., Denic, V., Bhamidipati, A., Punna, T., Ihmels, J., Anrews, B., Boone, C., Greenblatt, J., Weissman, J., and Krogan, N. (2005). Exploration of the function and organization of the yeast early secretory pathway through an epistatic miniarray profile. Cell *123*, 507-519.

Schulze, A., and Harris, A.L. (2012). How cancer metabolism is tuned for proliferation and vulnerable to disruption. Nature *491*, 364-373.

Shao, W. and Espenshade, P.J. (2012). Expanding roles for SREBP in metabolism. Cell Metabolism *16*, 414-419.

Shaw, C.S., Jones, D.A., and Wagenmakers, A.J. (2008) Network distribution of mitochondria and lipid droplets in human muscle fibres. Histochem. Cell Biol. **129**, 65-72

Simockova, M., Holic, R., Tahotna, D., Patton-Vogt, J., and Griac, P. (2008). Yeast Pgc1p (YPL206c) Controls the Amount of Phosphatidylglycerol via a Phospholipase C-type Degradation Mechanism. J Biol Chem *283*, 17107-17115.

Sorger, D., and Daum, G. (2002) Synthesis of triacylglycerols by the acyl-coenzyme A:diacyl-glycerol acyltransferase Dga1p in lipid particles of the yeast *Saccharomyces cerevisiae*. J. Bacteriol. **184**, 519-524

Sorger, D., Athenstaedt, K., Hrastnik, C., and Daum, G. (2004) A yeast strain lacking lipid particles bears a defect in ergosterol formation. J. Biol. Chem. **279**, 31190-31196

Sozio, M.S., S. Liangpunsakul, and D. Crabb. (2010). The role of lipid metabolism in the pathogenesis of alcoholic and nonalcoholic hepatic steatosis. Semin Liver Dis, *30* 378-390.

Stolz, J. and Sauer, N. (1999). The fenpropimorph resistance gene FEN2 from Saccharomyces cerevisiae encodes a plasma membrane H+-pantothenate symporter. J Biol Chem *274*, 18747-18752.

Swinnen, J.V., Bekers, A., Brusselmans, K., Organe, S., Segers, J., Timmermans, L., Vanderhoydonc, F., Deboel, L., Derua, R., Waelkens, E., De Schrijver, E., Van de Sande, T., Noel, A., Foufelle, F., and Verhoeven, G. (2005) Mimicry of a cellular low energy status blocks tumor cell anabolism and suppresses the malignant phenotype. Cancer Res *65*, 2441-2448.

Swinnen, J.V., Brusselmans, K., and Verhoeven, G. (2006). Increased lipogenesis in cancer cells: new players, novel targets. Curr Opin Clin Nutr Metab Care *9*, 358-365.

Szymanski, K.M., Binns, D., Bartz, R., Grishin, N.V., Li, W.P., Agarwal, A.K., Garg, A., Anderson, R.G., and Goodman, J.M. (2007). The lipodystrophy protein seipin is found at

endoplasmic reticulum lipid droplet junctions and is important for droplet morphology. Proc Natl Acad Sci USA *104*, 20890-20895.

Takeuchi, K., and Reue, K. (2009). Biochemistry, physiology, and genetics of GPAT, AGPAT, and lipin enzymes in triglyceride synthesis. Am J Physiol Endocrinol Metab *296*, E1195-E1209.

Thiam, A.R., Farese, R.V., and Walther, T.C. (2013). The biophysics and cell biology of lipid droplets. Nat Rev Mol Cell Biol *14*, 775-86.

Thiel, K., Heier, C., Haberl, V., Thul, P., Oberer, M., Lass, A., Jackle, H., and Beller, M. (2013) The evolutionarily conserved protein CG9186 is associated with lipid droplets, required for their positioning and for fat storage. J. Cell Sci. **126**, 2198-2212

Thoms, S., Debelyy, M., Connerth, M., Daum, G., and Erdmann, R. (2011) The putative *Saccharomyces cerevisiae* hydrolase Ldh1p is localized to lipid droplets. Euk. Cell **10**, 770-775

Tiwari, R., Koffel, R., and Schneiter, R. (2007). An acetylation/deacetylation cycle controls the export of sterols and steroids from S. cerevisiae. EMBO J *26*, 5109-5119.

Tiwari, R., and Schneiter, R. (2009) Sterol acetylation and export from yeast and mammalian cells. VDM Verlag Dr. Müller. ISBN 978-3-639-16998

Tong, A.H., Evanglista, M., Parsons, A.B., Xu, H., Bader, G.D., Page, N., Robinson, m., Raghibizadeh, S., Hogue, C.W., Bussey, H., Andrews, B., Tyers, M., and Boone, C. (2001). Systematic genetic analysis with ordered arrays of yeast deletion mutants. Science *294*, 2364–2368.

Tong, A.H., and Boone, C. (2006). Synthetic genetic array analysis in Saccharomyces cerevisiae. Methods Mol Biol *313*, 171–192.

Turró, S., M. Ingelmo-Torres, J.M. Estanyol, F. Tebar, M.A. Fernández, C.V. Albor, K. Gaus, T. Grewal, C. Enrich, and Pol, A. (2006) Identification and characterization of associated with lipid droplet protein 1: A novel membrane-associated protein that resides on hepatic lipid droplets. Traffic, *7* 1254-1269.

Umlauf, E., E. Csaszar, M. Moertelmaier, G.J. Schuetz, R.G. Parton, and R. Prohaska. (2004). Association of stomatin with lipid bodies. J Biol Chem *279*, 23699-23709.

Van Horn, C.G., Caviglia, J.M., Li, L.O., Wang, S., Granger, D.A., and Coleman, R.A. (2005). Characterization of recombinant long-chain rat acyl-CoA synthetase isoforms 3 and 6: identification of a novel variant of isoform 6. Biochemistry *44*, 1635-1642.

van Manen, H.J., Kraan, Y.M., Roos, D., and Otto, C. (2005) Single-cell Raman and fluorescence microscopy reveal the association of lipid bodies with phagosomes in leukocytes. Proc. Natl. Acad. Sci. USA **102,** 10159-10164

Verstrepen, K.J., Van Laere, S.D., Vercammen, J., Derdelinckx, G., Dufour, J.P., Pretorius, I.S., Winderickx, J., Thevelein, J.M., and Delvaux, F.R. (2004) The *Saccharomyces cerevisiae* alcohol acetyl transferase Atf1p is localized in lipid particles. Yeast **21**, 367-377

Viennois, E., Mouzat, K., Dufour, J., Morel, L., Lobacaro, J., and Baron, S. (2012). Selective liver X receptor modulators (SLiMs): What use in human health?. Mol Cell Endocr *351*, 129-141.

Wakil, S.J., and Abu-Elheiga, L.A. (2008). Fatty acid metabolism: target for metabolic syndrome. J Lipid Res *50*, S138-S143.

Wang, C.W., and Lee, S.C. (2012) The ubiquitin-like (UBX)-domain-containing protein Ubx2/Ubxd8 regulates lipid droplet homeostasis. J. Cell Sci. **125**, 2930-2939

Wang, C.W., Miao, Y.H., and Chang, Y.S. (January 16, 2014) Size control of lipid droplets in budding yeast requires a collaboration of Fld1 and Ldb16. J. Cell Sci. 10.1242/ jcs.137737

Walther, T.C., and Farese, R.V. (2012) Lipid droplets and cellular lipid metabolism. Annu. Rev. Biochem. **81,** 687-714

Wan, H.C., R.C. Melo, Z. Jin, A.M. Dvorak, and P.F. Weller. (2007). Roles and origins of leukocyte lipid bodies: proteomic and ultrastructural studies. FASEB J *21*, 167-178.

Wanner, G., Formanek, H., and Theimer, R.R. (1981) The ontogeny of lipid bodies (spherosomes) in plant cells. Planta *151*, 109-123

Warburg, O. (1956). On the origin of cancer cells. Science *123*, 309-314.

Wellen, K.E., Hatzivassiliou, G., Sachdeva, U.M., Bui, T.V., Cross, J.R., and Thompson, C.B. (2009). ATP-citrate lyase links cellular metabolism to histone acetylation. Science *324*, 1076-1080.

Weng, J., Chen, C.Y., Pinzone, J.J., Ringel, M.D., Chen, C.S. (2006). Beyond peroxisome proliferator-activated receptor gamma signaling: the multi-facets of the antitumor effect of thiazolidinediones. Endocr Relat Cancer *13*, 401-413.

Wilfling., F., Wang, H., Haas, J., Krahmer, N., Gould, T., Uchida, A., Cheng, J., Graham, M., Christiano, R., Frohlich, F., Liu X., Buhman, K., Coleman, R., Bewersdorf, J., Farese, R.F., and Walther, T. (2013). Triacylglycerol synthesis enzymes mediate lipid droplet growth by relocalizing from the ER to lipid droplets. Dev Cell *24*, 384-399.

Wilfling, F., Haas, J.T., Walther, T.C., Farese, Jr., R.V. (2014) Lipid Droplet Biogenesis. Curr. Opin. Cell Biol. In Press.

Williams, K., Argus, J., Zhu, Y., Wilks, M., Marbois, B., York, A., Kidani, Y., Pourzia, A., Akhavan, D., Lisiero, D., Komisopouou, E., Henkin, A., Soto, H., Chamberlain, B., Vergnes, l., Jung, M., Torres, J., Liau, L., Christofk, H., Prins, R., Mischel, P., Reue, K., Graeber, T., and Bensinger, S. (2013) An essential requirement for the SCAP/SREBP signaling axis to protect cancer cells from lipotoxicity. Cancer Res. Online First.

Wise, D.R., DeBerardinis, R.J., Mancuso, A., Sayed, N., Zhang, X.Y., Pfeiffer, H.K., Nissim, I., Daikhin, E., Yudkoff, M., McMahon, S.B., and Thompson, C.B. (2008). Myc regulates a transcriptional program that stimulates mitochondrial glutaminolysis and leads to glutamine addiction. Proc Natl Acad Sci *105*, 18782-18787.

Wymann, M.P., and Schneiter, R. (2008). Lipid signalling in disease. Nat Rev Mol Cell Biol *9,* 162-176.

Xu, N., Zhang, S.O., Cole, R.A., McKinney, S.A., Guo, F., Haas, J., Bobba, S., Farese, R.V., and Mak, H.Y. (2012). The FATP1-DGAT2 complex facilitates lipid droplet expansion at the ER-lipid droplet interface. J Cell Biol *198*, 895-911.

Yamashita, Y., Kumabe, T., Cho, Y.Y., Watanabe, M., Kawagishi, J., Yoshimoto, T., Fujino, T., Kang, M.J., and Yamamoto, T.T. (2000). Fatty acid induced glioma cell growth is mediated by the acyl-CoA synthetase 5 gene located on chromosome 10q25.1-q25.2, a region frequently deleted in malignant gliomas. Oncogene *19,* 5919-5925.

Yang, H., Hsu, C., Yang, J., and Yang, W. (2012) Monodansylpentane as a blue-fluorescent lipid-droplet marker for multi-color live-cell imaging. PLoS ONE **7**, e32693

Yokoyama, Y., and Mizunuma, H. (2010). Peroxisome proliferator-activated receptor and epithelial ovarian cancer. Eur J Gynaecol Oncol *31*, 612-615.

Zaugg, K., Yao, Y., Reilly, P.T., Kannan, K., Kiarash, R., Mason, J., Huang, P., Sawyer, S.K., Fuerth, B., Faubert, B., Kalliomaki, T., Elia, A., Luo, X., Nadeem, V., Bungard, D., Yalavarthi, S., Growney, J.D., Wakeham, A., Moolani, Y., Silvester, J., Ten, A.Y., Bakker W., Tsuchihara, K., Berger, S., Hill, R.P., Jones, R.G., Tsao, M., Robinson, M.O., Thompson, C.B., Pan, G., and Mak, T.W. (2011). Carnitine palmitoyltransferase 1C promotes cell survival and tumor growth under conditions of metabolic stress. Genes Dev *25*, 1041-1051.

Zhou, W., Tu, Y., Simpson, P.J., and Kuhajda, F.P. (2009). Malonyl-CoA decarboxylase inhibition is selectively cytotoxic to human breast cancer cells. Oncogene *28*, 2979-2987.

Zinser, E, Paltauf, F., and Daum, G. (1993) Sterol composition of yeast organelle membranes and subcellular distribution of enzymes involved in sterol metabolism. J. Bacteriol. **175**, 2853-2858

Zou, Z., Tong, F., Faergeman, N.J., Borsting, C., Black, P.N., and Dirusso, C.C. (2003). Vectorial acylation in Saccharomyces cerevisiae. Fat1p and fatty acyl-CoA synthetase are interacting components of a fatty acid import complex. J Biol Chem *278*,16414-16422.

Zinser, E., F. Paltauf, and Daum, G. (1993). Sterol composition of yeast organelle membranes and subcellular distribution of enzymes involved in sterol metabolism. J Bacteriol *175*, 2853-2858.

Züchner, S., Dallman, J., Wen, R., Beecham, G., Naj, A., Farooq, A., Kohli, M.A., Whitehead, P.L., Hulme, W., Konidari, I., Edwards, Y.J., Cai, G., Peter, I., Seo, D., Buxbaum, J.D.,

Haines, J.L., Blanton, S., Young, J., Alfonso, E., Vance, J.M., Lam, B.L., and Pericak-Vance, M.A. (2011) Whole-exome sequencing links a variant in DHDDS to retinitis pigmentosa. Am. J. Hum. Genet. **88**, 201-206

Zweytick, D., K. Athenstaedt, and G. Daum. (2000). Intracellular lipid particles of eukaryotic cells. Biochim Biophys Acta *1469*, 101-120.

Appendix: Protocols developed in Farese Lab

1. *In Vitro* Cholesteryl-Acetate Deacetylase Activity Assay (Say1 Assay)
2. *In Vitro* Cis-Isoprenyl Transferase Activity Assay (Rer2 Assay)
3. Western Blots from Cell Fractions
4. Whole Cell Yeast Western Blots
5. Yeast UPR assay by UPRE-lacZ
6. Yeast Lipid Extraction and Thin Layer Chromatography (TLC)
7. Screen for Yeast Growth on Various Carbon Sources

In vitro cholestryl-acetate deacetylase activity assay (Say1 assay)

Cell Fractionation

1. Grow 250mL cells to stationary phase.
   Do not grow them for too long as the longer cells are in stationary phase the thicker their cell walls become and so the more refractory there are to spheroplasting.
2. Centrifuge 4,000rpm for 5 min.
3. Resuspend in 25mL washing buffer and move to 50mL Falcon tubes.
4. Shake 10 min at 30C.
5. Centrifuge 4,000rpm for 5min.
6. Resuspend in 25mL spheroplast buffer.
7. Centrifuge 4,000rpm for 5min.
8. Weigh pellets.
9. Resuspend in XmL spheroplast buffer (to .2g/mL).
10. Add 20mg/g Zymolyase 20T. Incubate in 30C shaker 1hr.
    You can also use Zymolyase 100T at 4mg/g or lyticase at 3150U/g.
11. Centrifuge 4,000rpm for 5min.
12. Wash with 10mL cold lysis buffer. All steps from here ON ICE.
13. Centrifuge 4,000rpm for 5min.
14. Resuspend spheroplasts in 1-2 mL lysis buffer.
    You want to use the smallest volume that you can because the denser the cell suspension is the better the cells break in the homogenizer.
15. Manually homogenize in a dounce homogenizer for 40 strokes.
    I use a 7-mL homogenizer. If you have a smaller one that's great, just don't go larger.
16. Pour dounced cells into a 15mL falcon tube. Rinse the dounce with 1 mL lysis buffer and collect to minimize cell lysis stuck to the dounce. Your total volume should be about 3-3.5mL.
17. Centrifuge 4C 300g 30min. Collect 200uL as your whole cell fraction. Transfer the rest of the supernatant to 2mL tubes for TLS-55.
    There will be many unbroken cells in the first spin which is why you collect your whole cell fraction after the first spin and not before.
18. Centrifuge 4C 100,0000g 30min (TLS-55 34,200rpm).
19. Slice off LD fraction by slicing off the top 300-500uL.
20. Collect the rest of the supernatant as the cytoplasm.
21. Gently rinse the 100K pellet twice with 1mL lysis buffer and resuspend the 100K pellet in 250uL lysis buffer.
22. Optional: Add 1mL lysis buffer to the LD fraction. Spin max speed 10m 4C. Insert a syringe underneath the floating LD layer and remove 1mL. Repeat.
    This reduces the amount of cytoplasm in the LD fraction but requires additional time and handling of the samples and can be a source of loss of LD protein as well.

Assay

23. Extract the radioactive substrate immediately before running the assay by running it on TLC (petroleum ether: diethyl ether: acetic acid (70:30:2)), scraping the CA band, extracting it in 3 mL 2:1 $CHCl_3$:MetOH twice, drying it, and resuspending it in EtOH.

24. Calculate the protein concentration of each fraction.
    You will probably need to make 1:5 dilutions to be in the linear range of the Bradford assay.
25. Transfer 200ug protein in 50uL lysis buffer of each cell fraction (WC, M, C, LD) to 1.5 mL eppendorf tubes. Also run a no-protein control lane.
26. Add 150uL of assay buffer.
27. Incubate 30C 60m with shaking.
28. Stop assay by adding 300uL CHCl3.
29. Add 600 uL MetOH. Vortex well until clear (~5min).
30. Add 300 uL acidified water. Vortex 1m.
31. Centrifuge max speed 2m RT to get two layers. Upper aqueous, lower organic.
32. Discard upper layer.
33. Add 300uL choloroform and 600 uL acidified water.
34. Vortex 1m. Centrifuge.
35. Transfer lower organic layer to fresh tube and dry under nitrogen.

TLC

36. Saturate TLC chamber with petroleum ether: diethyl ether: acetic acid (70:30:2) for 1-2 hrs before TLC run.
37. Add 40uL CHCl3:MetOH (1:1) to each tube. Vortex and load to silica gel TLC plates. Run a cold cholesterol standard on each end of the TLC plate.
38. Run for 35m. Leave under hood to evaporate solvent.
39. Expose the plate to iodine and image.
    This is so that you can measure the Rf value of cholesterol each experiment.
40. Expose to phosphor imaging screen 3 days and scan on the Typhoon.
    Note that the free cholesterol band will be a minor band when compared to all sorts of other bands you see on the plate.

Wash Buffer [Make Fresh]	For 150mL
.1M TrisCl pH9.0	15mL 1M TrisCl pH9.0
10mM DTT	.231g DTT

Spheroplast Buffer	For 150mL
1.3M Sorbitol	23.7g sorbitol
25mM Hepes-KOH pH7.5	2.5mL 1M Hepes-KOH pH7.5
20mM DTT	.31g DTT
5mM MgCl2	.75mL 1M $MgCl_2$

Lysis Buffer	for 50mL
200mM Sorbitol	1.54g sorbitol
10mM Hepes-KOH pH7.5	.5mL 1M Hepes-KOH pH7.5
100mM NaCl	1mL 5M NaCl
5mM $MgCl_2$	.25mL 1M $MgCl_2$
1mM EDTA	.5mL .1M EDTA

Assay Buffer [Final]	for 50mL 2X Assay Buffer
100mM phosphate buffer pH 6.9	10mL 1M phosphate buffer pH 6.9
.3% Triton X-100	.3mL Triton X-100

Mix per reaction [200uL finished reaction size]:
[200ug protein in 50uL sample]
100uL buffer
39uL water
10uL 10mg/mL in EtOH cold cholesteryl acetate
1.43 ul 14C-cholesteryl acetate (.143 uCi of 55uCi/mmol)

Total amounts per rxn:
2.6 nmol 14C-cholesteryl acetate (.143 uCi of 55uCi/mmol)
23.4 nmol cholesteryl acetate

Acidified water	for 50mL
2.8% ortho-phosphoric acid	1.65mL 85% H_3PO_4
	48.35 mL water

100mL 1M phosphate buffer pH 6.9
52mL 1M Na_2HPO_4
48mL 1M NaH_2PO_4

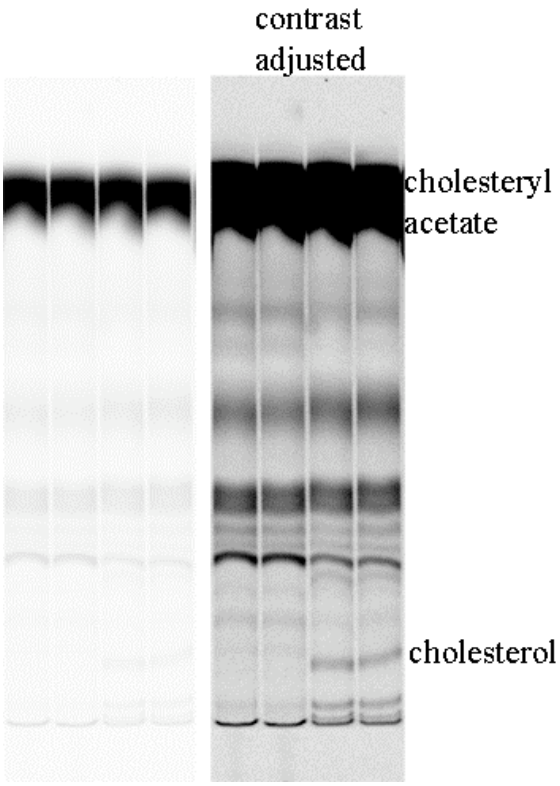

Sample of experimental results. Free cholesterol is present in lanes 3-4. Identity of other bands is unknown.

In Vitro Cis-Isoprenyl Transferase Activity Assay (Rer2 Assay)

Cell Fractionation

1. Grow 250mL cells to stationary phase.
   Do not grow them for too long as the longer cells are in stationary phase the thicker their cell walls become and so the more refractory there are to spheroplasting.
2. Centrifuge 4,000rpm for 5 min.
3. Resuspend in 25mL washing buffer and move to 50mL Falcon tubes.
4. Shake 10 min at 30C.
5. Centrifuge 4,000rpm for 5min.
6. Resuspend in 25mL spheroplast buffer.
7. Centrifuge 4,000rpm for 5min.
8. Weigh pellets.
9. Resuspend in XmL spheroplast buffer (to .2g/mL).
10. Add 20mg/g Zymolyase 20T. Incubate in 30C shaker 1hr.
    You can also use Zymolyase 100T at 4mg/g or lyticase at 3150U/g.
11. Centrifuge 4,000rpm for 5min.
12. Wash with 10mL cold lysis buffer. All steps from here ON ICE.
13. Centrifuge 4,000rpm for 5min.
14. Resuspend spheroplasts in 1-2 mL lysis buffer.
    You want to use the smallest volume that you can because the denser the cell suspension is the better the cells break in the homogenizer.
15. Manually homogenize in a dounce homogenizer for 40 strokes.
    I use a 7-mL homogenizer. If you have a smaller one that's great, just don't go larger.
16. Pour dounced cells into a 15mL falcon tube. Rinse the dounce with 1 mL lysis buffer and collect to minimize cell lysis stuck to the dounce. Your total volume should be about 3-3.5mL.
17. Centrifuge 4C 300g 30min. Collect 200uL as your whole cell fraction. Transfer the rest of the supernatant to 2mL tubes for TLS-55.
    There will be many unbroken cells in the first spin which is why you collect your whole cell fraction after the first spin and not before.
18. Centrifuge 4C 100,0000g 30min (TLS-55 34,200rpm).
19. Slice off LD fraction by slicing off the top 300-500uL.
20. Collect the rest of the supernatant as the cytoplasm.
21. Gently rinse the 100K pellet twice with 1mL lysis buffer and resuspend the 100K pellet in 250uL lysis buffer.
22. Optional: Add 1mL lysis buffer to the LD fraction. Spin max speed 10m 4C. Insert a syringe underneath the floating LD layer and remove 1mL. Repeat.
    This reduces the amount of cytoplasm in the LD fraction but requires additional time and handling of the samples and can be a source of loss of LD protein as well.

Assay

23. Calculate the protein concentration of each fraction.
    You will probably need to make 1:5 dilutions to be in the linear range of the Bradford assay.

24. Transfer 100ug protein to each cell fraction (WC, M, C, LD) to 16x100mm glass tubes and bring volume to 75.8uL with water. Also run a no-protein control lane.
25. Create a master mix with FPP, 14C-IPP, and 5X reaction buffer and transfer 24.2 uL to each reaction tube.
26. Incubate 30C 1h with gentle shaking.
    I do this in the rocking waterbath in the radioactive room with the waterbath set to 30C and the bottom 1" of the tubes in the water.
27. Quench the reaction by adding 2mL $CHCl_3$:MeOH (2:1).
    Your life will be a lot easier and your experiment more accurate if you have a repeat pipetter for this part of the assay.
28. Add .8mL .9% NaCl.
    This further separates the hydrophobic products from unreacted water soluble IPP.
29. Suck the aqueous phase from the top of the tube and put it to rad waste.
30. Wash the organic phase 3 times with 2mL $CHCl_3$:MeOH:dH_2O (3:48:47), sucking off the upper aqueous phase each time and putting it to rad waste.
31. Dry samples under nitrogen.

TLC:

32. Saturate TLC chamber with hexane:ethyl acetate (80:20) for 1-2 hrs before TLC run.
41. Add 50uL n-hexane to each tube. Vortex and load to silica gel TLC plates. Repeat 50uL load. Run a cold dolichol standard on each end of the TLC plate.
42. Run until the solvent reaches the top of the TLC plate.
43. Expose the plate to iodine and image.
    This is so that you can measure the Rf value of dolichol each experiment.
44. Expose to phosphor imaging screen 3 days and scan on the Typhoon.
45. Either on the computer or on a true-size print of the phosphor image, measure the distance from the origin to the dolichol band. On your TLC plate, gently draw in pencil a 1" distance around the dolichol band. Scrape each lane in this 1" block and count on the scintillation counter.
    The distance to the dolichol band can vary across the TLC plate so you may need to make multiple measurements.

Wash Buffer [Make Fresh]	For 150mL
.1M TrisCl pH9.0	15mL 1M TrisCl pH9.0
10mM DTT	.231g DTT

Spheroplast Buffer	For 150mL
1.3M Sorbitol	23.7g sorbitol
25mM Hepes-KOH pH7.5	2.5mL 1M Hepes-KOH pH7.5
20mM DTT	.31g DTT
5mM MgCl2	.75mL 1M $MgCl_2$

Cis-IPTase reaction buffer	for 10mL 5X buffer
60mM HEPES, pH 8.5	5mL .6M HEPES pH 8.5
5mM $MgCl_2$	250uL 1M $MgCl_2$
2mM DTT	(500uL .2M DTT add fresh)

2mM NaF	500uL .2M NaF
2mM sodium orthovanadate	500uL .2M sodium orthovanadate

cis-IPTase reaction	For each 100uL rxn
100ug protein	
50uM FPP (Sigma F6892)	2.2uL FPP ammonium salt (MeOH:ammonia soln)
45uM 14C-IPP (ARC 0541)	2uL 14C-IPP
cis-IPTase reaction buffer	20uL 5X cis-IPTase reaction buffer
H_2O	to 100uL

Sample assay TLC.
Total cpm are not indicative of cis-IPTase activity because of presence of label in non-dolichol/polyprenol lipids.

Western Blot Protocol

Based on Ken Harrison's Method

Pour Gel

Resolving Gel	8.5%	10%	12.5%
30% acrylamide	2.125	2.5	3.125
4X Resolving buffer	1.875mL	1.875mL	1.875mL
diH2O	3.5mL	3.125mL	2.5mL
10%APS	50uL	50uL	50uL
TEMED	10uL	10uL	10uL
	7.5mL	7.5mL	7.5mL

Overlay with 1mL H2O. Wait 15m.

Stacking Gel

650uL 30% Acrylamide (in cold room)
1.25mL stacking buffer
3.05mL water
25uL 10%APS (ok at RT for 1 mo)
5uL TEMED

Add comb.
Wait 30m.

Resolving buffer is 1.5M Tris pH8.8. 36.3g Tris Base in 150mL water. pH8.8 using concentrated HCl. Bring volume to 200mL.
Stacking buffer is .5M Tris pH 6.8. 12.1g Tris Base in 150mL water. pH6.8 using concentrated HCl. Bring volume to 200mL.

Protein Assay – Bio-Rad Dc Protein Assay

Mix 1mL Reagent A
20uL Reagent S

Put into each well of a 96-well plate:

5uL sample (and standards) in duplicated
25uL AS mixture
200uL Reagent B

Wait 10min.
Read A750

Use BSA protein standards 10mg/mL, 5, 2.5, 1.25, .625, .325

Run Gel

Rinse lanes with water bottle over sink. Suck out water with aspirator.
Assemble cassette. Lanes face in.
Fill with running buffer (carbuoy by sink).

If running large volumes, fill empty lanes with 1X blue juice.
80V until hits resolving
up to 100V (~70mA)

Transfer

Set up cassette
Black side down – sponge – watman – gel – nitrocellulose – watman – sponge
Place in transfer box with red facing front

Transfer Buffer 1X – OR use 10X purchased buffer stock near sink
    3.2g Tris Base
    14.4g glycine
    in 1L H2O
Use 800mL buffer and 200mL MetOH for 1L of transfer buffer

250-300mA 2hrs (for 50-100kD proteins)
200-250mA 4hrs (for high MW proteins)
70-100mA 16hrs (to transfer O/N)

Block

Use Bio-Rad 1X TBS/Casein Blocking Buffer (stored in cold room) diluted to .1X with TBS (Ken's bench)
Make 50mL
Trim the nitrocellulose to the edge of where the gel was
Block RT 30min-1hr

Primary

In 2mL, primary antibody in .1X TBS/Casein Buffer diluted with TBS-T (next to sink)
Rock O/N cold room

Wash 3X 10min

Secondary

In 2mL, secondary antibody in .1X TBS/Casein Buffer diluted with TBS and .01% SDS
1 hr RT

Wash 8X 5minutes

Yeast Whole Cell Western Blot

Based on Ken Harrison's Protocol
8/11

1. Pellet 7.5 OD yeast
2. Wash in 10mM Tris pH 7.5
3. Resuspend 7.5 OD yeast/750uL Ken's Buffer. Add 200uL beads.
4. Vortex in the cold room 15min.
5. Spin 2k rpm 5min to pellet beads. Transfer liquid to new tube.
6. Spin max rpm 15min. Transfer sup to new tube.
7. Do protein assay on samples.
8. Add 6X blue juice to 50ug of protein. Boil 15 min. Load gel.

Ken's Buffer:	for 20mL
50mM Tris-Cl pH 7.4	1mL 1M Tris-Cl pH 7.4
150mM NaCl	3mL 1M NaCl
5mM EDTA	200uL 500mM EDTA
.1% NP-40	
Roche Complete Protease Inhibitor	1 Complete Mini Pellet
Pefabloc SC	3mg/10mL

Yeast UPR assay by UPRE-lacZ

EC 5/12 (Based on protocol By Huajin Wang.)

Optimized for use with FYPl141 aka pPW984 2X UPRE-lacZ, 2micron, URA3

Materials:

- Y-PER yeast protein extraction reagent (Thermo Fisher scientific PI-78991)
- 2xZ buffer (500mL): [Need 250uL/sample]
  - $Na_2HPO_4.7H_2O$ 16.1g or anhydrous 8.5g
  - $NaH_2PO_4.H_2O$ 5.5g
  - KCl 0.75g
  - $MgSO_4.7H_2O$ 0.246g
  - Add ddH_2O to 500mL, Adjust pH to 7.0.
  - Store at 4°C. (Do NOT autoclave)
  - **Add 270 µl (50mM) BME/100 ml of 1xZ buffer prior to use.**
- ONPG buffer: [Need 100uL/sample]
  - 4 mg/ml in 1xZ-buffer (with BME)
  - Make fresh every time or freeze at -20°C.
- 1M Na_2CO_3 in ddH_2O (to stop reaction)

Procedure:

1. Start O/N culture RT from a streaked plate. Do NOT let them get above OD1. They are very sensitive to growth phase. Do NOT ever let them reach stationary.
2. Grow cells w/ shaking at 30°C until reach OD600 0.4-0.5. Collect 2mL of culture and record OD of collected sample.
3. Add 5mM DTT for 3hrs as positive control (50uL of 1M DTT/10mL culture)
4. Harvest cells by centrifugation at full speed 1m
5. Pellet can be frozen at -80, or proceed to ONPG assay.

ONPG assay:

1. Warm up reagents and cell pellet to 30°C before assay
2. Lyse cells with 250 µl YPER+ 250 µl 2x Zbuffer (with BME) (combine and add at once)
3. Add 100 µl ONPG buffer to 500 ul of cell lysate
4. Incubate at 30°C for 1-30 min, depending on the reaction. Stop reaction when the tube reaches a light-medium yellow color and record time. Try not to collect at minimum or maximum of time range. If you've reached the color of a yellow crayon, you've gone too far.
5. Add 400 µl of 1M Na_2CO_3 to stop reaction
6. Spin down cell debris at 13,000rpm, 1min
7. Transfer 900uL of supernatant to cuvette and measure absorbance at OD420.

Calculate assay units as:
1000*(OD420)/(time(min)*volume collected*OD600)

Yeast Lipid Extraction and TLC Protocol

Erin Currie

1. Grow 10mL yeast overnight.
2. Take OD. To continue with the same number of cells in each sample, use all 10mL of the sample with the smallest OD and proportionately less volume for other samples. You want to use somewhere between 5-10 ODs total.
3. Spin down in glass tubes for 3m at 3000K in desktop centrifuge.
4. Resuspend in 1mL water. Pellet (3m at 3000K in desktop centrifuge).
5. Resuspend in 300uL water.
6. Add 2mL fresh $CHCl_3$/MetOH (1:1) using glass pipette.
7. Add glass beads (~300uL worth. Estimate based on the volume it takes in the tube).
8. Vortex 5 minutes. (Need to vortex all tubes by hand. Multi-tube head doesn't work).
9. Spin down (3m at 3000K in desktop centrifuge), transfer supernatant into fresh glass tube using Pasteur pipettes (supernatant should be one phase).
    a. If they have 2 aqueous phases, add 1mL more $CHCl_3$/MetOH. Vortex 1m. Respin.
10. Dry under N_2. (Can store tightly parafilmed at -20°C for a few days).
11. Add 70uL chloroform/tube (one at a time). Vortex. Slowly dot onto center of loading lane.
12. Load 1uL 100ug/uL cholesterol/cholesterol ester/DG/TG standard.
13. Run in solvent until it reaches the top (~45 min).

Charring

1. Dip TLC plate in 10% CuSO4 (w/v) and 8% phosphoric acid for 20s.
2. Char in hot oven until bands are visible. Temperature and time can vary.

Glass beads - .5mm Glass Beads (Soda Lime), BioSpec Products #11079105
Glass tubes – FisherBrand disposable culture tubes, borosilicate glass 16x100mm, Cat #14-961-29

Solvent systems:

80mL hexane	25mL Methylacetate	100mL hexane
20mL ethyl ether	25mL ispropanol	For squalene
1mL acetic acid	25mL chloroform	
For standard neutral lipid analysis	10mL methanol	
	9mL .25% KCl	
	For phospholipid separation	

YPD	YPGlycerol	YPDO	YPO	YPD + .2% Tween40	YPD + 10ug/mL Terbinafine	YPD + EtOH	YPD + 500ng/uL Tm	YPD + DMSO
2.5g Yeast Extract	2.5g Yeast Extract	2.5g Yeast Extract	2.5g Yeast Extract	2.5g Yeast Extract	2.5g Yeast Extract	2.5g Yeast Extract	2.5g Yeast Extract	2.5g Yeast Extract
5g Peptone	5g Peptone	5g Peptone	5g Peptone	5g Peptone	5g Peptone	5g Peptone	5g Peptone	5g Peptone
5g Dextrose		5g Dextrose	250 uL oleic acid	5g Dextrose	5g Dextrose	5g Dextrose	5g Dextrose	5g Dextrose
		250 uL oleic acid	500 uL Tween40	500 uL Tween40				
		500 uL Tween40	5g Agar	5g Agar	5g Agar	5g Agar	5g Agar	5g Agar
5g Agar	5g Agar	5g Agar	250mL diH2O	250mL diH2O	250mL diH2O	250mL diH2O	250mL diH2O	250mL diH2O
250mL diH2O	225mL diH2O	250mL diH2O	autoclave	autoclave	autoclave	autoclave	autoclave	autoclave
autoclave	autoclave	autoclave			2.5mL 1mg/mL Terb in EtOH	2.5mL EtOH	12.5 uL 5mg/mL Tm in DMSO	12.5 uL DMSO
	25mL 30% glycerol							

SCD	SCGlycerol	SCDO	SCO	SCD + .2% Tween40
5g Agar	5g Agar	5g Agar	5g Agar	5g Agar
175mL diH2O	175mL diH2O	175mL diH2O	175mL diH2O	175mL diH2O
		250 uL oleic acid	250 uL oleic acid	
		500 uL Tween40	500 uL Tween40	500 uL Tween40
autoclave	autoclave	autoclave	autoclave	autoclave
25mL YNB	25mL YNB	25mL YNB	25mL YNB	25mL YNB
25mL 20% Dextrose	25mL 30% glycerol	25mL 20% Dextrose		25mL 20% Dextrose
25mL SCM	25mL SCM	25mL SCM	25mL SCM	25mL SCM

Screen for Growth on Carbon Sources

3/12 EC

Pour 250mL of plate media. Makes 4 Nunc Omnitray 86mm x 128mm plates (Single Well with Lid #242811) and 8 100mm x 15mm round Petri dish plates (normal plate dishes). Allow plates to dry several days.

Clone single colonies into 100uL YPD in 96 well round bottom plates. Grow 2 colonies/strain. Grow 2-3 days at 30° in open plastic bag with damp paper towels. Do not use outermost wells as they will dehydrate.

Perform a 10-fold dilution of the saturated wells into YPD and grow 4-5 hrs to get back into log phase.

Perform 5x 5-fold OR 10-fold serial dilutions in diH_2O. Fill each well with 80uL of diH_2O and add 20uL from larger dilution OR 90uL with 10uL.

Spot 3uL of each dilution onto a plate starting from the most dilute to the least.

Grow and image on the gelDoc using reflective white light. Image => Conversion => 8-bit grayscale and save onto flash drive

Oleic acid SIGMA O1383 stored at -20C
Tween40 SIGMA P1504 stored at RT
Terb in EtOH stored at -20C

Publishing Agreement

It is the policy of the University to encourage the distribution of all theses, dissertations, and manuscripts. Copies of all UCSF theses, dissertations, and manuscripts will be routed to the library via the Graduate Division. The library will make all theses, dissertations, and manuscripts accessible to the public and will preserve these to the best of their abilities, in perpetuity.

Please sign the following statement:

I hereby grant permission to the Graduate Division of the University of California, San Francisco to release copies of my thesis, dissertation, or manuscript to the Campus Library to provide access and preservation, in whole or in part, in perpetuity.

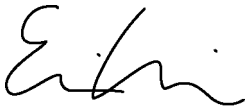

4/26/14

Author Signature | Date